**RODRIGO TEIXEIRA AVILA**

# PHYSIOLOGICAL AND HYDRAULIC MECHANISMS OF DROUGHT TOLERANCE IN PLANTS: IMPLICATIONS OF $CO_2$ AND IRRADIANCE

Thesis submitted to the Plant Physiology Graduate Program of the Universidade Federal de Viçosa in partial fulfillment of the requirements for the degree of *Doctor Scientiae*.

Adviser: Fábio Murilo DaMatta

**VIÇOSA - MINAS GERAIS**
**2020**

**RODRIGO TEIXEIRA AVILA**

# PHYSIOLOGICAL AND HYDRAULIC MECHANISMS OF DROUGHT TOLERANCE IN PLANTS: IMPLICATIONS OF $CO_2$ AND IRRADIANCE

Thesis submitted to the Plant Physiology Graduate Program of the Universidade Federal de Viçosa in partial fulfillment of the requirements for the degree of *Doctor Scientiae*.

APPROVED: February 17, 2020.

Assent:

Rodrigo Teixeira Avila
Author

Fábio Murilo DaMatta
Adviser

*To my parents.*

## ACKNOWLEDGEMENTS

In order to reach some really important people, I need to start with a few words in Portuguese.

Agradeço, primeiramente, a Deus por ter me dado força e perseverança para seguir em frente diante de inúmeros desafios.

Aos meus pais, Alaíde e Jorge, meu irmão Jorge Luís e minha companheira de todas as horas, Analu, o meu eterno agradecimento pelo amor incondicional. Vocês são parte majoritária desta vitória.

Ao meu orientador, Fábio DaMatta, por ser responsável pelo meu treinamento em toda a minha trajetória acadêmica, desde a iniciação científica até a finalização de meu doutorado. Obrigado pela paciência, e por todos os ensinamentos.

Aos meus amigos do Programa de Fisiologia Vegetal da UFV. Obrigado por me auxiliarem nas disciplinas e nos experimentos. Sem vocês, eu não teria chegado até aqui.

Aos amigos do futebol. Construímos uma verdadeira família. Vocês me ensinaram que existe vida além da academia e o quanto é valoroso uma grande amizade.

A todos os Professores e funcionários da Pós-graduação de Fisiologia Vegetal e da UFV com os quais trabalhei. Vocês me ensinaram a ter disciplina nos estudos e afazeres acadêmicos. Obrigado pela convivência tão enriquecedora.

Ao Professor Scott McAdam e todos os amigos que me recepcionaram tão bem na Purdue University durante meu treinamento sanduíche. Sem dúvida, ess foi a experiência mais extraordinária de minha vida.

À Universidade Federal de Viçosa pelas oportunidades concedidas a mim ao longo de minha vida acadêmica.

À Coordenação de Aperfeiçoamento de Pessoal de Nível Superior (CAPES) e ao Conselho Nacional de Pesquisa e Desenvolvimento Científico e Tecnológico (CNPq) pela concessão de minhas bolsas de estudo.

A todos que de alguma forma me ajudaram a cumprir essa etapa tão importante de minha vida. O meu sincero, muito obrigado!

*“Eu quase que nada não sei. Mas desconfio de muita coisa.”.*
(João Guimarães Rosa)

## ABSTRACT

AVILA, Rodrigo Teixeira, D.Sc., Universidade Federal de Viçosa, February, 2020. **Physiological and hydraulic mechanisms of drought tolerance in plants: implications of $CO_2$ and irradiance**. Adviser: Fábio Murilo DaMatta.

Herein, it is present a series of experiments divided into four chapters with the purpose to immerse deep into some physiological and hydraulic responses to drought and also how some of them interact with environmental variability such as elevated [$CO_2$] and irradiance. On the first two chapters it is presented drought responses of coffee plants, one of the most important commodities worldwide, under elevated (700 ppm) and ambient (400 ppm) [$CO_2$] On the first chapter we found that drought-stressed 700-plants were able to keep hydraulic conductance for longer, transpiring more than 400-plants. Correlative evidence is shown that aquaporins may play major roles in these processes. In addition, Well-watered 700-plants displayed lower whole-plant transpiration rates than their 400-counterparts. This was not associated with maximum $g_s$ *per se*, but rather with an increased stomatal closure rate upon vapor pressure deficit transitions, which occur innumerous times over the course of the day. On the second chapter we found that elevated [$CO_2$] improved carbon assimilation, water use-efficiency and biomass accumulation regardless watering, in addition to decreasing the oxidative pressure under drought conditions. Elevated [$CO_2$] also promoted key allometric adjustments linked to drought tolerance, *e.g.* more biomass partitioning towards roots with a deeper root system. Improved growth under enhanced air [$CO_2$] was unlikely to have been associated with global changes on hormonal pools but rather with shifts on carbon fluxes. Altogether, results from the chapters 1 and 2 suggest that [$CO_2$] is perceived by the plant as a key environmental factor having profound implications on how plants respond to drought, thus permitting 700-plants to have an improved fitness under drought when compared to 400-plants. In the third and fourth chapters, efforts were focused on analyzing hydraulic aspects of several different species. O the third chapter, we focused on finding anatomical drivers related to inter- and intraspecific xylem embolism resistance. Vessel lumen fraction was the only anatomical trait measured that correlated with xylem embolism resistance across scales and species. Light was

found to drive only minor differences in stem and not leaf embolism resistance. Our data suggest that conduits highly dispersed in a matrix of imperforate elements may be better protected against the spread of embolism than conduits that are packed in close proximity, which may contribute to our understanding of the mechanisms behind air-seeding. Finally at the fourth chapter, it is presented deep insights into the possible existence of a well-established water potential threshold beyond which vessels and tracheids will embolize We found that, in vessel-based xylem species, individual xylem conduits had a more well-defined water potential at which embolism occur, with considerable pre-existing embolism being able to influence the vulnerability of the xylem. In contrast, conduits in tracheid-based xylem did not display a well-defined individual water potential threshold at which embolism occurs and thus pre-existing embolism did not alter the vulnerability of xylem.

Keywords: Elevated $CO_2$. Drought. Coffee. Embolism, Xylem.

## RESUMO

AVILA, Rodrigo Teixeira, D.Sc., Universidade Federal de Viçosa, fevereiro de 2020. **Mecanismos fisiológicos e hidráulicos da tolerância a seca: implicações de $CO_2$ e irradiância**. Orientador: Fábio Murilo DaMatta.

Ao longo deste trabalho, apresenta-se uma série de experimentos divididos em quatro capítulos analisando-se respostas fisiológicas e hidráulicas de plantas à seca e sua interação com fatores ambientas tais como concentração de $CO_2$ ($[CO_2]$) e irradiância. Nos dois primeiros capítulos, são apresentadas respostas de plantas de café à seca sob $[CO_2]$ elevada (700 ppm) ou ambiente (400 ppm). No primeiro capítulo, observou-se que sob elevada $[CO_2]$, plantas sob estresse hídrico foram capazes de manter a condutância hidráulica e estomática por mais tempo associado a um aumento da abundância de transcritos de aquaporinas. Além disso, plantas irrigadas aclimatadas a elevada $[CO_2]$ apresentaram taxas de transpiração, em nível de planta inteira, mais baixas quando comparadas com plantas aclimatadas a $[CO_2]$ ambiente. Tal fato não foi associado à máximas condutâncias estomáticas em si, mas ao aumento da taxa de fechamento estomático em respostas a incrementos de déficit de pressão de vapor, que ocorrem inúmeras vezes ao longo do dia. Já no segundo capítulo, observou-se que a $[CO_2]$ elevada aumentou a assimilação de carbono, a eficiência no uso da água e o acúmulo de biomassa, independentemente do regime hídrico, além de diminuir a pressão oxidativa em condições de seca. A $[CO_2]$ elevada também promoveu ajustes alométricos importantes associados à tolerância à seca, tais como uma maior partição de biomassa para raízes. Além disso, observou-se que o incremento do crescimento sob o aumento da $[CO_2]$ não parece ter associado a mudanças globais nas concentrações hormonais, mas sim devido a mudanças no fluxo de carbono. Em suma, os resultados dos capítulos um e dois sugerem que o $CO_2$ é percebido pela planta como um fator ambiental essencial, com profundas implicações na forma como as plantas respondem à seca, permitindo assim que plantas aclimatadas à elevada $[CO_2]$ apresentem melhor performance em comparação a plantas de $[CO_2]$ ambiente. No terceiro e quarto capítulos, focou-se na análise de aspectos hidráulicos de várias espécies diferentes. No terceiro capítulo, concentrou-se na busca por fatores anatômicos determinantes para a variação intra e interespecífica da resistência ao embolismo do xilema. A

fração do lúmen de vasos foi a única característica anatômica medida que se correlacionou com a resistência ao embolismo ao longo de espécies e órgãos das plantas. Verificou-se que a luz determina apenas pequenas alterações na resistência do caule enquanto não altera a resistência de folhas ao embolismo. Acredita-se que vasos altamente dispersos em uma matriz de elementos imperfurados podem ser melhor protegidos contra a propagação do embolismo do que os que são dispostos próximos uns aos outros. Finalmente, no quarto capítulo, são apresentados novos *insights* sobre a possível existência de um limiar de potencial hídrico além do qual vasos e traqueídeos embolizam. Observou-se que, em espécies de xilemas baseados em vasos, os condutos individuais de xilema tinham um potencial limítrofe mais bem definido no qual o embolismo ocorre. Dessa maneira, a vulnerabilidade do xilema ao embolismo pode ser alterada pela presença de embolismo pré-existentes. Por outro lado, os xilemas baseados em traqueídeos não exibem um limiar de potencial hídrico bem definido, por isso a embolia pré-existente não alterou a vulnerabilidade do xilema.

Palavras-chave: $CO_2$ elevado. Seca. Café. Embolia. Xilema.

## SUMMARY

**General introduction**

Plant survivorship and fitness depend on how they are able to interact with environmental factors in order to ultimately capture $CO_2$ and resources for growth and reproduction. The way and how plants can fastly sense and translate environmental signals into physiological responses is determined along evolution and breeding, matching environmental requirements such as humidity, temperature and light and nutrient availability. A multiplicity of strategies has been selected, by nature or human force, determining the current ecological and cultivational distribution range of plants around the world. However, plants are now facing a fast change on climate. On one hand, the foreseeing disruption of rainfall patterns may force plants to face challenges they might not be adapted to (IPCC, 2014). On the other hand, rising $CO_2$ concentration ($[CO_2]$) is believed to mitigate the effects of more severe and frequently drought events including a reinforcement of plant defense against stresses such as drought *(AbdElgawad et al.*, 2016). How plant strategies against drought will respond to a possible rainfall patterns disruption remain to be solved. Therefore, a deeper understanding of all these strategies and their interaction with climate changes is required for future actions in order to guarantee ecological and agronomical sustainability.

Earlier plant responses to drought include a decreased stomatal opening, thus avoiding excessive water loss through the stomatal pore that could put xylem under harmful water potentials (Martin-StPaul *et al.*, 2017). This extremely important process is mainly controlled by ABA which is rapidly produced in leaves of angiosperms and gymnosperms triggering stomatal responses (McAdam and Brodribb, 2015; McAdam *et al.*, 2016; Brodribb and McAdam, 2017). Further, the water movement and distribution through plant tissues also need to be precisely regulated to avoid desiccation of tissues and waste of the available water. Most of this regulation is controlled by aquaporins abundance and activity. In roots, they determine the axial flow while in leaves they are responsible for coordinating leaf hydraulic responses and even stomatal behavior (Maurel *et al.*, 2015; Maurel *et al.*, 2016). Decrease of water loss by stomatal pore and the regulation of water movement through aquaporins are important pathways to regulate the whole plant hydraulics, which altogether have profound impacts on how plants deal with drought events.

The stomatal control of transpiration, although extremely important for plant survive, may lead to a depletion in internal [$CO_2$] which can bring a series of events with harmful consequences for the plant. $CO_2$ scarcity at the RuBisCO active site decreases dramatically the usage of NADPH leading to an impairment of the electron chain reaction which ultimately leads to increased oxidative pressure favoring the formation of reactive oxygen species (ROS). This might lead to membrane and protein damaging disrupting cell function which, in extreme cases, may cause death of foliar tissues. However, accumulation of a number of osmotic active compounds might prevent these tissues from being damaged. It is often observed an increased number of compatible solutes in plant cells under drought, most of them with ROS-scavengers properties, thereby decreasing oxidative pressure. Amino acids, glucose, fructose, polyamines and several other compounds can be accumulated at the cytoplasm, vacuole and even at the nucleus permitting the Maintenance of the hydration state of membranes and proteins (Cyr *et al*., 1990; Ha *et al*., 1998; Babita *et al*., 2010; Nolan *et al.*, 2017). This strategy can additionally avoid more water loss through osmotic adjustments.

At a long-term scale, plants may acclimate to drought by an intricate system controlled mainly by hormone contents and signaling and the energetic status of the plant. The interaction between ABA, ethylene, jasmonic acid, cytokinin and gibberellins and carbon metabolism can lead to remarkable changes in transcription patterns which also may permit the necessary physiological responses required for plant survive under drought (de Ollas *et al*., 2015; Verma *et al*., 2016; Pavlů *et al*., 2018). By doing so plants can change their morphology by building smaller and thicker leaves, deeper roots, higher root to shoot ratios which can permit them to decrease transpiration, reach water in deeper layers of the soil and keep higher hydraulic conductance, with ultimate consequences on avoiding drought severity.

All of the described physiological strategies that plants employ to endure drought were selected throughout the course of evolution. However, plants are facing climate changes much faster them in a normal plant evolutional scale. Thus, the environment in which plants evolved might change drastically in the next few decades. Changes in the pattern of rainfall (Schlaepfer *et al*., 2017) with profound implication on timing, severity and frequency of drought events and

increases in temperature (Dore, 2005) are believed to possibly disrupt the distributional and cultivational range of species leading to a massive plant mortality. In this scenario, rising [$CO_2$] is believed to mitigate, at least partially, the harmful effect of climate changes. Increased [$CO_2$] can improve net photosynthesis rates and biomass accumulation (Ainsworth and Long, 2005; Leakey *et al*., 2009). However, how elevated [$CO_2$] will modulate and interfere the way plants sense and respond to drought remain under intense debate. How will all of these strategies deal with this changing scenario? Will elevated [$CO_2$] by itself permit plants to endure more intense and frequent drought events? A lot of gaps remain to be solved before we can answer these questions, including a deeper understanding of plant responses to drought at the hydraulic level, a relatively new scientific field.

As the soil continuously dries out, the last level of defense against drought stress it is xylem resistance to embolism, the last way plants can undertake hydraulic failure. Water transportation through xylem conduits occur *via* negative pressure, and because of that, the water inside the conduits it is at the so called metaphasic state. In this state, water it is prompt to go from liquid to the vapor phase inside the conduits. This may happen through the occurrence of a nucleation in which an air bubbles are sucked into the conduit ultimately causing the complete disruption of the water continuum, the embolism (Zimmermann, 1983). Embolism can spread through xylem conduits, thus disrupting permanently, in most cases, the transportation of water and eventually leading to a complete hydraulic failure that ultimately causes plant death (Brodribb and Cochard, 2009). Currently, xylem resistance against embolism is believed to be one of the most important strategies for plant survive against drought stress (Lens *et al*., 2013). In this way, the water potential at which 50% of xylem conduits are embolized, the $P_{50,}$ is an important metric that has been correlated with the distributional range of several species. Xylem conduit dimensions as diameter and length (Hacke *et al*., 2009; Blackman *et al*., 2010), pit membrane structure in angiosperms (Choat *et al*., 2008; Brodersen *et al*., 2014; Li *et al*., 2016), torus and margo sealing capacity in gymnosperms (Choat and Pittermann, 2009; Hacke and Jansen, 2009) and cell-wall thickness (Hacke *et al*., 2001; Blackman *et al*., 2010) have been associated with $P_{50}$. In addition, $P_{50}$ is not just correlated with distributional range through contrasting environments in terms of water

availability but also explains different susceptibilities to drought within the same individual in which is not rare to find a growing gradient of resistance from leaves to stems prolonging towards the root system (Cardoso *et al*., 2019; Lucani *et al*., 2019). Also, different microenvironments within a canopy with contrasting irradiance has been shown to determine profound anatomical changes triggering alterations on $P_{50}$ (Barigah *et al*., 2006; Plavcová *et al*., 2011). Although a lot of efforts have been made to understand the anatomical drivers of xylem resistance, we still have much more to discovery in this field. We still poorly comprehend how connectivity between conduit, conduits distribution at xylem and lumen fraction may interfere on xylem resistance against embolism, for example.

Herein, I present a series of experiments divided into four chapters with the purpose to immerse deep into some physiological and hydraulic responses to drought and also how some of them interact with environmental variability such as elevated [$CO_2$] and irradiance. On the first two chapters I focused on studying drought responses of coffee plants, one of the most important commodities worldwide, under elevated [$CO_2$]. At the first chapter I investigate hydraulic aspects, including stomatal behavior and aquaporins expression and their implications to the transpiration process. In the second chapter I focused on how elevated [$CO_2$] might mitigate diffusional limitations (which are inherent of this species) in coffee plants under drought and how this could alleviate the oxidative pressure under stressful conditions. In the third and fourth chapters I analyze hydraulic aspects of several different species. Specifically, at the third chapter I present an analysis of anatomical drivers of xylem resistance to embolism over 13 species evolved in a range of different environments. Finally, at the fourth chapter, by submitting several species to cycles of dehydration and rehydration, I present deep insights into the possible existence of a well-established water potential threshold beyond which vessels and tracheids will embolize. Hopefully this compilation of results from several experiments shall increase the current knowledge about drought responses *per se* and how this phenomenon interacts with other environmental factors.

**References**

**AbdElgawad H, Zinta G, Beemster GTS, Janssens IA, Asard H** (2016) Future climate $CO_2$ levels mitigate stress impact on plants: increased defense or

decreased challenge? *Front Plant Sci* **7**: 1–7

**Ainsworth EA, Long SP** (2005) What have we learned from 15 years of free-air $CO_2$ enrichment (FACE)? A meta-analytic review of the responses of photosynthesis, canopy properties and plant production to rising $CO_2$. *New Phytol* **165**: 351–372

**Babita M, Maheswari M, Rao LM, Shanker AK, Rao DG** (2010) Osmotic adjustment, drought tolerance and yield in castor ( Ricinus communis L.) hybrids. *Environ Exp Bot* **69**: 243–249

**Barigah TS, Ibrahim T, Bogard A, Lagneau LA, Montpied P** (2006) Irradiance-induced plasticity in the hydraulic properties of saplings of different temperate broad-leaved forest tree species. *Tree Physiol* **26**: 1505–1516

**Blackman CJ, Brodribb TJ, Jordan GJ** (2010) Leaf hydraulic vulnerability is related to conduit dimensions and drought resistance across a diverse range of woody angiosperms. *New Phytol* **188**: 1113–1123

**Brodersen C, Jansen S, Choat B, Rico C, Pittermann J** (2014) Cavitation resistance in seedless vascular plants: the structure and function of interconduit pit membranes. *Plant Physiol* **165**: 895–904

**Brodribb TJ, Cochard H** (2009) Hydraulic failure defines the recovery and point of death in water-stressed conifers. *Plant Physiol* **149**: 575–584

**Brodribb TJ, McAdam SAM** (2017) Evolution of the Stomatal Regulation of Plant Water Content. *Plant Physiol* **174**: 639–649

**Cardoso AA, Batz TA, Mcadam SAM** (2019) Xylem embolism resistance determines leaf mortality during drought in *Persea americana*. Plant Physiol. doi: 10.1201/9781351072571

**Choat B, Choat B, Cobb AR, Jansen S** (2008) Structure and function of bordered pit: new discoveries and impacts on whole-plant hydraulic function. *New Phytol* **177**: 608–626

**Choat B, Pittermann J** (2009) New insights into bordered pit structure and cavitation resistance in angiosperms and conifers. *New Phytol* **182**: 557–560

**Cyr DR, Buxton GF, Webb DP, Dumbroff EB** (1990) Accumulation of free amino acids in the shoots and roots of three northern conifers during drought. *Tree Physiol* **6**: 293–303

**Dore MHI** (2005) Climate change and changes in global precipitation patterns: what do we know? *Environ Int* **31**: 1167–1181

**Ha HC, Sirisoma NS, Kuppusamy P, Zweier JL, Woster PM, Casero RA** (1998) The natural polyamine spermine functions directly as a free radical scavenger. *Proc Natl Acad Sci U S A* **95**: 11140–11145

**Hacke UG, Jacobsen AL, Pratt RB** (2009) Xylem function of arid-land shrubs from California, USA: An ecological and evolutionary analysis. *Plant, Cell Environ* **32**: 1324–1333

**Hacke UG, Jansen S** (2009) Embolism resistance of three boreal conifer species varies with pit structure. *New Phytol* **182**: 675–686

**Hacke UG, Sperry JS, Pockman WT, Davis SD, Mcculloh KA** (2001) Trends in wood density and structure are linked to prevention of xylem implosion by negative pressure. *Oecologia* **126**: 457–461

**Leakey ADB, Ainsworth EA, Bernacchi CJ, Rogers A, Long SP, Ort DR** (2009) Elevated $CO_2$ effects on plant carbon, nitrogen, and water relations: Six important lessons from FACE. *J Exp Bot* **60**: 2859–2876

**Lens F, Tixier A, Cochard H, Sperry JS, Jansen S, Herbette S** (2013) Embolism resistance as a key mechanism to understand adaptive plant strategies. *Curr Opin Plant Biol* **16**: 287–292

**Li S, Lens F, Karimi Z, Klepsch MM** (2016) Intervessel pit membrane thickness as a key determinant of embolism resistance in angiosperm xylem. *IAWA J* **37**: 152–171

**Lucani CJ, Brodribb TJ, Jordan G, Mitchell PJ** (2019) Intraspecific variation in drought susceptibility in *Eucalyptus globulus* is linked to differences in leaf vulnerability. *Funct Plant Biol* **46**: 286–293

**Martin-StPaul N, Delzon S, Cochard H** (2017) Plant resistance to drought depends on timely stomatal closure. Ecol Lett 1–11

**Maurel C, Boursiac Y, Luu DT, Santoni V, Shahzad Z, Verdoucq L** (2015) Aquaporins in plants. *Physiol Rev* **95**: 1321–1358

**Maurel C, Verdoucq L, Rodrigues O** (2016) Aquaporins and plant transpiration. *Plant Cell Environ* **39**: 2580–2587

**McAdam SAM, Brodribb TJ** (2015) The evolution of mechanisms driving the stomatal response to vapor pressure deficit. *Plant Physiol* **167**: 833–843

**McAdam SAM, Sussmilch FC, Brodribb TJ** (2016) Stomatal responses to vapour pressure deficit are regulated by high speed gene expression in angiosperms. *Plant Cell Environ* **39**: 485–491

**Nolan RH, Tarin T, Santini NS, McAdam SAM, Ruman R, Eamus D** (2017) Differences in osmotic adjustment, foliar abscisic acid dynamics, and stomatal regulation between an isohydric and anisohydric woody angiosperm during drought. *Plant Cell Environ* **40**: 3122–3134

**de Ollas C, Arbona V, Gómez-Cadenas A** (2015) Jasmonic acid interacts with abscisic acid to regulate plant responses to water stress conditions. *Plant Signal Behav* **10**: e1078953

**Pavlů J, Novák J, Koukalová V, Luklová M, Brzobohatý B, Černý M** (2018) Cytokinin at the crossroads of abiotic stress signalling pathways. *Int J Mol Sci* **19**: 1–36

**Plavcová L, Hacke UG, Sperry JS** (2011) Linking irradiance-induced changes in pit membrane ultrastructure with xylem vulnerability to cavitation. *Plant, Cell Environ* **34**: 501–513

**Schlaepfer DR, Bradford JB, Lauenroth WK, Munson SM, Tietjen B, Hall SA, Wilson SD, Duniway MC, Jia G, Pyke DA, *et al*** (2017) Climate change reduces extent of temperate drylands and intensifies drought in deep soils. *Nat Commun*. doi: 10.1038/ncomms14196

**Verma V, Ravindran P, Kumar PP** (2016) Plant hormone-mediated regulation of stress responses. *BMC Plant Bio*l **16**: 1–10

**Zimmermann MH** (1983) Xylem structure and the ascent of sap. Springer-Verlag. doi: 10.1139/b81-248

# CHAPTER 1

## Changes in stomatal function and plant hydraulic conductance delay coffee dehydration during drought under elevated [$CO_2$]

**Abstract**

Rising air $CO_2$ concentration ([$CO_2$]) is believed to mitigate the negative impacts of global climate changes such as increased air temperatures and drought events. Nonetheless, how elevated [$CO_2$] affects the way plants sense and respond to drought remains a critical unknown. In this study, potted coffee (*Coffea arabica* L.) plants were cultivated under contrasting air [$CO_2$] (c. 400 ppm or 700 ppm) in open top chambers under greenhouse conditions. After a 5-month exposure to [$CO_2$] treatments, plants were submitted to a progressive, controlled soil water deficit down to 20% soil field capacity. Well-watered 700-plants displayed lower whole-plant transpiration rates than their 400-counterparts. During drought, 700-plants delayed tissue dehydration and were able to maintain higher plant hydraulic conductances for longer, while transpiring more when compared to 400-plants. Differences in transpiration rates were not associated with maximum stomatal conductance or foliar ABA levels, but rather with an increased stomatal closure rate upon transitions in leaf-to-air vapor pressure deficit. Evidence is shown that aquaporins may play key roles in altering stomatal function and plant hydraulic conductance. Altogether, our results suggest that elevated [$CO_2$] has marked implications on how coffee plants respond to soil water deficit, ultimately permitting 700-plants to have an improved fitness under drought when compared to 400-plants.

**Key words:** aquaporin, *Coffea arabica*, elevated [$CO_2$], hydraulic conductance, stomatal response, whole-plant transpiration.

**Abbreviations:** *A,,* net photosynthetic rate; ABA, abscisic acid; *CaPiP*, *Coffea arabica* plasma membrane intrinsic protein; *CaTiP*, *Coffea arabica* tonoplast intrinsic protein; DP, polar diameter of stomata; FC, soil field capacity; FOV, field of view; $g_{s,}$ stomatal conductance; $g_{s\ initial,}$ maximum stomatal conductance at low leaf-to-air vapor pressure deficit; $g_{s\ final,}$ stomatal conductance at high leaf-to-air vapor pressure deficit; $K_{plant,}$ whole-plant hydraulic conductance; OTC, open top chamber; PPFD, photosynthetic photon flux density; SD, stomatal density; SI, stomatal index; SLAC1, S-type anion channel; *T*, whole-plant transpiration over the day; $T_m$, whole-plant transpiration between predawn and midday; UPLC-MS/MS, ultra-performance liquid chromatography - tandem mass spectrometer; VD, vein density; VPD, leaf-to-air vapor pressure deficit; $VPD_s$, stomatal sensitivity to leaf-to-air vapor pressure deficit; [$CO_2$], atmospheric $CO_2$ concentration; $\Psi_{md}$, midday leaf water potential; $\Psi_{pd,}$ predawn leaf water potential; $\Psi_w$, water potential

## Introduction

The increase of atmospheric $CO_2$ concentration ($[CO_2]$) coupled with rising air temperatures and unpredictability of rainfall patterns constitute major components of global climate change. Drought events are predicted to increase in frequency and intensity in many areas of the globe (IPCC, 2014), thus imposing considerable constraints to plant growth and productivity (Wang et al., 2018). In addition, rises in leaf-to-air vapor pressure deficit (VPD) are also expected, which can potentially result in further limitations to leaf gas exchange and ultimately in plant mortality (Grossiord et al., 2020). Nonetheless, rising $[CO_2]$ is believed to mitigate the negative effects of drought in plants due to enhancements in both net photosynthetic rate ($A$) and water-use efficiency as a result of the increased $[CO_2]$ inside leaves (Prentice *et al.*, 2001; Ainsworth & Long, 2005; Keenan *et al.*, 2013). Such positive effect of increased $[CO_2]$ is likely to occur alongside changes in the way plants sense and respond to drought (Brodribb and McAdam, 2013), and further studies are required in order to unveil such mechanisms.

Improved water economy and acquisition are common strategies allowing plants to cope with water-limited conditions. Stomatal closure, in response to increases in foliar abscisic acid (ABA) levels, represents one of the earliest plant responses minimizing excessive water loss during drought (Martin-StPaul et al., 2017, Creek et al., 2020). Guard cells are also able to sense rapid and numerous changes in VPD leading to a well-described ABA-dependent stomatal closure (McAdam & Brodribb, 2014, 2015; McAdam *et al.*, 2016, Cardoso et al., 2018). In addition, whole-plant hydraulic conductance is also regulated through changes in aquaporin function, favoring a better compartmentalization and distribution of water through plants tissues (Parent *et al.*, 2009). Aquaporins, which are intrinsic membrane proteins responsible for efficiently transport water from cell-to-cell, play major roles in defining plant hydraulic conductances, and they have been demonstrated to be responsive to drought (Maurel *et al.*, 2015, 2016; Miniussi *et al.*, 2015). By regulating the activity of aquaporins, plants are able to control the water transport across tissues and cells, including the stomatal ones (Grondin *et al.*, 2015).

Noticeably, stomatal conductance ($g_s$) has been widely, but not universally, reported to decrease under enhanced $[CO_2]$ (Engineer *et al.*, 2016).

The $CO_2$-induced stomatal closure is believed to occur via aquaporin PIP2;1, which facilitates the entrance of $CO_2$ into the guard cell, where it is converted to $HCO_3^-$. This leads to activation of an S-type anion channel (SLAC1), which results in guard cell turgor loss, and ultimately stomatal closure (Maurel *et al.*, 2016). Enhanced [$CO_2$] can also result in stomatal anatomy modifications, including changes in stomatal density, index and size (Woodward, 1987; Ramalho et al., 2013; Xu *et al.*, 2016), which collectively lead to a lower maximum $g_s$. In addition, decreases in $g_s$ at enhanced [$CO_2$] have also been reported to be triggered by hydraulic adjustments (declines in leaf and root hydraulic conductances), which suggests a close coordination between vapor and liquid water transport (Hao *et al.*, 2018). Nevertheless, in some species, such as coffee (Ramalho *et al*., 2013; Ghini *et al*., 2015; Rodrigues *et al*., 2016), $g_s$ appears to be unresponsive to elevated [$CO_2$] under well-watered conditions, but the underlying mechanism associated with this behavior is a critical unknown. Additionally, whether such unresponsiveness is maintained under drought condition and how it could affect plant water-use efficiency and drought tolerance deserve a deeper examination.

In this study, we cultivated coffee (*Coffea arabica* L.) plants under elevated [$CO_2$], and exposed them to a progressive, controlled drought stress. Coffee, one of the most globally traded agricultural commodities, was selected for its stomata unresponsiveness to [$CO_2$] at least up to 700 ppm (Ramalho *et al.*, 2013; Ghini *et al.*, 2015; DaMatta *et al.*, 2016; Rodrigues *et al.*, 2016) and high sensitivity to VPD (Batista *et al.*, 2012; Martins *et al.*, 2019). A number of questions were addressed: (i) Could the unresponsiveness of $g_s$ to elevated [$CO_2$] be kept under drought? How could the expected changes in hydraulic adjustments impact $g_s$ at enhanced [$CO_2$] in combination with drought? (iii) Would an enhanced [$CO_2$] alter the stomata responses to VPD? (iv) Could the possible alterations in stomatal function and plant hydraulics be associated with alteration in aquaporins transcript patterns? To answer these questions, we combined measurements of whole-plant transpiration, plant hydraulic conductance, measurements of $g_s$, stomatal responses to VPD, and aquaporin transcripts abundance. We discuss our data by emphasizing the implications of stomatal function and hydraulics on whole-plant transpiration, and how this could improve drought tolerance of coffee plants under elevated [$CO_2$].

## Material and Methods

### *Plant material, experimental conditions and sampling*

The experiment was conducted in Viçosa (20º45'S, 42º15'W, 650-m altitude), south-eastern Brazil. Coffee (*Coffea arabica* L. cv. IAC 44) seedlings were grown in open-top chambers (OTC) (1.15 m diameter and 1.40 m height) that were placed inside a greenhouse with controlled air temperature (30/25 ± 2ºC, day/night) and naturally fluctuating air humidity and photosynthetic photon flux density (PPFD). Thirty-four seedlings were transplanted (mid-March 2017) to 12 L pots containing a mixture of soil, sand and composted manure (3:2:1, v/v/v) until achieving 5-6 leaf pairs. After that, the most 24 vigorous seedlings were chosen (mid-April 2017). These seedlings were then submitted to two air $CO_2$ treatments: ambient (386 ± 20 ppm) or elevated [$CO_2$] (723 ± 83 ppm) using the above quoted OTC. For sake of simplification, these concentrations are hereafter referred to as 400 or 700 ppm. $CO_2$ fumigation was accomplished from 06:00 to 18:00 h. [$CO_2$] was checked weekly by using portable $CO_2$ sensors (model CO277, Akso Produtos Eletrônicos, São Leopoldo, Brazil), which were used and calibrated following manufacturer recommendations. Air temperature and humidity, which were measured daily using specific sensors (model 1400-104, Lincoln, NE, USA), did not vary among the different OTC.

During the first five months, all of the seedlings were regularly watered so that the soil water content was maintained near to field capacity (FC). Subsequently, plants from each $CO_2$ treatment were divided into two groups. In the first group (*i.e.*, well-watered plants), plants remained watered as described above. The plants from the second group (*i.e.*, drought-stressed plants) were not watered until the soil water content reached approximately 50% FC (c. five days). They were then maintained at 50% FC for additional 22 days. Subsequently the soil water content was reduced to 37.5% FC (by suspending irrigation for three days) and plants were kept at 37.5% FC for an additional 22 days. Also by suspending irrigation for two days soil water content reached 25% FC, and plants were maintained under this condition for 30 days. Finally, soil water content was decreased down to 20% FC, and plants were kept at this condition for five days. Further details concerning the control of soil moisture have been reported by Cavatte et al. (2012) and Menezes-Silva et al. (2017). Each one of the four $CO_2$

chambers contained three plants from the first group and three from the second one. Routine agricultural practices for coffee bean cultivation, including fertilization and control of insect and pathogen attack were used in both well-watered and water-limited plants.

Unless otherwise stated, samplings and measurements were performed on completely expanded leaves from the third or fourth leaf pair from the apex of plagiotropic branches after 72 or 79 days upon drought imposition, *i.e.* 25% or 20% of FC. For biochemical analyses, leaf tissues were collected at 11:30-12:30 h (solar time) and then flash frozen in liquid nitrogen with subsequent storage at -80ºC until analysis.

*Hydraulic parameters*

Leaves were collected, maintained inside zip lock bags with damp paper towel during 5 min, and then the water potential ($\Psi_w$) was measured at both predawn (4:30-5:30 h) ($\Psi_{pd}$) and midday ($\Psi_{md}$) using a Scholander pressure chamber (model 1000, PMS Instruments, Albany, NY, USA).

The plant hydraulic conductance ($K_{plant}$) was estimated as whole-plant transpiration per unit leaf area divided by the leaf-to-soil $\Psi_w$ difference, with soil $\Psi_w$ estimated from leaf $\Psi_{pd}$ (Cavender-Bares et al., 2007; Nardini and Salleo, 2000). Transpiration was gravimetrically computed between predawn and midday ($T_m$) using a balance (0.1 g precision), whereas total leaf area was measured using maximum leaf length and width dimensions, as described in Antunes *et al.* (2008). $K_{plant}$ was then calculated as $K_{plant} = T_m/[-(\Psi_{md} - \Psi_{pd})]$ and expressed as mmol $H_2O$ $m^{-2}$ $s^{-1}$ $MPa^{-1}$. Additionally, whole-plant transpiration ($T$) over the drought period imposition was determined daily by weighting the pots at 18:00 h with data normalized by the total leaf area, and expressed in mmol $H_2O$ $m^{-2}$ $s^{-1}$.

The $g_s$ was measured at the leaf level using a portable infrared gas analyzer (model LI-6400XT, Li-COR Biosciences INC., Nebraska, USA), under an artificial PPFD of 1000 µmol $m^{-2}$ $s^{-1}$, and 400 or 700 ppm [$CO_2$], between 08:00 and 09:00 hwhen $g_s$ was previously observed to be at its maximum values.

*Leaf anatomy*

Leaves, collected and prepared as described in Menezes-Silva *et al.* (2015), were used for measuring vein density (VD), stomatal density (SD),

stomatal index (SI), and stomatal polar diameter (DP). One c. 200 $mm^2$ section was taken from the middle of the lamina of each leaf, avoiding major veins. Five fields of view (FOV) at 4× magnification and five FOV at 10× magnification were photographed from each leaf section using a digital camera mounted on an Olympus Microscope (AX70TRF, Olympus Optical, Japan). VD was calculated as the sum of the vein length divided by the FOV area using 4× magnification images. SD, SI and DP were measured using 10× magnification images. For all measurement, we utilized the image analysis program Image Pro-Plus (version 4.5, Media Cybernetics, Silver Spring, USA).

*VPD curves*

To perform VPD curves, we selected the four well-watered 400- and 700-plants with the most similar $g_s$, as stomatal responses are strongly affected by initial $g_s$ ($g_{s\ initial}$) (see Oren *et al.* 1999). We were unable to collect useful data for drought-stressed plants, precisely because $g_{s\ initial}$ was very low and variable. For each plant, a fully expanded leaf was enclosed in a 40-$cm^2$ conifer chamber (Li6400-22 L, Li-Cor, Lincoln, NE, USA) connected to the infrared gas analyzer described above. The initial conditions inside the chamber were: 25°C, 400 or 700 ppm [$CO_2$] (depending on the $CO_2$ treatment), 1000 µmol photons $m^{-2}$ $s^{-1}$ at the leaf surface, and 0.91 ± 0.18 kPa of VPD. The initial low VPD was controlled by a portable dew point generator (LI-610, LI-COR Inc., Lincoln, NE, USA). Leaves remained under these conditions until gas exchange reached a stable maximum, which was logged every 60 s to build the kinetics of the stomatal responses. The initial plateau (5 min) was used to determine $g_{s\ initial}$. In the next step, VPD was rapidly increased to 2.46 ± 0.43 kPa by forcing the air through the desiccant container attached to the LI-COR. The leaf was maintained at high VPD until stabilization of leaf gas exchange (final plateau), when the new steady-state $g_s$ at high VPD ($g_{s\ final}$) was determined. VPD sensitivity ($VPD_s$) was determine as $VPD_s = [((g_{s\ initial} - g_{s\ final})/g_{s\ initial})\ x100]/(\text{High VPD} - \text{Low VPD})$. Finally, stomatal closure rate to VPD transitions was estimated as the coefficient of the linear phase of VPD transition curves and expressed in mmol $H_2O$ $m^{-2}$ $s^{-1}$ $min^{-1}$. We also performed the reverse VPD transition, *i.e.* plants acclimated to 400 ppm [$CO_2$] were submitted to a VPD transition at 700 ppm [$CO_2$] and *vice-versa*.

*Aquaporin expression*

Specific primers were used to assess the expression of six genes coding for aquaporin plasma membrane (4) and tonoplast (2) intrinsic proteins (PiPs and TiPs respectively). From these six genes, only three PiPs (*CaPiP2;1*, *CaPiP1;2* and *CaPiP2;2*) and one TiP (*CaTiP1;1*) had their transcripts amplified. These genes were previously demonstrated to be the most responsive to drought stress in coffee plants (Miniussi *et al*. 2015). RNA was extracted according to the methodology described by Ramalho *et al*. (2018) using three biological replicates that were collected in well-watered and drought-stressed plants under 25 and 20% FC, thus a total of six biological replicates were taken into account. The next step was to verify the RNA integrity on 1% (w/v) agarose gels. Further, RNA concentration was spectrophotometrically determined before and after the samples had been submitted to a DNAse I digestion (Amplification Grade DNAse I, Invitrogen) which was performed according to the manufacturer's instructions. Subsequently, cDNA synthesized using a SuperScript III First-Strand Synthesis SuperMix for qRT-PCR (Invitrogen). The PCR program was as follows: 95°C for 3 min, and 40 cycles of 95°C for 10 s, 65°C for 15 s, and 72°C for 15 s. For the analysis of gene expression, real time PCR (Step One PlusTM Real Time PCR System, Applied Biosystems, CA, USA) with the SYBR green fluorescence detection (Applied Biosystems1) system was employed using the Platinum1 SYBR1 Green qPCR SuperMix-UDG with ROX kit. The transcript levels were then assessed by the standard curves of each selected gene and normalized using the coffee malate dehydrogenase gene as recommended by Martins *et al.* (2017). The determination of the target gene expression levels was calculated by 2-ΔΔCT method (Livak & Schmittgen, 2001).

*Foliar abscisic acid*

ABA was extracted from leaves, and quantified exactly as described by Martins et al. (2019). The samples were automatically injected into a UPLC-MS/MS system using an Agilent 1200 Infinity Series coupled to a mass spectrometry type triple quadrupole (QqQ), model 6430 (Agilent Technologies, Santa Clara, CA, USA). A calibration curve was established to determine the absolute foliar ABA levels.

*Growth parameters*

Non-destructive growth traits were assessed every 21 days. In addition to total leaf area (see above), plant height (from the soil level until the end of the orthotropic branch) and stem diameter at the soil level were also assessed.

*Experimental design and statistical analyses*

Plants were subjected to four treatment combinations, in a 2 x 2 factorial (two [$CO_2$] and two levels of available water in the soil). Data were analyzed following a completely randomized design, as a matter of simplification, given that all the chambers were inside the same greenhouse and submitted to the same conditions. In addition, pot positions inside the chambers were daily randomly changed during the weighting of pots. Six plants in individual pots per treatment combination were considered as replicates. The analyses were based on two-way ANOVA followed by the Student *t*-test comparing [$CO_2$] within each watering condition and *vice versa*. The relative expression ratio of each target gene was computed based on its real-time PCR efficiency and the crossing point difference of a target sample versus control. All statistical analyses were performed using the *R* programming language, version 3.4.0 (*R*core Team, 2018). A 95% confidence level was adopted for all tests.

**Results**

Decreased soil moisture to 50 or 37.5% FC did not affect both $\Psi_{pd}$ and $\Psi_{md}$ regardless of $CO_2$ treatments. At 25% FC, $\Psi_{pd}$ and $\Psi_{md}$ remained at control levels in 700-plants, but were lower in drought-stressed 400-plants than in their well-watered counterparts. At 20% FC, both $\Psi_{pd}$ and $\Psi_{md}$ were lower in drought-stressed than in well-watered individuals, independently of $CO_2$ (Table 1).

Over time, $g_s$ of well-watered plants oscillated according to the conditions inside the greenhouse (Fig. 1A). Similar $g_s$ values were observed between well-watered plants cultivated at either 400- or 700 ppm of $CO_2$. However, in drought-stressed plants, some $g_s$ differences were observed in response to [$CO_2$] treatments. The greater difference was observed at 37.5% FC, when $g_s$ values of 700-plants were more than two-fold higher over the 400-plants (Fig. 1A), but this difference was attenuated at lower FC levels, becoming null at 20% FC.

The $K_{plant}$ oscillated less in response to the greenhouse conditions over time, and it was also unresponsive to [$CO_2$] in well-watered plants over the course of this study, which displayed an averaged $K_{plant}$ of 1.17 mmol $m^{-2}$ $s^{-1}$ $MPa^{-1}$ (Fig. 1B). In contrast, in drought-stressed plants, higher values of $K_{plant}$ (*c*. 100%) were observed in 700- than in 400-plants at 37.5 or 25% FC. This difference disappeared at 20% FC, when $K_{plant}$ reached values of approx. 0.30 and 1.0 mmol $m^{-2}$ $s^{-1}$ $MPa^{-1}$ under drought and well irrigated conditions, respectively, regardless of [$CO_2$].

Averaged *T* values were higher in well-watered than in drought-stressed plants (Fig. 1C). Overall, until *c*. 40 days upon drought imposition (when soil moisture corresponded to 50-37.5% FC), plants displayed the highest *T* in parallel with the highest VPD (mean values ranging from *c*. 1.5 to 4.0 kPa; Fig. 1D). During this period, contrasting *T* responses to [$CO_2$] were observed, depending on water availability. Under well-watered conditions, the 400-plants transpired more than 700-plants (averaging on 2.0 and 1.5 mol $H_2O$ $m^{-2}$ $s^{-1}$, respectively), while under drought an inverse pattern was noted, *i.e.* lower *T* in 400- than in 700-plants (averaging on 0.6 and 1.0 mol $H_2O$ mol $m^{-2}$ $s^{-1}$, respectively). In contrast, during the last 40 days (which coincided with the rainy season and mean VPD < 1.5 kPa), differences in *T* patterns across treatments were reduced independently of $CO_2$ treatments. However, a clear trend of higher *T* in well-watered 400-plants (averaging on 0.93 mol $H_2O$ $m^{-2}s^{-1}$) than in the plants from the other three treatments (averaging on 0.66 mol $H_2O$ $m^{-2}s^{-1}$) could be observed.

We additionally assessed the stomatal behavior upon VPD transitions by evaluating both the stomatal closure rate and stomatal sensitivity to increasing VPD in well-watered plants (Fig. 2). Interestingly, although maximum $g_s$ did not respond to $CO_2$ *per se*, stomatal closure rate was significantly higher (78%) in 700- than in 400-plants (Fig. 2A). This contrasting pattern is well illustrated in Fig. 2C, as denoted by the steeper decrease in $g_s$ overtime in 700- than in 400-plants upon fast VPD transitions. Such stomatal closure rates were unrelated to ABA levels (Fig. S1) as well as to stomatal morphology (*i.e*. SD, SI and PD, Table S1), all of which remained unaltered in response to $CO_2$ and watering treatments. Interestingly, when proceeding the reverse VPD transition curves, 700-plants presented stomatal closure rates similar to those of 400-plants, which, in turn,

maintained the same behavior as when submitted to transitions under 400 ppm of [$CO_2$] (Fig. S2 and S3). Finally, the stomatal sensitivity to VPD was unresponsive regardless of treatments (Fig. 2B and Fig.S3).

To gain additional insights on the alterations in stomatal behavior and plant hydraulic, we further examined aquaporin gene expression in leaves and roots. Overall, drought affected the expression of aquaporin genes in leaves (Fig. 3), but only in 700-plants, *e.g.* decreased transcript abundance of *CaTiP1;1* (60%) and CaPiP1;1 (90%). On the other hand, [$CO_2$] had a striking effect on the expression of aquaporin genes. The leaves of 700-plants displayed higher transcript abundance of all genes we analyzed (from 3 up to 40 folds) when compared to 400-plants independently of watering treatments with the exception of *CaPiP2;2*, which remained unresponsive to [$CO_2$]. No alterations on the aquaporin transcript abundance were found in roots (data not shown).

Finally, we assessed some growth responses. Total leaf area, plant height and stem diameter increased over time, and were significantly higher in the 700- than in 400-plants irrespective of watering (Fig. S4).

**Discussion**

Coffee plants cultivated under elevated air [$CO_2$] were submitted to a gradual, moderate drought stress similar to naturally found in most Brazilian coffee producing areas (*cf.* Martins *et al.*, 2019). Overall, enhanced [$CO_2$] delayed coffee plant dehydration during drought, as judged from their higher $\Psi_w$ at 20 or 25% FC (significantly only for the latter) when compared with the 400-plants. Such response seemed to be linked to both the higher $K_{plant}$ over the drought imposition and enhanced stomatal closure rate to VPD observed under elevated [$CO_2$].

As reported earlier for coffee (Ramalho et al., 2013; Ghini et al., 2015), $g_s$ was essentially unresponsive to elevated [$CO_2$] under well-watered conditions. This response was mostly maintained under drought condition, as noted by the similar $g_s$ values (at 25 or 20% FC) of 400- and 700-plants under drought stress. We suggest that differences in $g_s$ in response to drought, as found at 37.5% or 25% FC, were unlikely to have been directly associated with $CO_2$ supply *per se*, but rather through changes in $K_{plant}$. The same differences in $K_{plant}$ can also explain to a great a extent the differences in $T$ that were observed between 400-

and 700-plants under drought. In addition, we suggest that the lower *T* observed in the 700-plants over their 400-counterparts might have resulted from a faster stomatal response of 700-plants to rising VPD.

We suggest that both the increased $K_{plant}$ and stomatal closure rate in plants cultivated under elevated [$CO_2$] might be due to differences in aquaporins transcripts (and presumably aquaporin abundance). In fact, the transcript levels of aquaporins have been well correlated with protein abundance (Lopez *et al.*, 2003; Alexandersson *et al.*, 2005; Hachez *et al.*, 2012) and hydraulic responses (Miniussi *et al.*, 2015). Therefore, it is tempting to suggest that the greater expression of *CaTIP1;1*, *CaPiP1;2* and *CaPiP2;1* on the leaves of drought-stressed 700-plants might be associated with a higher $K_{plant}$ when compared to their 400-counterparts. This suggestion is reinforced by the fact that major limitations to water transport in coffee occur at the leaf level (Tausend *et al.*, 2000) and are dominated by extra-vascular tissues (Gascò *et al.*, 2004). Taken this information into account, and that we did not find differences in leaf vein density (Table S1), it is therefore expected that aquaporins may play major roles in facilitating water flow through leaf tissues. Higher $K_{plant}$ could in turn concur for a better water status in 700-plants, allowing them to keep stomata open for longer upon increasing drought severity, thus likely improving their leaf gas exchange.

Leaf transpiration depends on several factors, like temperature, air humidity, air turbulence and boundary layer resistance (Rawson *et al.*, 1977; Collatz *et al.*, 1991; Bunce, 1997). This complexity makes transpiration an extremely dynamic process. Interestingly, under well-watered conditions the 400- and 700-plants displayed different *T* despite showing the same maximum $g_s$. This apparent conflicting result could arise, *a priori,* from the varying approaches to measure $g_s$ (instantaneous measurements that were performed when $g_s$ peaks, at constant air flux and turbulence, irradiance and VPD in the chamber of the gas analyzer) and *T* (a long-term measurement that computes all environmental oscillations). Nevertheless, we suggest that the uncoupling between $g_s$ and *T* in coffee plants under elevated [$CO_2$], as here reported for the first time, should have rather been related to stomatal responses to VPD. Interestingly, in well-watered conditions the 700-plants displayed a faster stomata closure upon rapid increases in VPD when compared to 400-plants. This phenotype was lost when

the 700-plants were submitted to a VPD transition at 400 ppm and behaved similarly as their 400-counterparts.

Given that the PiP2;1 aquaporin is involved in a $CO_2$-dependent stomatal closure (Maurel *et al.*, 2016) and it was up-regulated under elevated [$CO_2$], it is tempting to suggest that the faster stomatal closure in 700-plants might be at least partially associated with increased activity of PiP2;1. This would lead to an easier and faster entrance of $CO_2$ into the guard cells at elevated [$CO_2$] conditions, and thus triggering a faster stomatal response. Additionally, PiP2;1 role in stomatal closure also requires an ABA-dependent activation of OST1 which could explain why in constant VPD no decrease in ABA was found in 700-plants (Grondin *et al.*, 2015). Other possibilities affecting this response, as changes in leaf ABA content and increased stomatal density or decreases in stomatal size, could be ruled out given that no alterations in stomatal anatomy or sensitivity to VPD transitions, as well as leaf ABA pools, were found. Altogether, our results suggest that plants acclimated to elevated [$CO_2$] are somehow primed to a [$CO_2$]-dependent response that leads to a faster stomatal closure to rising VPD. This should contribute to decrease leaf transpiration with increasing air evaporative demand, which may ultimately concur to postpone drought stress development.

In conclusion, well-watered 700-plants displayed lower whole-plant transpiration rates than their 400-counterparts. This was not associated with maximum $g_s$ *per se* or with foliar ABA levels, but rather with an increased stomatal closure rate upon VPD transitions, which occur innumerous times over the course of the day. In addition, drought-stressed 700-plants delayed tissue dehydration and were able to keep higher $K_{plant}$ for most of the period of drought imposition, while transpired more than 400-plants. Evidence is shown that aquaporins may play a major role in these processes. Altogether, our results suggest that enhanced [$CO_2$] has marked implications on how coffee plants respond to drought, permitting the 700-plants to have an improved growth under drought when compared to 400-plants. Finally, our novel results pointed that rising [$CO_2$] can partially mitigate the negative impacts of drought on coffee, as had already been noted on the mitigating effects of enhanced [$CO_2$] on heat stress (Martins *et al.*, 2016; Rodrigues *et al.*, 2016). Therefore, rises in [$CO_2$] are expected to

play key roles to help the sustainability of coffee production in a scenario of global climate change.

**Acknowledgements**

Postdoctoral (AAC) and research (FMD) fellowships granted respectively by Brazilian Federal Agency for Support and Evaluation of Graduate, Brazil (CAPES, Finance Code 001) and by National Council for Scientific and Technological Development, Brazil (CNPq, Grant 308652/2014-2) are acknowledged. We also thank scholarships to undergraduate and graduate students by these agencies and by the Foundation for Research Assistance of Minas Gerais State, Brazil (FAPEMIG). Finally, we thank Núcleo de Análises de Biomoléculas (NUBIOMOL) for providing the facilities to perform the ABA analyses, and Fundação para a Ciência e a Tecnologia for supporting JDCR (UID/04129/2020, LEAF and UIDP/04035/2020, GeoBioTec).

**Author's contributions**

RTA, conception and design, execution of experiments, data analyses and interpretation, writing; AAC, data analyses and interpretation, writing; WLA, execution of experiments; LCC, execution of experiments, data analyses and interpretation; KLGM, execution of experiments; MLB, execution of experiments; RPBS, execution of experiments; LAO, execution of experiments; DSB, execution of experiments; SCVM, conception and design, data analyses and interpretation; JDCR, conception and design, data analyses and interpretation, writing; FMD, conception and design, data analyses and interpretation, project administration, funding acquisition, writing.

**References**

**Ainsworth EA, Long SP**. **2005**. What have we learned from 15 years of free-air $CO_2$ enrichment (FACE)? A meta-analytic review of the responses of photosynthesis, canopy properties and plant production to rising $CO_2$. *New Phytologist* **165**: 351–372.

**Alexandersson E, Fraysse L, Sjövall-Larsen S, Gustavsson S, Fellert M, Karlsson M, Johanson U, Kjellbom P**. **2005**. Whole gene family expression and drought stress regulation of aquaporins. *Plant Molecular Biology* **59**: 469–484.

**Antunes WC, Pompelli MF, Carretero DM, DaMatta FM**. **2008**. Allometric models for non-destructive leaf area estimation in coffee (*Coffea arabica* and *Coffea canephora*). *Annals of Applied Biology* **153**: 33–40.

**Batista KD, Araújo WL, Antunes WC, Cavatte PC, Moraes GABK, Martins SCV, DaMatta FM**. **2012**. Photosynthetic limitations in coffee plants are chiefly governed by diffusive factors. *Trees - Structure and Function* **26**: 459–468.

**Brodribb TJ, McAdam SAM. 2013.** Unique responsiveness of angiosperm stomata to elevated $CO_2$ explained by calcium signalling. *PloS one* **8**: 11.

**Bunce JA**. **1997**. Does transpiration control stomatal responses to water vapour pressure deficit? *Plant, Cell and Environment* **20**: 131–135.

**Cavatte PC, Oliveira ÁAG, Morais LE, Martins SC V, Sanglard LMVP, DaMatta FM**. **2012**. Could shading reduce the negative impacts of drought on coffee? A morphophysiological analysis. *Physiologia Plantarum* **144**: 111–122.

**Cardoso AA, Brodribb TJ, Lucani CJ, DaMatta FM, McAdam SAM. 2018.** Coordinated plasticity maintains hydraulic safety in sunflower leaves. *Plant, Cell and Environment* **41** 2567–2576.

**Cavender-Bares J, Sack L, Savage J. 2007.** Atmospheric and soil drought reduce nocturnal transpiration in live oaks. *Tree Physiology* 27: 611–620.

**Collatz GJ, Ball JT, Grivet C, Berry JA**. **1991**. Physiological and environmental regulation of stomatal conductance, photosynthesis and transpiration: a model that includes a laminar boundary layer. *Agricultural and Forest Meteorology* **54**: 107–136.

**Creek D, Lamarque LJ, Torres-Ruiz JM, Parise C, Burlett R, Tissue DT, Delzon S. 2020.** Xylem embolism in leaves does not occur with open stomata: evidence from direct observations using the optical visualization technique. *Journal of Experimental Botany* **71**: 1151–1159.

**DaMatta FM, Godoy AG, Menezes-Silva PE, Martins SC V, Sanglard LMVP, Morais LE, Torre-Neto A, Ghini R**. **2016**. Sustained enhancement of photosynthesis in coffee trees grown under free-air $CO_2$ enrichment conditions: disentangling the contributions of stomatal, mesophyll, and biochemical limitations. *Journal of Experimental Botany* **67**: 341–352.

**Engineer CB, Hashimoto-Sugimoto M, Negi J, Israelsson-Nordström M, Azoulay-Shemer T, Rappel WJ, Iba K, Schroeder JI**. **2016**. $CO_2$ sensing and $CO_2$ regulation of stomatal conductance: advances and open questions. *Trends in Plant Science* **21**: 16–30.

**Gascò A, Nardini A, Salleo S**. **2004**. Resistance to water flow through leaves of *Coffea arabica* is dominated by extra-vascular tissues. *Functional Plant Biology* **31**: 1161–1168.

**Ghini R, Torre-Neto A, Dentzien AFM, Guerreiro-Filho O, Iost R, Patrício FRA, Prado JSM, Thomaziello RA, Bettiol W, DaMatta FM**. **2015**. Coffee growth, pest and yield responses to free-air $CO_2$ enrichment. *Climatic Change* **132**: 307–320.

**Grondin A, Rodrigues O, Verdoucq L, Merlot S, Leonhardt N, Maurel C**. **2015**. Aquaporins contribute to ABA-triggered stomatal closure through OST1-mediated phosphorylation. *Plant Cell* **27**: 1945–1954.

**Grossiord C, Buckley TN, Cernusak LA, Novick KA, Poulter B, Siegwolf RT, Sperry JS, McDowell NG**. 2020. Plant responses to rising vapor pressure deficit. *New Phytologist* in press.

**Hachez C, Veselov D, Ye Q, Reinhardt H, Knipfer T, Fricke W, Chaumont F**. **2012**. Short-term control of maize cell and root water permeability through plasma membrane aquaporin isoforms. *Plant, Cell and Environment* **35**: 185–198.

**Hao GY, Holbrook NM, Zwieniecki MA, Gutschick VP, BassiriRad H**. **2018**. Coordinated responses of plant hydraulic architecture with the reduction of stomatal conductance under elevated $CO_2$ concentration. *Tree Physiology* **38**: 1041–1052.

**IPCC. 2014.** Proceedings of the 5th Assessment Report, WGII, Climate Change 2014: Impacts, Adaptation, and Vulnerability; Cambridge University Press, Cambridge, U.K.

**Keenan TF, Hollinger DY, Bohrer G, Dragoni D, Munger JW, Schmid HP, Richardson AD**. **2013**. Increase in forest water-use efficiency as atmospheric

carbon dioxide concentrations rise. *Nature* **499**: 324–327.

**Livak KJ, Schmittgen TD**. **2001**. Analysis of relative gene expression data using real-Time quantitative PCR and the 2−ΔΔCT method. *Methods* **25**: 402–408.

**Lopez F, Bousser A, Sissoëff I, Gaspar M, Lachaise B, Hoarau J, Mahé A**. **2003**. Diurnal regulation of water transport and aquaporin gene expression in maize roots: contribution of PIP2 proteins. *Plant and Cell Physiology* **44**: 1384–1395.

**Martin-StPaul N, Delzon S, Cochard H. 2017.** Plant resistance to drought depends on timely stomatal closure. *Ecology Letters* **20**:1437–1447.

**Martins MQ, Fortunato AS, Rodrigues WP, Partelli FL, Campostrini E, Lidon FC, DaMatta FM, Ramalho JC, Ribeiro-Barros AI**. **2017**. Selection and validation of reference genes for accurate RT-qPCR data normalization in *Coffea spp.* under a climate changes context of interacting elevated [$CO_2$] and temperature. *Frontiers in Plant Science* **8**: 307.

**Martins SCV, Sanglard ML, Morais LE, Menezes-Silva PE, Mauri R, Avila RT, Vital CE, Cardoso AA, DaMatta FM**. **2019**. How do coffee trees deal with severe natural droughts? An analysis of hydraulic, diffusive and biochemical components at the leaf level. *Trees - Structure and Function* **33**: 1679–1693.

**Maurel C, Boursiac Y, Luu DT, Santoni V, Shahzad Z, Verdoucq L**. **2015**. Aquaporins in plants. *Physiological Reviews* **95**: 1321–1358.

**Maurel C, Verdoucq L, Rodrigues O**. **2016**. Aquaporins and plant transpiration. *Plant, Cell and Environment* **39**: 2580–2587.

**McAdam SAM, Brodribb TJ**. **2014**. Separating active and passive influences on stomatal control of transpiration. *Plant Physiology* **164**: 1578–1586.

**McAdam SAM, Brodribb TJ**. **2015**. The evolution of mechanisms driving the stomatal response to vapor pressure deficit. *Plant Physiology* **167**: 833–843.

**McAdam SAM, Sussmilch FC, Brodribb TJ**. **2016**. Stomatal responses to vapour pressure deficit are regulated by high speed gene expression in angiosperms. *Plant, Cell and Environment* **39**: 485–491.

**Menezes-Silva PE, Cavatte PC, Martins SC V, Reis J V., Pereira LF, Ávila RT, Almeida AL, Ventrella MC, DaMatta FM**. **2015**. Wood density, but not leaf hydraulic architecture, is associated with drought tolerance in clones of *Coffea canephora*. *Trees - Structure and Function* **29**: 1687–1697.

**Menezes-Silva PE, Sanglard LMVP, Ávila RT, Morais LE, Martins SCV,**

**Nobres P, Patreze CM, Ferreira MA, Araújo WL, Fernie AR, *et al.* 2017**. Photosynthetic and metabolic acclimation to repeated drought events play key roles in drought tolerance in coffee. *Journal of Experimental Botany* **68**: 4309–4322.

**Miniussi M, Del Terra L, Savi T, Pallavicini A, Nardini A**. **2015**. Aquaporins in *Coffea arabica* L.: identification, expression, and impacts on plant water relations and hydraulics. *Plant Physiology and Biochemistry* **95**: 92–102.

**Nardini A, Salleo S.2000.** Limitation of stomatal conductance by hydraulic traits: Sensing or preventing xylem cavitation? *Trees - Structure and Function* **15**: 14–24

**Oren R, Sperry JS, Katul GG, Pataki DE, Ewers BE, Phillips N, Schäfer KVR**. **1999**. Survey and synthesis of intra- and interspecific variation in stomatal sensitivity to vapour pressure defict. *Plant, Cell and Environment* **22**: 1515–1526.

**Parent B, Hachez C, Redondo E, Simonneau T, Chaumont F, Tardieu F**. **2009**. Drought and abscisic acid effects on aquaporin content translate into changes in hydraulic conductivity and leaf growth rate: a trans-scale approach. *Plant Physiology* **149**: 2000–2012.

**Prentice I, Farquhar G, Fasham M**. **2001**. The carbon cycle and atmospheric carbon dioxide. *Climate Change 2001: The Scientific Basis*: 183–237.

**Ramalho JC, Rodrigues AP, Semedo JN, Pais IP, Martins LD, Simões-Costa MC, Leitão AE, Fortunato AS, Batista-Santos P, Palos IM, *et al.* 2013**. Sustained photosynthetic performance of *Coffea* spp. under long-term enhanced [$CO_2$]. *PLoS One* **8**: 1–19.

**Ramalho JC, Rodrigues AP, Lidon FC, Marques LMC, Leitão AE, Fortunato AS, *et al*.** 2018. Stress cross-response of the antioxidative system promoted by superimposed drought and cold conditions in *Coffea* spp. *PLoS One* **2018**: 13(6).

**Rawson HM, Begg JE, Woodward RG**. **1977**. The effect of atmospheric humidity on photosynthesis, transpiration and water use efficiency of leaves of several plant species. *Planta* **134**: 5–10.

**Rodrigues WP, Martins MQ, Fortunato AS, Rodrigues AP, Semedo JN, Simões-Costa MC, Pais IP, Leitão AE, Colwell F, Goulao L, *et al.* 2016**. Long-term elevated air [$CO_2$] strengthens photosynthetic functioning and mitigates the impact of supra-optimal temperatures in tropical *Coffea arabica* and *C. canephora* species. *Global Change Biology* **22**: 415–431.

**Tausend PC, Goldstein G, Meinzer FC**. **2000**. Water utilization, plant hydraulic properties and xylem vulnerability in three contrasting coffee (*Coffea arabica*) cultivars. *Tree Physiology* **20**: 159–168.

**Wang Z, Li J, Lai C, Wang RY, Chen X, Lian Y. 2018.** Drying tendency dominating the global grain production area. *Global Food Security* **16**: 138–149.

**Woodward FI. 1987.** Stomatal numbers are sensitive to increases in $CO_2$ from pre-industrial levels. *Nature* **327**: 617–618.

**Xu Z, Jiang Y, Jia B, Zhou G**. **2016**. Elevated-$CO_2$ response of stomata and its dependence on environmental factors. *Frontiers in Plant Science* **7**: 1–15.

**Tables and figures**

**Table 1.** The effect of watering (well-watered or drought-stressed plants) and $CO_2$ supply (400 or 700 ppm) on the water potential at predawn ($\Psi_{pd}$) and midday ($\Psi_{md}$). For drought-stressed plants, measurements were made at 50, 37.5, 25 and 20% soil field capacity (FC). Different lowercase letters indicate differences between watering regimes within the same $CO_2$ supply; different capital letters indicate differences between $CO_2$ treatments within the same watering regime (Student *t*-test, α= 0.05; *n*= 6 ± SE).

| $\Psi_{pd}$ (MPa) | | | | | | | | | | | | |
|---|---|---|---|---|---|---|---|---|---|---|---|---|
| | 400 ppm | | | | | | 700 ppm | | | | | |
| FC (%) | Well-Watered | | | Drought | | | Well-Watered | | | Drought | | |
| 50 | -0.19 | ± 0.02 | Aa | -0.27 | ± 0.03 | Aa | -0.24 | ± 0.02 | Aa | -0.24 | ± 0.02 | Aa |
| 37.5 | -0.23 | ± 0.02 | Aa | -0.32 | ± 0.03 | Aa | -0.28 | ± 0.03 | Aa | -0.28 | ± 0.02 | Aa |
| 25 | -0.22 | ± 0.03 | Aa | -0.39 | ± 0.05 | Ab | -0.24 | ± 0.02 | Aa | -0.26 | ± 0.03 | Aa |
| 20 | -0.23 | ± 0.02 | Aa | -0.52 | ± 0.03 | Bb | -0.24 | ± 0.03 | Aa | -0.41 | ± 0.03 | Ab |
| $\Psi_{md}$ (MPa) | | | | | | | | | | | | |
| FC (%) | Well-Watered | | | Drought | | | Well-Watered | | | Drought | | |
| 50 | -0.51 | ± 0.01 | Aa | -0.73 | ± 0.06 | Aa | -0.68 | ± 0.08 | Aa | -0.58 | ± 0.06 | Aa |
| 37.5 | -0.60 | ± 0.02 | Aa | -0.87 | ± 0.07 | Aa | -0.77 | ± 0.08 | Aa | -0.66 | ± 0.06 | Aa |
| 25 | -0.59 | ± 0.04 | Aa | -1.25 | ± 0.11 | Ab | -0.71 | ± 0.13 | Aa | -0.92 | ± 0.17 | Aa |
| 20 | -0.73 | ± 0.06 | Aa | -1.45 | ± 0.04 | Ab | -0.78 | ± 0.10 | Aa | -1.46 | ± 0.06 | Ab |

**Table S1.** The effect of watering (well-watered or drought-stressed plants at 20% of soil field capacity) and $CO_2$ supply (400 or 700 ppm) on the vein density (VD, mm $mm^{-2}$), stomatal density (SD, $mm^{-2}$), stomatal index (SI) and stomatal polar diameter (DP, μm). Different lowercase letters indicate differences between water regimes within the same $CO_2$ supply; different capital letters indicate differences between $CO_2$ supply within each watering (Student *t*-test, α= 0.05; *n*= 6 ± SE).

| | 400 ppm | | | | 700 ppm | | | |
|---|---|---|---|---|---|---|---|---|
| | Well-Watered | | Drought | | Well-Watered | | Drought | |
| VD | 9.2 ± 0.3 | Aa | 9.6 ± 0.4 | Aa | 9.1 ± 0.3 | Aa | 9.4 ± 0.2 | Aa |
| SD | 177 ± 6 | Aa | 159 ± 8 | Aa | 166 ± 5 | Aa | 153 ± 4 | Aa |
| SI | 13.5 ± 0.2 | Aa | 12.70 ± 0.7 | Aa | 13.10 ± 0.60 | Aa | 12.2 ± 0.3 | Aa |
| DP | 27.1 ± 0.5 | Aa | 27.2 ± 0.4 | Aa | 27.2 ± 0.5 | Aa | 27.7 ± 0.3 | Aa |

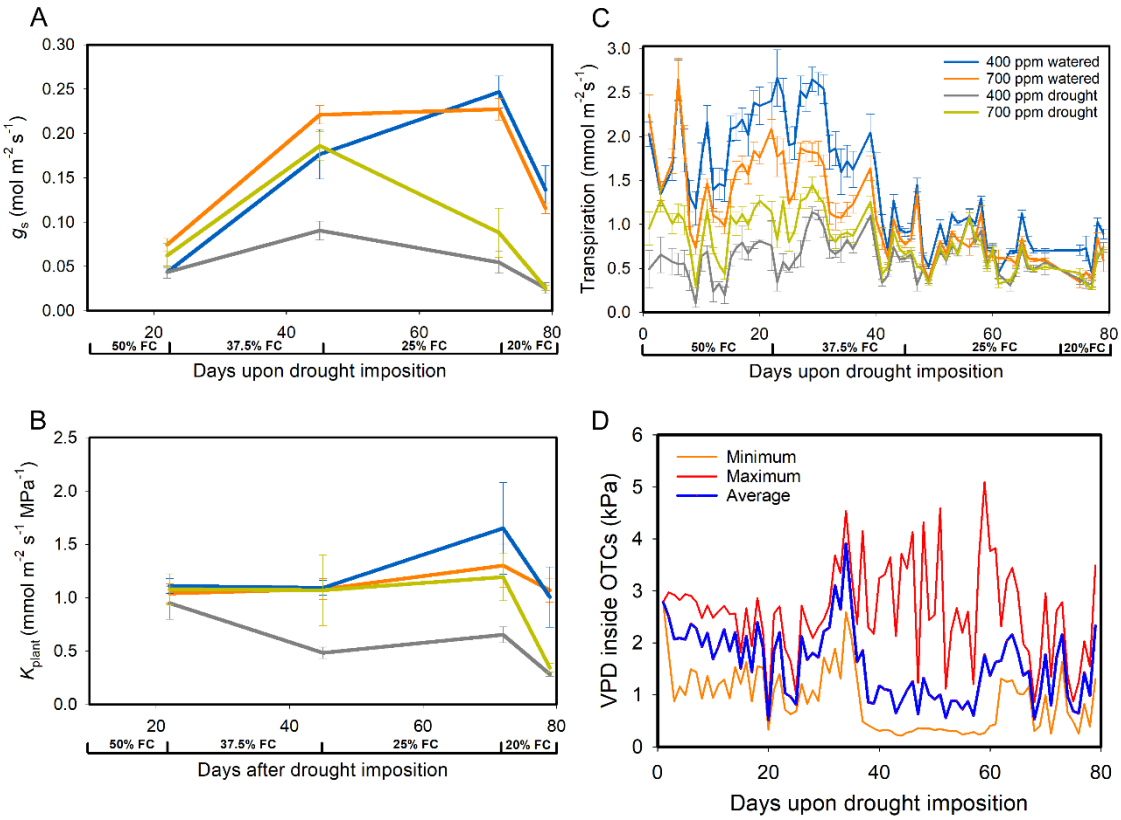


**Figure 1.** The effect of watering (well-watered or drought-stressed plants) and $CO_2$ supply (400 or 700 ppm) on the (A) stomatal conductance ($g_s$), (B) plant hydraulic conductance, and (C) whole-plant transpiration of coffee plants. For drought-stressed plants, measurements were made at 50, 37.5, 25 and 20% soil field capacity. *n*= 6 ± SE. (D) Minimum, mean and maximum values of vapor pressure deficit (VPD) inside the open top chamber are also presented.

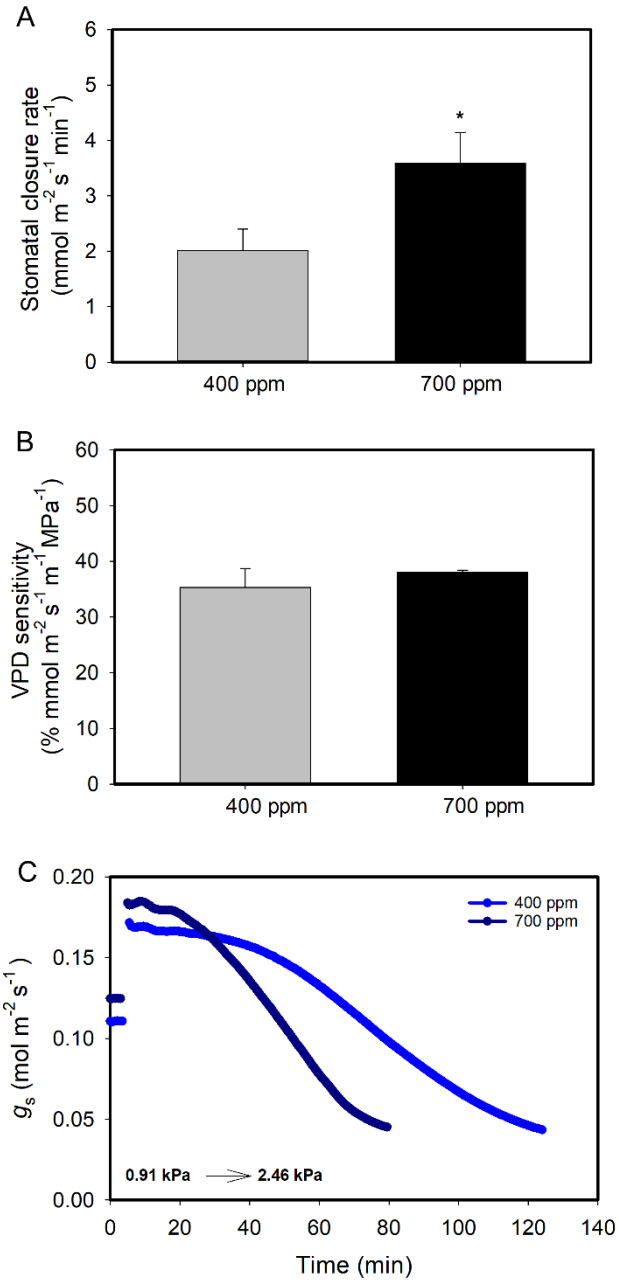


**Figure 2.** The effect of $CO_2$ supply (400 or 700 ppm) on the stomatal closure rate (A) and stomatal sensitivity to vapor pressure deficit (VPD) (B) in well-watered coffee plants. One replicate of each 400- (light blue) and 700-plants (dark blue) with similar initial stomatal conductances ($g_s$) is presented to demonstrate the differential stomatal closure rate following a step increase in VPD (C). Full data, including the reverse VPD transitions, are presented in Fig. S2 and Fig. S3. Asterisks (*) denote statistical significance between $CO_2$ treatments (Student *t-test*, α= 0.05; *n* = 4 ± SE).

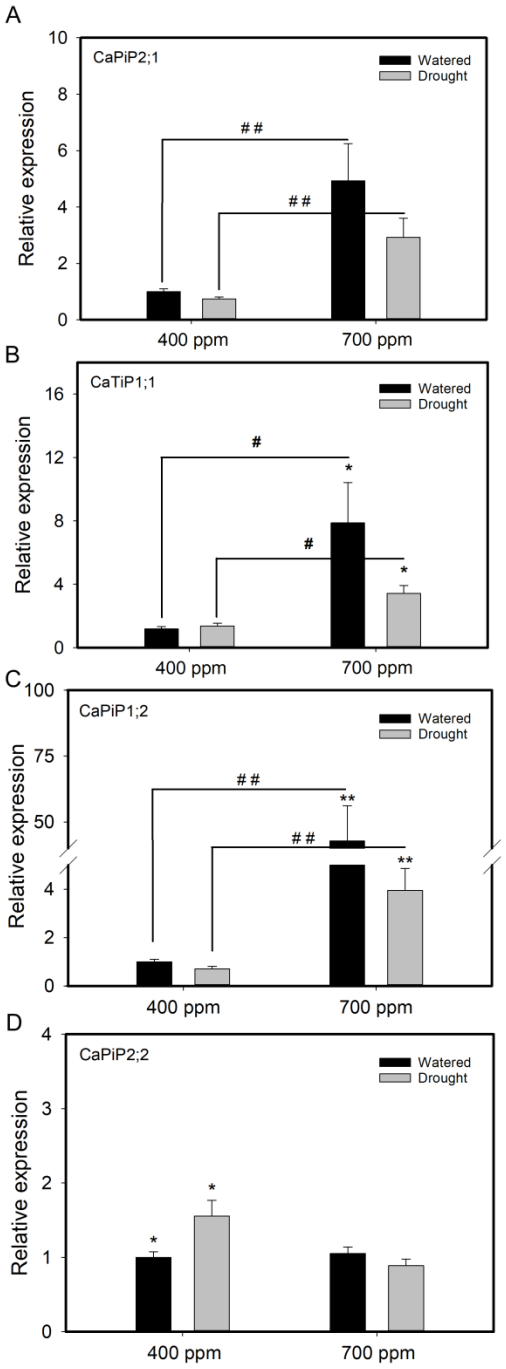


**Figure 3.** The effect of watering (well-watered or drought-stressed plants) and $CO_2$ supply (400 or 700 ppm) on the relative expression of aquaporins *CaPiP2;1* (A), *CaTiP1;1* (B), *CaPiP1;2* (C), and *CaPiP2;2* (D) in coffee leaves. For drought-stressed plants, measurements were made at 25 or 20% field capacity (three biological replicates). Asterisks (*, α= 0.05; **, α= 0.01) indicate differences between watering regimes within a same $CO_2$ supply; hashtags (#, α= 0.05; ##, α= 0.01) indicate differences between $CO_2$ treatments within a same watering regime (Student *t*-test).

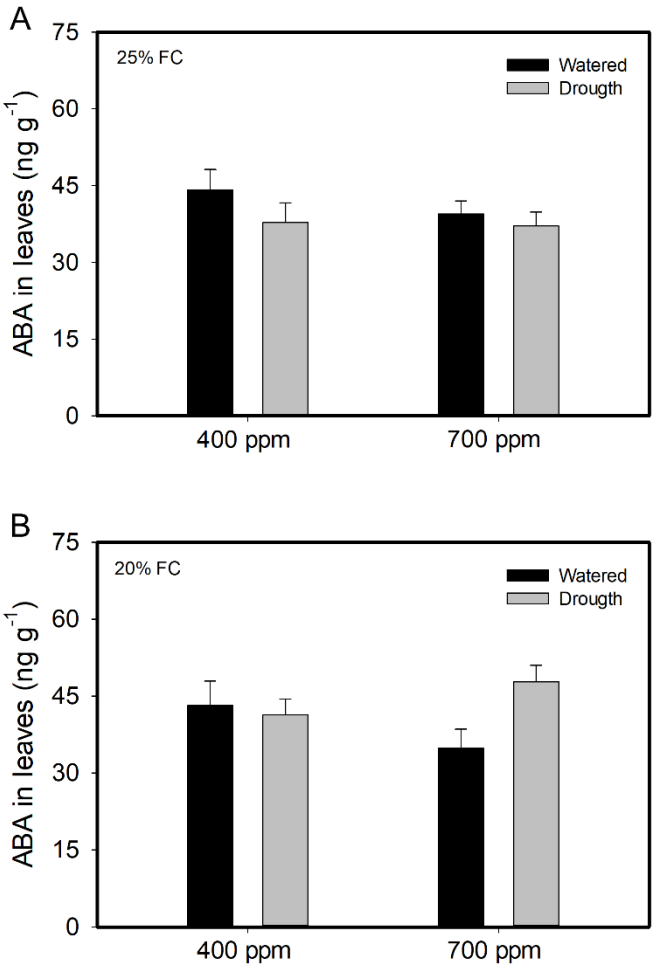


**Figure S1.** The effect of watering (well-watered or drought-stressed plants) and $CO_2$ supply (400 or 700 ppm) on foliar ABA levels on a dry weight basis. Data for drought-stressed plants at 25 (A) or 20% (B) soil field capacity (FC) are demonstrated (Student *t-test,* α= 0.05; *n*= 4 ± SE).

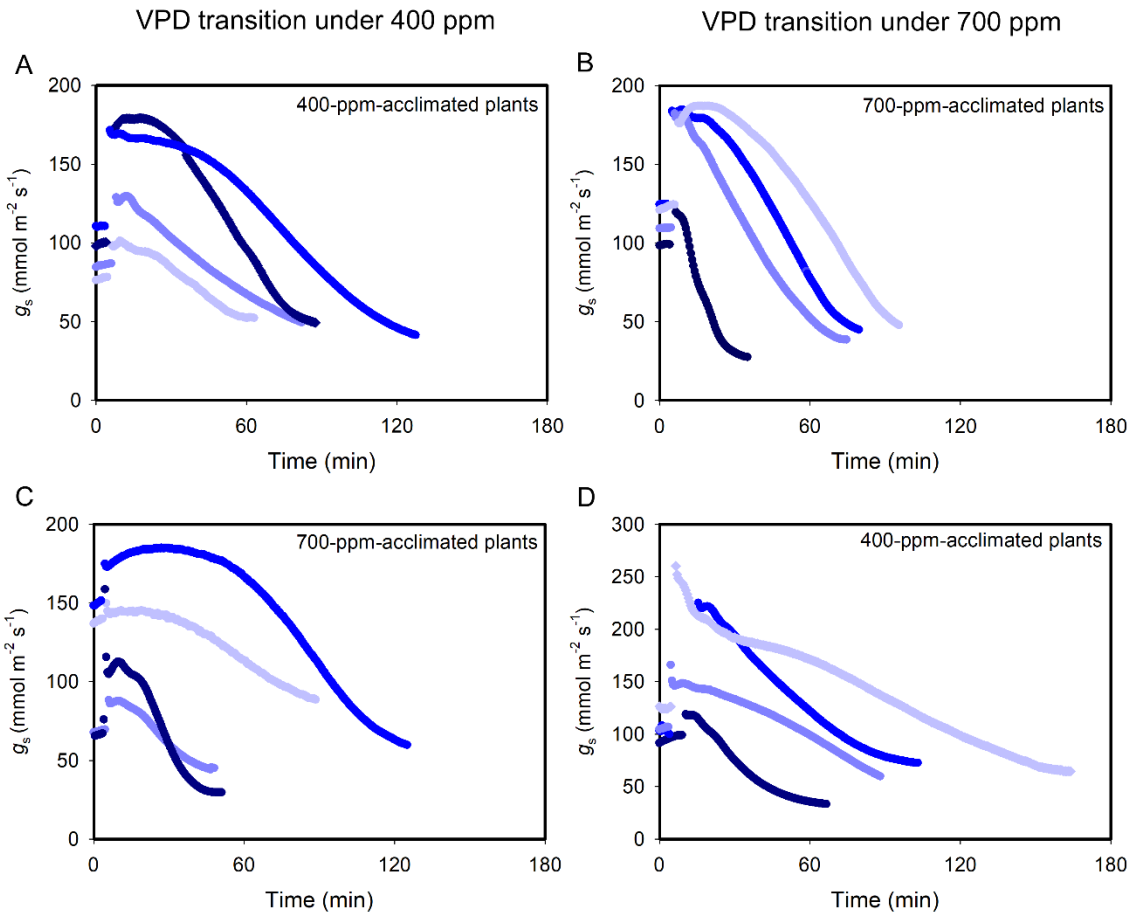


**Figure S2.** Full data of vapor pressure deficit (VPD) transition curves under 400 or 700 ppm [$CO_2$] of coffee plants acclimated to 400 or 700 ppm [$CO_2$]. Blue gradient, from darker to lighter color shades, highlights the gradient of inclination at the linear phase of stomatal closure. The lighter the blue, the slower stomatal response. Each curve represents one leaf.

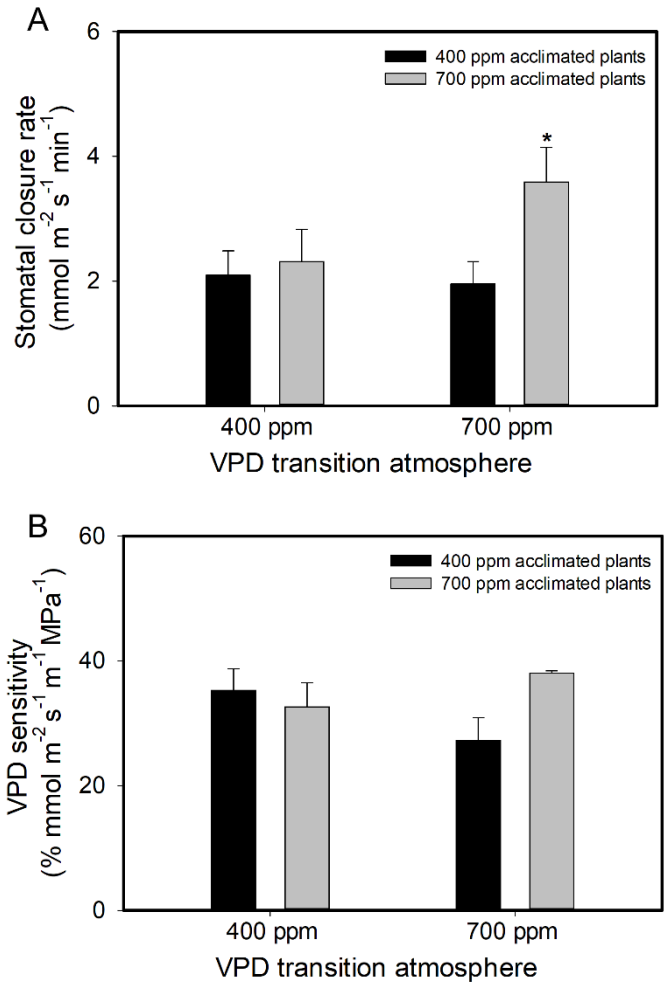


**Figure S3.** Stomatal closure rate (A) and vapor pressure deficit (VPD) sensitivity (B) of well-watered coffee plants acclimated to 400 or 700 ppm of $CO_2$ (grey and black bars, respectively) and submitted to a VPD transition at 400 or 700 ppm of $CO_2$. Asterisks (*) denote significance between treatments within and between each [$CO_2$] acclimation (Student *t-test,* α= 0.05; *n*= 4 ± SE).

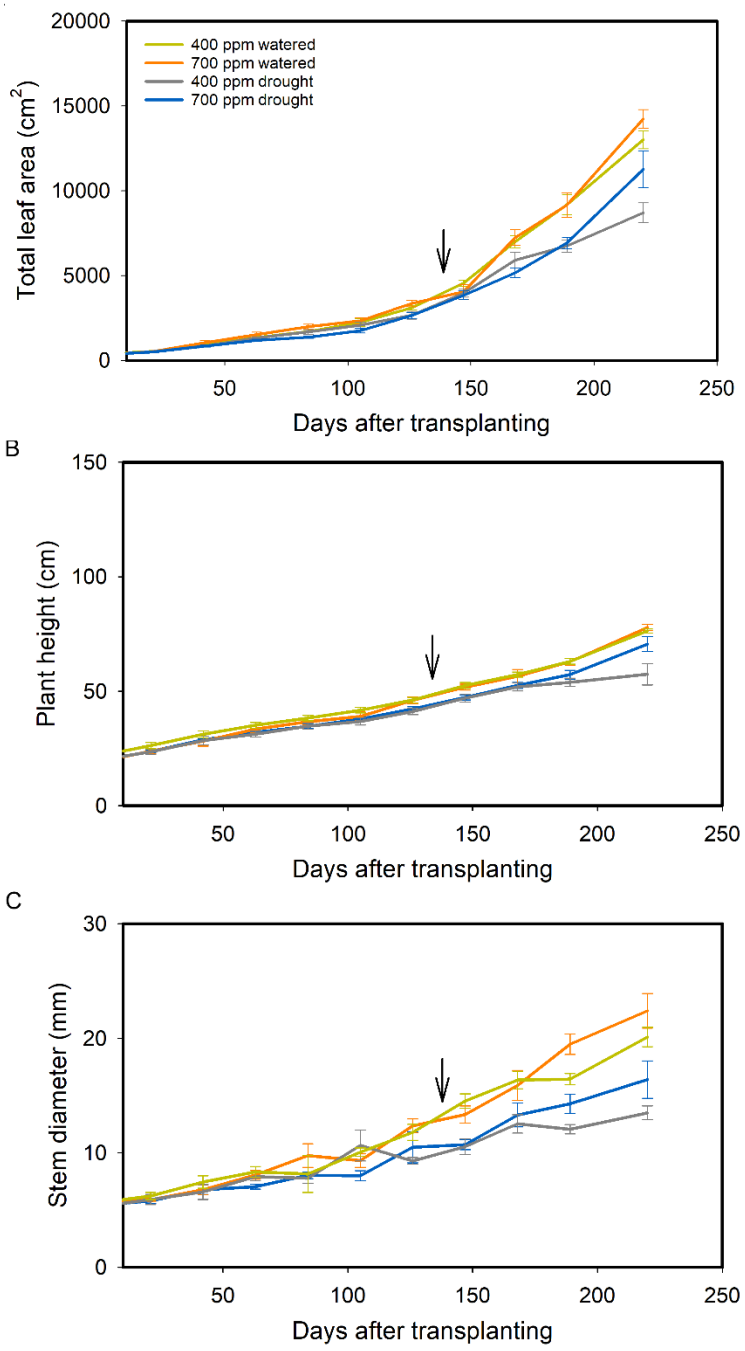


**Figure S4.** The effect of watering (well-watered or drought-stressed plants) and $CO_2$ supply (400 or 700 ppm) on the total leaf area (A), plant height (B) and stem diameter of at the soil level (C) of coffee plants over the course of the experiment. The black arrows indicate the beginning of drought imposition. *n*= 6 ± SE.

# CHAPTER 2

## Elevated air [$CO_2$] improves photosynthetic performance and alters biomass accumulation and partitioning in drought-stressed coffee plants

**Abstract**

Coffee (*Coffea arabica* L.) is an important global commodity grown in tropical areas where increased drought severity and frequency are believed to become progressively important due to climate changes. Nonetheless, rising air [$CO_2$] is thought to be able to mitigate heat and drought stresses. In this study, we tested how carbon assimilation and use are affected by elevated [$CO_2$] in combination with a progressive drought, and how this could impact shifts on biomass accumulation and partitioning. For that, we cultivated coffee plants in open top chambers under greenhouse conditions. Plants grown in 12-L pots were then submitted to ambient (386 ± 20 ppm) or elevated (723 ± 83 ppm) [$CO_2$] during approximately seven months, as well as to varying soil water availabilities (100, 50, 37.5, 25 or 20% of soil field capacity). Our results demonstrate that elevated [$CO_2$] improved carbon assimilation rates (>60%) with unaltered stomatal conductance and no signs of photosynthetic downregulation. This was accompanied by increases in water-use efficiency, respiration rates and biomass accumulation regardless of watering, and decreased photorespiration rates and oxidative pressure under drought. Improved growth under enhanced [$CO_2$] was more evident under drought than under full irrigation, and was unlikely to have been associated with global changes on hormonal pools, but rather with shifts on carbon fluxes. Finally, elevated [$CO_2$] promoted key allometric adjustments linked to drought tolerance, *e.g.*, more biomass partitioning towards roots with deeper roots. Collectively, our results offer novel and timely information on the mitigating ability of rising air [$CO_2$] on the photosynthetic performance and growth of coffee plants under drought conditions.

**Key words:** Allometric adjustments, drought stress, growth regulators, rising [$CO_2$], water-use efficiency.

**Abbreviations**

$A$, net $CO_2$ assimilation rate; ABA, abscisic acid; $C_i$, internal $CO_2$ concentration; $C_c$, chloroplastic $CO_2$ concentration; $F_m$, maximum fluorescence; $F_{m'}$, light-adapted maximum fluorescence; $F_s$, steady-state fluorescence yield; $F_v/F_m$, variable-to-maximum fluorescence ratio; $F_0$ , minimum fluorescence; ETR,

electron transport rate; FC, field capacity; $g_s$, stomatal conductance; LDM, leaf dry mass; LMR, leaf mass ratio; NPQ, coefficient for nonphotochemical quenching; OTCs, open top chambers; PPFD, photosynthetic photon flux density; PS, photosystem; $q_p$ , coefficient for photochemical quenching; $R_d$, daytime respiration; RDM, root dry mass; RMR, root mass ratio; $R_n$; nocturnal respiration; $R_p$, photorespiration; $R_p/A_{gross}$, photorespiration-to-gross photosynthesis ratio; RuBisCO, ribulose-1,5-bisphosphate carboxylase/oxygenase; RuBP, ribulose-1,5-bisphosphate; SDM, shoot dry mass; SMR, shoot mass ratio; TDM, total dry mass; TLA, total leaf area; TSS, total soluble sugars; $V_{cmax}$, maximum apparent carboxylation capacity; WUE, water-use efficiency; $\Psi_{pd}$, predawn water potential; $\Phi_{PSII}$, quantum yield of PSII non-cyclic electron transport

## Introduction

Ongoing and future predicted global climate changes have been mostly associated with increases in both atmospheric $CO_2$ concentration ($[CO_2]$) and air temperature, in addition to alterations in precipitation patterns. In terms of geological or evolutionary scales, these changes have occurred rapidly from the industrial revolution period onwards (IPCC, 2014), and are already impairing both natural and agricultural ecosystems. Therefore, plants are expected to face abiotic stresses, such as supra-optimal temperatures and limited water availability, to a greater extent than in the ambient where they naturally evolved. Nonetheless, elevated $[CO_2]$ is believed to potentially mitigate theses stressful factors (AbdElgawad et al., 2016; Rodrigues et al., 2016).

Elevated $[CO_2]$ often diminishes leaf stomatal aperture and stomatal density, thus leading to reductions in stomatal conductance ($g_s$) across many herbs and woody species (Woodward, 1987; Ainsworth and Rogers, 2007). Despite these reductions, net photosynthesis rates ($A$) are improved, which has been associated with an enhanced carboxylase activity of ribulose-1,5-bisphosphate carboxylase/oxygenase (RuBisCO) paralleling decreases in its oxygenase activity, thus ultimately reducing the photorespiration flux and reactive oxygen species (ROS) production (Ainsworth and Rogers, 2007; Leakey et al., 2009). As a consequence of the increased $A$, elevated $[CO_2]$ can potentially increase the net primary productivity of vegetation (Kimball, 1983; Norby et al., 2005) by providing additional carbon (fertilization effect). In parallel, a number of studies have demonstrated that enhanced $[CO_2]$ often stimulates plant growth by improving plant development processes such as cell division and elongation (Masle, 2000; Yong et al., 2000; Ferris et al., 2001; Lindroth et al., 2002; Taylor et al., 2003; Ribeiro et al., 2012). These processes are usually regulated by plant hormones, including auxins, gibberellins, cytokinins, abscisic acid (ABA) and polyamines (Galston and Sawhney, 1990; Yong et al., 2000; Lindroth et al., 2002; Masson et al., 2017), whose signaling are usually intimately related to carbon metabolism (Thompson et al., 2017). Taking all of the above information together, it is expected that $[CO_2]$-triggered alterations on hormonal pools and carbon fluxes could improve plant growth and crop sustainability in a scenario of global climate changes.

Plant acclimation to drought events essentially involves a number of adjustments at varying levels. Stomatal closure, for instance, is one of the first mechanisms displayed by plants during drought to reduce excessive water loss and prevent them from rapidly reaching critical water potentials (Brodribb and McAdam, 2017; Cardoso et al., 2018). Plants can also acclimate to drought stress via morphological and anatomical changes, *e.g.* producing thicker and smaller leaves with thicker cuticles favoring cooling while minimizing water losses (Nicotra et al., 2011; Duursma et al., 2019). In addition, plants can acclimate to drought via increasing assimilate partitioning towards the root system. Plants can therefore modify the shoot-to-root ratio by growing not just deeper roots but also roots that are better able to acquire water, thus ultimately avoiding drought stress (Pinheiro et al., 2005). This process relies on a considerable amount of energy, and an elevated air [$CO_2$] can provide an increasing assimilate availability due to higher *A* to support these shifts in growth and biomass allocation.

Coffee (*Coffea arabica* L. and *C. canephora* Pierre), one of the most important commodities worldwide, is grown in tropical areas where drought episodes are the main bottleneck affecting crop yields (DaMatta et al., 2010). Indeed, modelling studies have estimated dramatic effects on the coffee crop due to climate changes causing extensive reductions of suitable areas in most coffee producing countries ( DaMatta et al., 2018). Decreases in crop yield (Bunn et al., 2015; Craparo et al., 2015; Ovalle-Rivera et al., 2015), possible extinction of wild populations of *C. arabica* (Davis et al., 2019), greater pest incidence (Magrach and Ghazoul, 2015), and increased agricultural, social and economic vulnerabilities have been foreseen. However, most of these works were chiefly focused on the increasing air temperatures and/or altered precipitation patterns without considering the potential mitigating effects of $CO_2$ fertilization (DaMatta et al., 2018; DaMatta et al., 2019). Studies on the effects of elevated [$CO_2$] in *C. arabica* and *C. canephora* have found an increase of 34-49% in *A* coupled with unchanged $g_s$ (Ramalho et al., 2013). Such results obtained in plants cultivated in growth chambers are in line with field results obtained in free air $CO_2$ enrichment (FACE) system, with reports of an absence of photosynthetic downregulation after several years of $CO_2$ fertilization (Ghini et al., 2015; DaMatta et al., 2016; Rakočević et al., 2018) and increased coffee bean yields (DaMatta et al., 2019). Also important, a growing body of evidence suggests that elevated

air [$CO_2$] plays a crucial role in the coffee plant ability to acclimate to abiotic stresses such as supra-optimal temperatures. At 42/34°C (day/night), plants under enhanced [$CO_2$] displayed higher *A* (205-495%) than their counterparts submitted to ambient [$CO_2$] (Rodrigues et al., 2016), a fact that was accompanied by diminished excitation pressure, and strengthened photochemical efficiency and biochemical functioning (Martins et al., 2016; Rodrigues et al., 2016; Scotti-Campos et al., 2019). Enhanced [$CO_2$] also preserved mineral homeostasis (Martins et al., 2014) and improved the coffee bean quality at high temperatures (Ramalho et al., 2018).

Irrespective the facts described above, there is no information on the ability of the coffee crop to cope with drought stress in a scenario of enhanced air [$CO_2$]. Here we hypothesize that rising [$CO_2$] could positively affect coffee performance under drought conditions. Specifically, we aimed to test how carbon assimilation and use are affected by elevated [$CO_2$] and drought, and how this could impact shifts on biomass accumulation and partitioning. For this purpose, we designed an experiment using Open Top Chambers (OTCs), and performed a range of analysis encompassing from physiological and biometric assessments to hormonal and metabolite profiling approaches in coffee plants submitted to varying air [$CO_2$] and soil water availabilities.

## Material and methods

### *Plant material and experimental conditions*

The experiment was conducted in Viçosa (20º45'S, 42º15'W, 650-m altitude), Southeastern Brazil. Coffee (*C. arabica* L. cv IAC 44) seedlings were grown in OTCs (1.15 m diameter and 1.40 m height) inside a greenhouse with controlled temperature (30/25 ± 2ºC, day/night) and naturally fluctuating air humidity and photosynthetic photon flux density (PPFD). Thirty-four seedlings were transplanted (mid-March 2017) and grown in 12-L pots containing a mixture of soil, sand and composted manure (3:2:1, v:v:v) until achieving 5-6 leaf pairs, when the most vigorous and uniform 24 seedlings were selected (mid-April 2017). These seedlings were then submitted to two $CO_2$ treatments: ambient [$CO_2$] (386 ± 20 ppm) and elevated [$CO_2$] (723 ± 83 ppm) using the above quoted OTCs. For sake of simplification, these concentrations are hereafter referred to as 400 or

700 ppm. $CO_2$ fertilization was accomplished from 06:00 to 18:00 h. [$CO_2$] was measured weekly by using portable $CO_2$ sensors (model CO277, Akso Produtos Eletrônicos, São Leopoldo, Brazil), which were used and calibrated as recommended by the manufacturer.

During the first five months, all of the seedlings were regularly watered so that the soil water content was maintained near to field capacity (FC). Subsequently, plants from each $CO_2$ treatment were divided into two groups. In the first group (*i.e.*, well-watered plants), plants remained watered as described above. The plants from the second group (*i.e.*, drought-stressed plants) were not watered until the soil water content reached approximately 50% FC (c. five days). They were then maintained at 50% FC for additional 22 days. Subsequently the soil water content was reduced to 37.5% FC (by suspending irrigation for three days) and plants were kept at 37.5% FC for an additional 22 days. Also by suspending irrigation for two days soil water content reached 25% FC, and plants were maintained under this condition for 30 days. Finally, soil water content was decreased down to 20% FC, and plants were kept at this condition for five days. Further details concerning the control of soil moisture have been reported by Cavatte et al. (2012) and Menezes-Silva et al. (2017. Each one of the four $CO_2$ chambers contained three plants from the first group and three from the second one. Routine agricultural practices for coffee bean cultivation, including fertilization and control of insect and pathogen attack were used in both well-watered and water-limited plants.

The 7-months-old plants cultivated under both watering conditions were analysed and harvested for biochemical analyses. The long-term drought treatment allowed us to analyse leaves that were expanded during the period of water shortage. Unless otherwise stated, all of the samplings and measurements were performed on completely expanded leaves from the third or fourth leaf pairs from the apex of plagiotropic branches after 77 or 82 days upon drought imposition, *i. e.*, at 25% or 20% FC. Gas exchange and chlorophyll *a* fluorescence parameters were measured during two times: 08:00-09:00 h and 11:30-12:30 h (solar time). For biochemical analyses, leaf tissues were collected at the same time points and then flash frozen in liquid nitrogen with subsequent storage at -80ºC until analysis. Given that no major differences were found for data collected

between these two times s, only the data obtained at 11:30-12:30 h are presented in Results.

*Water potential, gas exchange and chlorophyll a fluorescence parameters*

The leaf water potential was determined at predawn ($\Psi_{pd}$) using a Scholander-type pressure chamber (model 1000, PMS Instruments, Albany, NY, USA). The gas exchange parameters [$A$, $g_s$, internal $CO_2$ concentration ($C_i$) and transpiration rate ($E$)] were measured simultaneously with chlorophyll *a* fluorescence parameters using a portable infrared gas analyser (model LI-6400XT, Li-COR Biosciences INC., Nebraska, USA) equipped with integrated fluorescence chamber heads (model LI-6400-40, Lincoln, NE, USA)]. Measurements were carried out at an artificial PPFD of 1000 μmol $m^{-2}$ $s^{-1}$ at the leaf level and at either 400 or 700 ppm of $CO_2$, according to the growth air [$CO_2$]. Further details have been described elsewhere (DaMatta *et al.*, 2016).

At predawn, the minimum fluorescence ($F_0$) was measured using a weak modulated measuring beam (*ca*. 0.03 μmol $m^{-2}$ $s^{-1}$). Subsequently, the maximal fluorescence ($F_m$) was measured by applying a saturating actinic light pulse (PAR of 8,000 μmol $m^{-2}$ $s^{-1}$) for 0.8 s. In light-adapted leaf tissues, the steady-state fluorescence yield ($F_s$) was measured after registering the gas exchange parameters. A saturating actinic light pulse (8,000 μmol $m^{-2}$ $s^{-1}$; 0.8 s) was applied to achieve the maximum fluorescence under light-adapted conditions ($F_m$'). The actinic light was then turned off, and a far-red illumination was applied (*ca*. 2 μmol $m^{-2}$ $s^{-1}$) to measure the initial fluorescence of the same light-adapted leaf ($F_0$'). Using the values of these parameters, the coefficient for photochemical quenching ($q_P$) was calculated as $q_P = (F_m' - F_s)/(F_m' - F_0')$, and the coefficient for non-photochemical quenching (NPQ) as $NPQ = (F_m/F_m') - 1$. The quantum yield of PSII non-cyclic electron transport ($\Phi_{PSII}$) was obtained as $\Phi_{PSII} = (F_m' - F_s)/F_m'$, from which the apparent electron transport rate (ETR) was calculated as $ETR = \Phi_{PSII} * PPFD * f * \alpha$, where $f$ is a factor that accounts for the partitioning of energy between PSII and PSI and is assumed to be 0.5, which indicates that the excitation energy is distributed equally between the two photosystems; and α is the leaf absorptance by the photosynthetic tissues and is assumed to be 0.84 (Maxwell and Johnson, 2000).

The rate of mitochondrial respiration in darkness ($R_n$) was measured at midnight and used to estimate light respiration ($R_d$) according to Lloyd *et al.* (1995) as $R_d = (0.5 – 0.05\ln(PPFD))R_n$. The photorespiratory rate of RuBisCO ($R_P$) were calculated as $R_P = 1/12[ETR – 4(A + R_d)]$ according to Valentini *et al.* (1995), after which the photorespiration-to-gross photosynthesis ratio ($R_P/A_{gross}$) was obtained by computing the values of $R_p$, $A$ and $R_d$, as described by DaMatta *et al.* (2016). Additionally, maximum apparent RuBisCO carboxylation capacity on a chloroplastic [$CO_2$] ($C_c$) basis ($V_{cmax}$) was estimated as the slope of the $A$-$C_i$ relationship by performing mini $A/C_i$ curves (air [$CO_2$] below 600 ppm) exactly as described by DaMatta *et al.* (2016). This procedure was successfully applied to well-watered plants but not to their drought-stressed counterparts which displayed intrinsically low $g_s$. We next estimated single-point $V_{cmax}$ on a $C_c$ basis for plants from all treatment combinations according to the methodology described by Wilson *et al.* (2000) and De Kauwe *et al.* (2016), using the kinetic properties of RuBisCO determined for coffee [as reported in Martins *et al.*, (2013)] and the values of $A$ and ETR measured at 08:00 h (when both $A$ and $g_s$ are at their maxima), followed by corrections to 25°C as described in Sharkey *et al*. (2007). Notably, values of $V_{cmax}$ as obtained using these two approaches were essentially similar for well-watered plants. We thus contend that our single-point $V_{cmax}$ estimations were reliable and therefore only these data are presented in Results.

*Hormonal profiling quantification*

Growth regulator pools were quantified using lyophilized leaf (20 mg) or root (80 mg) tissues. The extraction was performed as described by Müller *et al.* (2011) with modifications. 400 µL of extraction solution (methanol: isopropanol: acetic acid, 20:79:1, v:v:v) were added to the leaf and root grounded material. Following centrifugation (13,000 *g*, 10 min, 4°C), approximately 350 µL of supernatant of each sample were placed into a new tube. The extraction was performed twice and both supernatants were combined for further a final centrifugation (20,000 *g*, 5 min at 4°C) used to remove any remained tissue debris. Subsequently, 5 µL of each supernatant were automatically injected into the LC-MS/MS system through an Agilent 1200 Infinity Series coupled to a Mass Spectrometry type triple Quadrupole (QqQ), model 6430 (Agilent Technologies, Santa Clara, California,

USA). Chromatographic separation was accomplished on a Zorbax Eclipe Plus C18 column (1.8 µm, 2.1 x 50 mm) (Agilent) in series with a guard column Zorbax SB- C18, 1.8 µm (Agilent). The mobile phase used comprises a solution resulting from the mixture of different proportion of (A) 0.02% acetic acid in water and (B) 0.02% acetic acid in acetonitrile. The gradient between the solutions A and B was applied as follows (min/ %B): 0/5; 11/60; 13/95; 17/95; 19/5; 20/5. The flow rate was 0.3 mL $min^{-1}$ and the temperature of the column was 23°C. The ESI Ionization source (Electrospray Ionization) was used under a gas temperature of 300°C, nitrogen flow rate of 10 L $min^{-1}$, nebulizer pressure of 35 psi, and capillary voltage of 4000 V. Finally, the quantification was performed on the Skyline 4.1 software (MacLean et al., 2010) and the peak area of each hormone was integrated for individual replicates. In the case of ABA an internal standard pattern ([$^{2}$H6](+)-cis,trans-abscisic acid, OlchemIm, Olomouc, Czech Republic) was used.

Ethylene was quantified at the end of the experiment using approximately 3 g of fresh root samples. After washed during 2 min in water, samples were placed in 25 mL Erlenmeyer flasks containing 1 mL of deionized water. The flasks remained sealed for 24 h inside a chamber (Forma Scientific Inc., Ohio, USA). Following this incubation, ethylene that accumulated inside the Erlenmeyer flasks was then quantified exactly as described by Silva *et al.*( 2014).

*Metabolites*

Leaf and root samples were lyophilized at -48°C and crushed in a ball mill. Pure methanol was added to a 10 mg sample of ground tissue and the mixture was incubated at 70°C for 30 min. After centrifugation (16,200 *g,* 5 min, 4°C), the concentrations of hexoses (glucose plus fructose), sucrose and total amino acids in the supernatant, and starch from the methanol-insoluble pellet, were quantified as previously detailed (Praxedes *et al.*, 2006; Ronchi *et al.*, 2006). The levels of malate and fumarate were spectrophotometrically determined using the methanol-soluble phase exactly as reported elsewhere (Nunes-Nesi *et al.*, 2007).

*Growth traits*

The following growth traits were assessed every three weeks: total leaf area (TLA) (as described in Antunes et al., 2008) using leaf length and width dimensions, diameter of the orthotropic branch at soil level (DOB), plant height (from the soil level until the highest leaf pair). In addition, destructive measurements were also performed at the end of the experiment. Leaves, stems and roots were kept in an oven at 70°C until completely dried, when their dry masses were determined. The dry plants, and each organ thereof were then weighed to determine plant leaf dry mass (LDM); shoot dry mass (SDM); root dry mass (RDM) and total dry mass (TDM). Specific leaf area (SLA) was calculated as the ratio of TLA to LDM. We computed the DM partitioning as: leaf mass ratio (LMR: LDM/TDM); shoot mass ratio (SMR: SDM/TDM) and root mass ratio (RMR: RDM/TDM). We also calculated the RDM/TLA ratio as a proxy for plant hydraulic conductance.

*Electrolyte leakage assay*

Twelve discs per replicate (0.95 $cm^2$ each) were taken, washed and packed in filter bottles containing 20 mL of deionized water. After sealing, the plates were conditioned at 25°C for 12 h and then the initial conductivity of the medium was measured using a benchtop conductivity meter (model CD-4301 Lutron, Taipei, Taiwan). Subsequently, the plates were heated at 90°C, for 2h, in a drying oven and, after cooling their contents, the final conductivity was measured. Electrolyte leakage was then expressed as the percentage of conductivity relative to total conductivity (Scotti-Campos et al., 2019).

*Experimental design and statistical analyses*

The coffee plants were subjected to four treatment combinations, forming a 2 x 2 factorial (two [$CO_2$] and two levels of available water), in a completely randomized design as a matter of simplification given that all the chambers were inside the same greenhouse and submitted to the same conditions. In addition, pot positions inside the chambers were daily randomly changed during the weighting of pots. Six plants in individual pots per treatment combination as replicates were used. The analyses were based on two-way ANOVAs followed by the *Student t*-test ($\alpha = 0.05$; $n = 6 \pm SE$) comparing [$CO_2$] within each watering

regime and *vice versa*. All statistical analyses were performed using the *R* programming language, version 3.4.0 (*R*core Team, 2018).

## Results

*Elevated [$CO_2$] postponed decreases in predawn water potential under drought conditions*

The $\Psi_{pd}$ (Fig. 1) decreased significantly only when soil moisture reached 25% of FC, but only in drought-stressed 400-plants (-0.39 MPa) as compared to their respective control plants (-0.22 MPa). At 20% FC, however, $\Psi_{pd}$ was significantly lower in both drought-stressed 400- and 700-plants than in their well-watered counterparts (ca. -0.23 MPa), but the 700-plants still presented a significantly higher $\Psi_{pd}$ value (-0.41 MPa) than the 400-plants (-0.52 MPa).

*Elevated [$CO_2$] improved carbon assimilation by overcoming stomatal limitations*

Enhanced [$CO_2$] clearly improved (>60%) $A$ regardless of water availability levels (Fig 2A). Overall, decreases in $A$ upon drought imposition strictly followed reductions in $g_s$ (Fig. 2A, B). Indeed, $A$ was well correlated with $g_s$ regardless of treatment combinations ($r^2 \geq 0.81$; $P \leq 0.007$). Notably, compared with well-watered controls, drought-stressed 400-plants displayed earlier decreases (at 37.5% FC) in $A$, $g_s$ and $C_i$ than their 700-counterparts, which showed significant reductions in $g_s$ and $C_i$ (Fig. 2A-C) starting at 25% FC, whereas $A$ was significantly decreased only at 20% FC. In contrast to these alterations, $V_{cmax}$ on a $C_c$ basis was unresponsive to the treatments (Fig. 2D), suggesting that the overall oscillations in $A$ could not be associated with differences in biochemical capacity for $CO_2$ assimilation. The $R_D$ was systematically higher (*ca*. 48%) and $R_p/A_{gross}$ was consistently lower (between 34 and 63%) in the 700-plants than in the 400-ones regardless of water treatments (Fig 2E-F). In any case, $R_p/A_{gross}$ was higher in drought-stressed 400-plants than in their 700-counterparts at all watering conditions. In addition, water-use efficiency (WUE), calculated as the $A/E$ ratio, was significantly higher in 700- than in 400-plants regardless of watering (Fig. 2G). Nonetheless, enhanced [$CO_2$] improved WUE more under drought than under full irrigation, as found at 20% FC.

Similarly to *A*, ETR decreased at milder drought (37.5% FC) in 400-plants than the 700-ones, which in turn displayed significantly reduced ETR values only at 20% FC (Fig. 3A). In addition, ETR essentially tended to be higher in 700- than in 400-plants, although the difference was progressively attenuated with increasing drought severity. Interestingly, $q_P$ followed a similar pattern of variation to that of ETR, although most differences were not significant (Fig. 3A-B). The ETR*/A* ratio was decreased by enhanced [$CO_2$] regardless of watering. Drought-stressed 400-plants presented a remarkable higher ETR*/A* than their 700- counterparts at 25 or 20% FC (Fig. 3C), suggesting a higher chloroplast excitation pressure. In any case, NPQ remained invariant irrespective of treatments (data not shown), whereas only minor alterations were found in electrolyte leakage, *i.e.*, the drought-stressed 700-plants displayed a significantly lower leakage (*ca*. 20%) than their respective 400-plants (Fig. 3D).

*Minor alterations in major metabolites took place in response to [$CO_2$] and water treatments*

Overall, the two lowest water availability levels tested in this study promoted slight declines in foliar starch, glucose, fructose, total sugars and amino acid contents, under both [$CO_2$] conditions (Fig 4A- E). However, under elevated [$CO_2$] the content of these metabolites was generally higher in 700- than in 400-plants regardless at 25 or 20% FC. Sucrose (Fig. 4B), malate and fumarate (data not shown) content remained mostly unchanged irrespective of [$CO_2$] or water treatments. In roots, a few changes in metabolites were found. These changes were restricted to (*i*) starch, which was slightly increased in drought-stressed plants regardless of [$CO_2$], (*ii*) fumarate pools, which were higher in well-watered 700-plants than in 400-counterparts, and (*iii*) total amino acids, which were remarkably decreased by drought, but only in the 400-plants (Table S1).

*$CO_2$ enrichment improved growth independently of water availability*

Whereas biomass was not reduced significantly by drought, biomass accumulation (and TLA) was improved by $CO_2$ enrichment (Table 1). Notably, these improvements were more evident under drought, as denoted by the greater increases in biomass in drought-stressed 700-plants (59%) than in well-watered 700-plants (32%), when compared with their respective 400-counterparts.

Furthermore, drought-stressed 700-plants accumulated 27% more biomass than the well-watered 400-plants. Plant height and TLA were decreased by drought, but only in 400-plants. Interestingly, the drought-stressed 700-plants displayed higher RMR (42%), RDM/TLA (56%) and deeper roots than their 400-counterparts (Table 1, Fig. 5).

*Minor changes in hormone content were observed in response to the treatments*

Hormone contents did not respond to either drought or [$CO_2$] in both leaves and roots with the exception of polyamines (see below) and ABA in roots, which was 8 to 9 times higher in drought-stressed plants than in well-watered individuals regardless of [$CO_2$] (Table S2 and S3). Leaf pools of both putrescine and spermine increased significantly (>80%) in drought-stressed 400-plants relative to well-watered controls, whereas they were unresponsive to the treatments in 700-plants regardless of watering (Fig. 6).

**Discussion**

Coffee plants were submitted to a progressive reduction of soil water availability resulting in the imposition of a moderate drought stress that is typically found under normal rainfed, field conditions at most of Brazilian cultivation areas for coffee production (DaMatta et al., 2018). Under similar drought events , coffee plants are usually reported to display remarkable reductions in both $g_s$ and $A$ (Menezes-Silva et al., 2017) as also found in this study. Here we expand previous knowledge on how coffee plants cope with water shortage by demonstrating that enhanced air [$CO_2$] alleviates drought stress impacts *via* the reinforcement in $CO_2$ uptake, changes in biomass accumulation and partitioning favouring water acquisition, and decreases in oxidative pressure in the chloroplast electron transport chain.

Our results clearly demonstrate that drought-imposed limitations on photosynthesis were fundamentally based on increases in diffusive constraints, at least at the stomatal level, as deduced from the significant decreases in both $g_s$ and $C_i$ and invariant $V_{cmax}$. Accordingly, it is unlikely that moderate drought conditions led to biochemical impairments of $CO_2$ assimilation, which have been shown to occur only at severe drought stress (DaMatta et al., 1997; Ramalho et al., 2018). By enhancing [$CO_2$], diffusive constraints (which are intrinsically high

in coffee, particularly those related to limited stomata aperture even in well-irrigated plants (Martins et al., 2014; DaMatta et al., 2016)) were at least partially overcome, thereby allowing $CO_2$ to reach the chloroplast stroma at higher rates. This, in turn, resulted in higher carboxylation over oxygenation performed by RuBisCO, resulting in higher *A* (and WUE) and decreased photorespiration rates (lower $R_p/A_{gross}$ ratio) the 700-plants regardless of watering. In addition, we found no signs of photosynthetic downregulation in these plants, as judged from the unchanging $V_{cmax}$ and little, if any, alterations in carbohydrate contents in response to enhanced [$CO_2$].

Given that the increase in *A* under elevated [$CO_2$] implies in more ATP use for RuBP regeneration (Ainsworth and Rogers, 2007), we also examined if leaf photochemistry was adjusted to match the biochemical requirements for $CO_2$ fixation. Although the proportion of energy used through photochemistry ($q_p$) remained unchanged across treatments, ETR was generally higher in 700- than in 400-plants independently of watering. Additionally, we found that the ETR values were high enough to sustain the measured *A* values (Martins et al., 2013). Nevertheless, in the case of drought-stressed 400-plants, the ETR/*A* ratio enhanced remarkably with increasing drought severity, what are likely associated with an increase in (excessive) reducing power that might lead to oxidative stress and membrane damage. However, the higher oxidative pressure displayed by the drought-stressed 400-plants was accompanied by unaltered electrolyte leakage (a proxy for membrane damage) relative to the well-watered 400-plants, suggesting that effective oxidative damage did not occur. Considering that adjustments in nonphotochemical dissipation of the excess energy did not occur (invariant NPQ), alternative pathways such as enzymatic and nonenzymatic antioxidative routes might have acted to afford photoprotection (Pinheiro et al., 2004; Wujeska et al., 2013; Ramalho et al., 2018). Alternatively, the higher contents of polyamines such as putrescine and spermine could have helped to counteract the oxidative pressure in drought-stressed 400-plants, given that these polyamines act as ROS scavengers under adverse conditions (Galston and Sawhney, 1990; Ha et al., 1998).

Drought *per se* did not lead to significant decreases in biomass accumulation, possibly reflecting the moderate stress condition the plants were exposed to. However, enhanced [$CO_2$] remarkably improved plant growth. In

other plant species, such increases in plant growth has been associated with changes in hormone pools (Huang and Xu, 2015; Gamage et al., 2018; Burgess et al., 2019). Nonetheless, bulk foliar hormone contents were altered little, if at all, in this current study, and thus, should not be taken into account as a major factor explaining growth differences in coffee plants due to $CO_2$ supply. It is likely that in slow-growth woody species such as coffee, which has inherently low *A* due to marked diffusive limitations (Batista et al., 2012; Martins et al., 2014), the improved growth stimulated by enhanced [$CO_2$] could be more directly dependent on the regulation of carbon flux and content through plant tissues. Interestingly, despite the marked increases in *A* coupled with increases in leaf area at enhanced [$CO_2$] (high source strength), only minor differences in the content of starch, soluble sugars and amino acids were detected across treatments. Taken together, these facts may be taken as circumstantial evidence that carbon- and nitrogen-rich compounds have been directed towards growth, particularly in the 700-plants that therefore displayed a higher sink demand.

Improved root growth is believed to be triggered by increased ABA content and a larger carbon flux towards roots (Fujii et al., 2007; Jossier et al., 2009). In presence of ABA, kinases SnRK2 induce the expression of genes coding for proteins involved in root growth (Fujii et al., 2007). However, an intricate network also links ABA signalling to the energetic status of roots. In this way, ABA and SnRK1 are involved in the regulation of activity of several enzymes involved in carbon metabolism (Jossier *et al.*, 2009 and references therein). Although both 400- and 700-plants under drought stress presented remarkable increases in ABA content in roots, only the 700-plants were able to adjust biomass partitioning, which demands a considerable amount of energy (Gamage et al., 2018). We suggest that the 700-plants, by having a higher assimilate production and a higher carbon flux through respiration (higher respiration rates), also showed a more favorable energetic status to support the increased root growth upon drought imposition. This was accompanied by an increased RDM/TLA. Collectively, these allometric adjustments could contribute to improve water uptake, plant hydration, and, therefore, stomatal opening even under water limited conditions. Ultimately, this should concur to alleviate shoot xylem tension, thus preserving whole-plant hydraulic conductance.

## Conclusions

We herein presented insights on how coffee plants deal with drought under $CO_2$ enrichment conditions. Results demonstrate that elevated [$CO_2$] improved C- assimilation, WUE and biomass accumulation regardless of watering, in addition to decreasing the oxidative pressure in the chloroplast under drought conditions. Elevated [$CO_2$] also promoted key allometric adjustments linked to drought tolerance, *e.g.*, more biomass partitioning towards roots with a deeper root system. Improved growth under enhanced air [$CO_2$] was unlikely to have been associated with global changes on hormonal pools but rather with shifts on carbon fluxes. Collectively, our results offer novel and timely information on the mitigating ability of rising air [$CO_2$] on the photosynthetic performance and growth under drought stress conditions. This information is of utmost importance in the context of the present and ongoing climate change scenarios for the coffee crop sustainability.

## Acknowledgements

Research fellowships that were granted by the National Council for Scientific and Technological Development (CNPq, Brazil) to FMD are gratefully acknowledged. We thank the scholarships that were granted by the Brazilian Federal Agency for the Support and Evaluation of Graduate Education (CAPES; Financial Code 001), the Foundation for Research Assistance of Minas Gerais State, Brazil (FAPEMIG) and CNPq. We are also thankful to the Núcleo de Análises de Biomoléculas (NUBIOMOL) for providing the facilities to perform the hormonal profiling analyses, and the Fundação para a Ciência e a Tecnologia for supporting JDCR through the research units UID/04129/2020 (LEAF), UIDP/04035/2020 (GeoBioTec).

## References

**AbdElgawad H, Zinta G, Beemster GTS, Janssens IA, Asard H** (2016) Future climate $CO_2$ levels mitigate stress impact on plants: increased defense or decreased challenge? Front Plant Sci **7**: 1–7

**Ainsworth EA, Rogers A** (2007) The response of photosynthesis and stomatal conductance to rising [$CO_2$]: mechanisms and environmental interactions.

Plant Cell Environ **30**: 258–270

**Antunes WC, Pompelli MF, Carretero DM, DaMatta FM** (2008) Allometric models for non-destructive leaf area estimation in coffee (*Coffea arabica* and *Coffea canephora*). Ann Appl Biol **153**: 33–40

**Batista KD, Araújo WL, Antunes WC, Cavatte PC, Moraes GABK, Martins SC V, DaMatta FM** (2012) Photosynthetic limitations in coffee plants are chiefly governed by diffusive factors. Trees - Struct Funct **26**: 459–468

**Brodribb T J, McAdam S A** (2017) Evolution of the stomatal regulation of plant water content. Plant Physiol **174**: 639-649

**Burgess P, Chapman C, Zhang X, Huang B** (2019) Stimulation of growth and alteration of hormones by elevated carbon dioxide for creeping bentgrass exposed to drought. Crop Sci **59**: 1672–1680

**Cardoso, A. A., Brodribb, T. J., Lucani, C. J., DaMatta, F. M., & McAdam, S. A.** (2018). Coordinated plasticity maintains hydraulic safety in sunflower leaves. Plant, cell & environment, **41**(11): 2567-2576

**Cavatte PC, Oliveira ÁAG, Morais LE, Martins SC V, Sanglard LMVP, DaMatta FM** (2012) Could shading reduce the negative impacts of drought on coffee? A morphophysiological analysis. Physiol Plant **144**: 111–122

**Craparo ACW, Van Asten PJA, Läderach P, Jassogne LTP, Grab SW** (2015) *Coffea arabica* yields decline in Tanzania due to climate change: global implications. Agric For Meteorol **207**: 1–10

**DaMatta FM, Avila RT, Cardoso AA, Martins SCV, Ramalho JC** (2018) Physiological and agronomic performance of the coffee crop in the context of climate change and global warming: a review. J Agric Food Chem **66**: 5264–5274

**DaMatta FM, Godoy AG, Menezes-Silva PE, Martins SC V, Sanglard LMVP, Morais LE, Torre-Neto A, Ghini R** (2016) Sustained enhancement of photosynthesis in coffee trees grown under free-air $CO_2$ enrichment conditions: disentangling the contributions of stomatal, mesophyll, and biochemical limitations. J Exp Bot **67**: 341–352

**DaMatta FM, Grandis A, Arenque BC, Buckeridge MS** (2010) Impacts of climate changes on crop physiology and food quality. Food Res Int **43**: 1814–1823

**DaMatta FM, Maestri M, Barros RS** (1997) Photosynthetic performance of two

coffee species under drought. Photosynthetica **34**: 257–264

**DaMatta FM, Rahn E, Läderach P, Ghini R, Ramalho JC** (2019) Why could the coffee crop endure climate change and global warming to a greater extent than previously estimated? Clim Change **152**: 167–178

**Duursma R A, Blackman C J, Lopéz R, Martin-StPaul N K, Cochard H, Medlyn B E** (2019) On the minimum leaf conductance: its role in models of plant water use, and ecological and environmental controls. New Phytologist, **221**(2): 693-705

**Davis AP, Chadburn H, Moat J, O'Sullivan R, Hargreaves S, Lughadha EN** (2019) High extinction risk for wild coffee species and implications for coffee sector sustainability. Sci Adv **5**: 1–10

**Ferris R, Sabatti M, Miglietta F, Mills RF, Taylor G** (2001) Leaf area is stimulated in Populus by free air $CO_2$ enrichment (POPFACE), through increased cell expansion and production. Plant Cell Environ **24**: 305–315

**Fujii H, Verslues PE, Zhu JK** (2007) Identification of two protein kinases required for abscisic acid regulation of seed germination, root growth, and gene expression in Arabidopsis. Plant Cell **19**: 485–494

**Galston AW, Sawhney RK** (1990) Polyamines in plant physiology. Plant Physiol **94**: 406–410

**Gamage D, Thompson M, Sutherland M, Hirotsu N, Makino A, Seneweera** S (2018) New Insights into the cellular mechanisms of plant growth at elevated atmospheric carbon dioxide concentrations. Plant Cell Environ **41**: 1233-1246.

**Ghini R, Torre-Neto A, Dentzien AFM, Guerreiro-Filho O, Iost R, Patrício FRA, Prado JSM, Thomaziello RA, Bettiol W, DaMatta FM** (2015) Coffee growth, pest and yield responses to free-air $CO_2$ enrichment. Clim Change **132**: 307–320

**Ha HC, Sirisoma NS, Kuppusamy P, Zweier JL, Woster PM, Casero RA** (1998) The natural polyamine spermine functions directly as a free radical scavenger. Proc Natl Acad Sci U S A **95**: 11140–11145

**Huang B, Xu Y** (2015) Cellular and molecular mechanisms for elevated $CO_2$ – regulation of plant growth and stress adaptation. Crop Sci **55**: 1405–1424

**Jossier M, Bouly JP, Meimoun P, Arjmand A, Lessard P, Hawley S, Grahame Hardie D, Thomas M** (2009) SnRK1 (SNF1-related kinase 1) has a central

role in sugar and ABA signalling in *Arabidopsis thaliana*. Plant J **59**: 316–328

**De Kauwe MG, Lin YS, Wright IJ, Medlyn BE, Crous KY, Ellsworth DS, Maire V, Prentice IC, Atkin OK, Rogers A, et al** (2016) A test of the "one-point method" for estimating maximum carboxylation capacity from field-measured, light-saturated photosynthesis. New Phytol **210**: 1130–1144

**Kimball BA** (1983) Carbon dioxide and agricultural yield: an assemblage and analysis of 430 prior observations. Agron J **75**: 1–48

**Leakey ADB, Ainsworth EA, Bernacchi CJ, Rogers A, Long SP, Ort DR** (2009) Elevated CO2 effects on plant carbon, nitrogen, and water relations: Six important lessons from FACE. J Exp Bot **60**: 2859–2876

**Lindroth RL, Osier TL, Barnhill HRH, Wood S A** (2002) Effects of genotype and nutrient availability on phytochemistry of trembling aspen (*Populus tremuloides* Michx.) during leaf senescence. Biochem Syst Ecol **30**: 297–307

**Lloyd J, Grace J, Miranda AC, Meir P, Wong SC, Miranda HS, Wright IR, Gash JHC, Mc Intyre J** (1995) A simple calibrated model of Amazon rainforest productivity based on leaf biochemical properties. Plant Cell Environ **18**: 1129–1145

**MacLean B, Tomazela DM, Shulman N, Chambers M, Finney GL, Frewen B, Kern R, Tabb DL, Liebler DC, MacCoss MJ** (2010) Skyline: an open source document editor for creating and analyzing targeted proteomics experiments. Bioinformatics **26**: 966–968

**Magrach A, Ghazoul J** (2015) Climate and pest-driven geographic shifts in global coffee production: Implications for forest cover, biodiversity and carbon storage. PLoS One **10**: 1–15

**Martins MQ, Rodrigues WP, Fortunato AS, Leitão AE, Rodrigues AP, Pais IP, Martins LD, Silva MJ, Reboredo FH, Partelli FL, et al** (2016) Protective response mechanisms to heat stress in interaction with high [$CO_2$] conditions in *Coffea* spp. Front Plant Sci **7**: 1–18

**Martins SCV, Galmés J, Cavatte PC, Pereira LF, Ventrella MC, DaMatta FM** (2014) Understanding the low photosynthetic rates of sun and shade coffee leaves: Bridging the gap on the relative roles of hydraulic, diffusive and biochemical constraints to photosynthesis. PLoS One **9**: 1–10

**Martins SC V, Galmés J, Molins A, DaMatta FM** (2013) Improving the estimation of mesophyll conductance to $CO_2$: on the role of electron transport

rate correction and respiration. J Exp Bot **64**: 3285–3298

**Masle J** (2000) The effects of elevated $CO_2$ concentrations on cell division rates, growth patterns, and blade anatomy in young wheat plants are modulated by factors related to leaf position, vernalization, and genotype. Plant Physiol **122**: 1399–1415

**Masson PH, Takahashi T, Angelini R** (2017) Molecular mechanisms underlying polyamine functions in plants. Front Plant Sci **8**: 1–3

**Maxwell K, Johnson GN** (2000) Chlorophyll fluorescence: a practical guide. J Exp Bot **51**: 659–668

**Menezes-Silva PE, Sanglard LMVP, Ávila RT, Morais LE, Martins SCV, Nobres P, Patreze CM, Ferreira MA, Araújo WL, Fernie AR, et al** (2017) Photosynthetic and metabolic acclimation to repeated drought events play key roles in drought tolerance in coffee. J Exp Bot **68**: 4309–4322

**Müller M, Munné-Bosch S, Pan X, Welti R, Wang X, Dun E, Brewer P, Beveridge C, Davies P, Ross J, et al** (2011) Rapid and sensitive hormonal profiling of complex plant samples by liquid chromatography coupled to electrospray ionization tandem mass spectrometry. Plant Methods **7**: 37

**Nicotra AB, Leigh A, Boyce CK, et al** (2011) The evolution and functional significance of leaf shape in the angiosperms. Funct Plant Biol 38:535–552

**Norby RJ, DeLucia EH, Gielen B, Calfapietra C, Giardina CP, King JS, Ledford J, McCarthy HR, Moore DJP, Ceulemans R, et al** (2005) Forest response to elevated $CO_2$ is conserved across a broad range of productivity. Proc Natl Acad Sci **102**: 18052–18056

**Nunes-Nesi A, Carrari F, Gibon Y, Sulpice R, Lytovchenko A, Fisahn J, Graham J, Ratcliffe RG, Sweetlove LJ, Fernie AR** (2007) Deficiency of mitochondrial fumarase activity in tomato plants impairs photosynthesis via an effect on stomatal function. Plant J **50**: 1093–1106

**Pinheiro HA, DaMatta FM, Chaves ARM, Fontes EPB, Loureiro ME** (2004) Drought tolerance in relation to protection against oxidative stress in clones of *Coffea canephora* subjected to long-term drought. Plant Sci **167**: 1307–1314

**Praxedes SC, DaMatta FM, Loureiro ME, Maria MA, Cordeiro AT** (2006) Effects of long-term soil drought on photosynthesis and carbohydrate

metabolism in mature robusta coffee (*Coffea canephora* Pierre var. *kouillou*) leaves. Environ Exp Bot **56**: 263–273

**Rakočević M, Ribeiro RV, Marchiori PER, Filizola HF, Batista ER** (2018) Structural and functional changes in coffee trees after 4 years under free air $CO_2$ enrichment. Ann Bot 21:1065–1078

**Ramalho JC, Pais IP, Leitão AE, Guerra M, Reboredo FH, Máguas CM, et al**. (2018) Can elevated air [$CO_2$] conditions mitigate the predicted warming impact on the quality of coffee bean?. Front. Plant Sci. 9, 287.

**Ramalho JC, Rodrigues AP, Semedo JN, Pais IP, Martins LD, Simões-Costa MC, et al.** (2013) Sustained photosynthetic performance of *Coffea* spp. under long-term enhanced [$CO_2$]. PloS ONE 8(12): e82712.

**Ribeiro DM, Araujo WL, Fernie AR, Schippers JHM, Mueller-Roeber B** (2012) Action of gibberellins on growth and metabolism of *Arabidopsis* plants associated with high concentration of carbon dioxide. Plant Physiol **160**: 1781–1794

**Ronchi CP, DaMatta FM, Batista KD, Moraes GABK, Loureiro ME, Ducatti C** (2006) Growth and photosynthetic down-regulation in *Coffea arabica* in response to restricted root volume. Funct Plant Biol **33**: 1013–1023

**Scotti-Campos P, Pais IP, Ribeiro-Barros AI, Martins LD, Tomaz MA, Rodrigues WP, Campostrini E, Semedo JN, Fortunato AS, Martins MQ, et al** (2019) Lipid profile adjustments may contribute to warming acclimation and to heat impact mitigation by elevated [CO2] in *Coffea* spp. Environ Exp Bot. **167**: 103856 **TD, Bernacchi CJ, Farquhar GD, Singsaas EL** (2007) Fitting photosynthetic carbon dioxide response curves for C3 leaves. Plant Cell Environ **30**: 1035–1040

**Silva PO, Medina EF, Barros RS, Ribeiro DM** (2014) Germination of salt-stressed seeds as related to the ethylene biosynthesis ability in three *Stylosanthes* species. J Plant Physiol **171**: 14–22

**Taylor G, Tricker PJ, Zhang FZ, Alston VJ, Miglietta F, Kuzminsky E** (2003) Spatial and temporal effects of free-air $CO_2$ enrichment ( POPFACE ) on leaf growth , cell expansion and cell production in a closed canopy of poplar 1. Plant Physiol **131**: 177–185

**Thompson M, Gamage D, Hirotsu N, Martin A, Seneweera S** (2017) Effects of elevated carbon dioxide on photosynthesis and carbon partitioning: a

perspective on root sugar sensing and hormonal crosstalk. Front Physiol **8**: 1–13

**Valentini R, Epron D, De Angelis P, Matteucci G, Dreyer E** (1995) In situ estimation of net CO2 assimilation, photosynthetic electron flow and photorespiration in Turkey oak (*Q. cerris* L.) leaves: diurnal cycles under different levels of water supply. Plant Cell Environ **18**: 631–640

**Wilson KB, Baldocchi DD, Hanson PJ** (2000) Spatial and seasonal variability of photosynthetic parameters and their relationship to leaf nitrogen in a deciduous forest. Tree Physiol **20**: 565–578

**Woodward FI. (1987)**. Stomatal numbers are sensitive to increases in $CO_2$ from pre-industrial levels. Nature **327**: 617–618

**Wujeska A, Bossinger G, Tausz M** (2013) Responses of foliar antioxidative and photoprotective defence systems of trees to drought: a meta-analysis. Tree Physiol **33**: 1018–1029

**Yong JW, Wong SC, Letham DS, Hocart CH, Farquhar GD** (2000) Effects of elevated [$CO_2$] and nitrogen nutrition on cytokinins in the xylem sap and leaves of cotton. Plant Physiol **124**: 767–780

**Tables and Figure legends**

**Table 1**. The effect of watering (well-watered or drought-stressed plants) and $CO_2$ supply (400 or 700 ppm) on total biomass (TDM); root mass ratio (RMR); shoot mass ratio (SMR); leaf mass ratio (LMR); total leaf area (TLA); plant height; specific leaf area (SLA) and root dry mass-to-total leaf area ratio (RDM/TLA). Measurements were made at the end of the experiment. Different lowercase letters indicate differences between watering regimes within a same $CO_2$ supply; different capital letters indicate differences between $CO_2$ treatments within a same watering regime (*Student t*-test, α= 0.05; *n*= 6 ± SE).

| | **400 ppm** | | | | | | **700 ppm** | | | | | |
|---|---|---|---|---|---|---|---|---|---|---|---|---|
| **Parameters** | **Well-watered** | | | **Drought** | | | **Well-watered** | | | **Drought** | | |
| TDM (g) | 249 ± 28 | Ba | | 200 ± 12 | Ba | | 329 ± 13 | Aa | | 317 ± 18 | Aa | |
| RMR | 0.15 ± 0.01 | Aa | | 0.12 ± 0.01 | Ba | | 0.13 ± 0.02 | Aa | | 0.17 ± 0.01 | Aa | |
| SMR | 0.85 ± 0.01 | Aa | | 0.88 ± 0.01 | Aa | | 0.87 ± 0.01 | Aa | | 0.83 ± 0.01 | Ba | |
| LMR | 0.69 ± 0.01 | Aa | | 0.73 ± 0.01 | Aa | | 0.67 ± 0.01 | Ab | | 0.64 ± 0.01 | Ba | |
| TLA ($m^2$) | 1.13 ± 0.11 | Ba | | 0.87 ± 0.06 | Ba | | 1.42 ± 0.06 | Aa | | 1.30 ± 0.05 | Aa | |
| Height (cm) | 70.6 ± 3.3 | Aa | | 57.4 ± 4.7 | Bb | | 77.9 ± 1.4 | Aa | | 76.3 ± 0.8 | Aa | |
| SLA ($m^2$ $kg^{-1}$) | 14.1 ± 0.2 | Aa | | 13.8 ± 0.26 | Aa | | 12.5 ± 0.3 | Bb | | 12.2 ± 0.2 | Bb | |
| RDM/TLA (g $cm^{-2}$) | 33.3 ± 2.6 | Aa | | 26.8 ± 3.1 | Ba | | 29.9 ± 3.5 | Aa | | 41.9 ± 4.6 | Aa | |

**Table S1.** The effect of watering (well-watered or drought-stressed plants) and $CO_2$ supply (400 or 700 ppm) on the root contents (on a dry weight basis) of starch, glucose (Glu), fructose (Fru), sucrose (Suc), total soluble sugar (TSS), malate (Mal), fumarate (Fum) and total amino acids (TAA). Measurements were made at the end of the experiment. Different lowercase letters indicate differences between watering regimes within a same $CO_2$ supply; different capital letters indicate differences between $CO_2$ treatments within a same watering regime (*Student t*-test, α= 0.05; *n*= 6 ± SE).

| | **400 ppm** | | | | | | **700 ppm** | | | | | |
|---|---|---|---|---|---|---|---|---|---|---|---|---|
| **Metabolites** | **Well-watered** | | | **Drought** | | | **Well-watered** | | | **Drought** | | |
| Starch (mg $g^{-1}$) | 19.5 ± 0.7 | Ab | | 22.8 ± 0.8 | Aa | | 19.9 ± 0.2 | Ab | | 23.7 ± 0.5 | Aa | |
| Glu (µmol $g^{-1}$) | 2.47 ± 0.67 | Aa | | 1.21 ± 0.07 | Aa | | 2.12 ± 0.38 | Aa | | 1.57 ± 0.15 | Aa | |
| Fru (µmol $g^{-1}$) | 4.38 ± 1.43 | Aa | | 2.16 ± 0.41 | Aa | | 2.73 ± 0.72 | Aa | | 1.78 ± 0.22 | Aa | |
| Suc (µmol $g^{-1}$) | 22.1 ± 1.2 | Aa | | 20.9 ± 1.2 | Aa | | 20.0 ± 0.5 | Aa | | 24.6 ± 0.89 | Aa | |
| TSS (µmol $g^{-1}$) | 30.5 ± 3.4 | Aa | | 26.1 ± 0.4 | Aa | | 25.0 ± 1.5 | Aa | | 27.9 ± 0.5 | Aa | |
| Mal (µmol $g^{-1}$) | 7.8 ± 1.8 | Aa | | 7.7 ± 1.2 | Aa | | 11.2 ± 1.3 | Aa | | 9.2 ± 0.5 | Aa | |
| Fum (µmol $g^{-1}$) | 5.96 ± 0.86 | Ba | | 5.92 ± 0.86 | Aa | | 9.37 ± 0.96 | Aa | | 6.47 ± 0.74 | Aa | |
| TAA (mmol $g^{-1}$) | 17.5 ± 2.5 | Aa | | 7.5 ± 1.8 | Bb | | 13.3 ± 3.8 | Aa | | 15.6 ± 2.6 | Aa | |

**Table S2.** The effect of watering (well-watered or drought-stressed plants) and air [$CO_2$] (400 or 700 ppm) on the leaf contents (on a dry weight basis) of 1-aminocyclopropane-1-carboxylic acid (ACC), abscisic acid (ABA), zeatin, methyl jasmonate (MeJA), salicylic acid (SA), spermidine (Spd) content on leaves. Measurements were made when soil moisture (drought treatments) reached 25 or 20% of field capacity (FC). Different lowercase letters indicate differences between watering regimes within a same $CO_2$ supply; different capital letters indicate differences between $CO_2$ treatments within a same watering regime (*Student t*-test, α= 0.05; *n*= 6 ± SE).

| | **Hormonal profiling in leaves** | | | | | | | | | | | | | | | |
|---|---|---|---|---|---|---|---|---|---|---|---|---|---|---|---|---|
| **[$CO_2$]** | **400 ppm** | | | | | | | **700 ppm** | | | | | | | | |
| **Hormone** | **Well-watered** | | | | **Drought** | | | | **Well-watered** | | | | **Drought** | | | |
| | **25% FC** | | | | | | | | | | | | | | | |
| ACC (μg $g^{-1}$) | 2.27 | ± | 0.20 | Aa | 1.61 | ± | 0.03 | Ba | 2.85 | ± | 0.21 | Aa | 2.86 | ± | 0.17 | Aa |
| ABA (ng $g^{-1}$) | 44.2 | ± | 3.9 | Aa | 37.8 | ± | 3.8 | Aa | 39.4 | ± | 2.6 | Aa | 37.1 | ± | 2.8 | Aa |
| Zeatin (ng $g^{-1}$) | 390 | ± | 38 | Aa | 318 | ± | 19 | Aa | 307 | ± | 17 | Aa | 287 | ± | 14 | Aa |
| MeJA (ng $g^{-1}$) | 31.5 | ± | 3.3 | Aa | 25.3 | ± | 3.7 | Aa | 18.0 | ± | 2.4 | Ba | 15.6 | ± | 2.2 | Ba |
| SA (ng $g^{-1}$) | 280 | ± | 78 | a | 123 | ± | 10 | a | 83 | ± | 31 | a | 227 | ± | 110 | a |
| Spd (μg $g^{-1}$) | 1.23 | ± | 0.03 | a | 1.12 | ± | 0.13 | a | 0.52 | ± | 0.07 | b | 0.52 | ± | 0.06 | b |
| | **20% FC** | | | | | | | | | | | | | | | |
| ACC (μg $g^{-1}$) | 2.65 | ± | 0.13 | Aa | 1.92 | ± | 0.14 | Aa | 3.13 | ± | 0.19 | Aa | 3.10 | ± | 0.28 | Aa |
| ABA (ng $g^{-1}$) | 43.2 | ± | 4.7 | Aa | 41.30 | ± | 3.1 | Aa | 34.8 | ± | 3.7 | Aa | 47.8 | ± | 3.19 | Aa |
| Zeatin (ng $g^{-1}$) | 260 | ± | 13 | Aa | 240 | ± | 21 | Aa | 226 | ± | 16 | Aa | 214 | ± | 17 | Aa |
| MeJA (ng $g^{-1}$) | 9.1 | ± | 0.8 | Aa | 13.7 | ± | 1.8 | Aa | 13.4 | ± | 1.2 | Aa | 9.3 | ± | 1.0 | Aa |
| SA (ng $g^{-1}$) | 177 | ± | 54 | Aa | 181 | ± | 59 | Aa | 239 | ± | 47.0 | a | 197 | ± | 60 | Aa |
| Spd (μg $g^{-1}$) | 0.43 | ± | 0.10 | Aa | 0.42 | ± | 0.06 | Aa | 0.19 | ± | 0.03 | Ba | 0.22 | ± | 0.04 | Ba |

**Table S3.** The effect of watering (well-watered or drought-stressed plants) and $CO_2$ supply (400 or 700 ppm) on the root contents (on a dry weight basis) of 1-aminocyclopropane-1-carboxylic acid (ACC), abscisic acid (ABA), zeatin, methyl jasmonate (MeJA), salicylic acid (SA) and spermidine (Spd). Measurements were made at the end of the experiment, when soil moisture was 20% of field capacity. Different lowercase letters indicate differences between watering regimes within a same $CO_2$ acclimation; different capital letters indicate differences between $CO_2$ treatments within a same watering regime (*Student t-test,* α= 0.05; *n*= 6 ± SE).

| | **Root hormonal profiling** | | | | | | | | | | | | | | | |
|---|---|---|---|---|---|---|---|---|---|---|---|---|---|---|---|---|
| | **400 ppm** | | | | | | | | **700 ppm** | | | | | | | |
| **Hormone** | **Well-watered** | | | | **Drought** | | | | **Well-watered** | | | | **Drought** | | | |
| ACC (ng $g^{-1}$) | 439 | ± | 42 | Aa | 247 | ± | 33 | Aa | 456 | ± | 162 | Aa | 259 | ± | 24 | Aa |
| ABA (ng $g^{-1}$) | 0.35 | ± | 0.25 | Ab | 3.10 | ± | 0.56 | Aa | 0.36 | ± | 0.09 | Ab | 3.01 | ± | 0.6 | Aa |
| Zeatin (ng $g^{-1}$) | 1507 | ± | 192 | Aa | 1071 | ± | 110 | Aa | 1330 | ± | 186 | Aa | 942 | ± | 137 | Aa |
| MeJA (ng $g^{-1}$) | 32.1 | ± | 2.9 | Ba | 29.4 | ± | 1.6 | Aa | 40.0 | ± | 2.6 | Aa | 33.0 | ± | 1.5 | Aa |
| GA3 (ng $g^{-1}$) | 55.6 | ± | 9.1 | Aa | 64.3 | ± | 2.7 | Aa | 43.2 | ± | 9.7 | Aa | 44.8 | ± | 8.4 | Aa |
| GA4 (ng $g^{-1}$) | 34.1 | ± | 2.4 | Aa | 31.1 | ± | 5.7 | Aa | 36.6 | ± | 4.2 | Aa | 36.6 | ± | 4.9 | Aa |
| JA (ng $g^{-1}$) | 1006 | ± | 186 | Aa | 787.3 | ± | 321 | Aa | 1200 | ± | 490 | Aa | 910.1 | ± | 372 | Aa |
| SA (ng $g^{-1}$) | 38.5 | ± | 4.6 | Aa | 37.3 | ± | 5.2 | Aa | 51.4 | ± | 9.4 | Aa | 39.3 | ± | 3.1 | Aa |
| Spd (µg $g^{-1}$) | 0.52 | ± | 0.03 | Aa | 0.63 | ± | 0.17 | Aa | 0.23 | ± | 0.02 | Aa | 0.45 | ± | 0.1 | Aa |
| Put (µg $g^{-1}$) | 1.29 | ± | 0.22 | Aa | 1.07 | ± | 0.17 | Aa | 0.79 | ± | 0.30 | Aa | 1.08 | ± | 0.2 | Aa |
| Spe (µg $g^{-1}$) | 57.3 | ± | 6.0 | Aa | 48.9 | ± | 8.2 | Aa | 43.8 | ± | 7.6 | Aa | 75.6 | ± | 4.2 | Aa |

## Figures

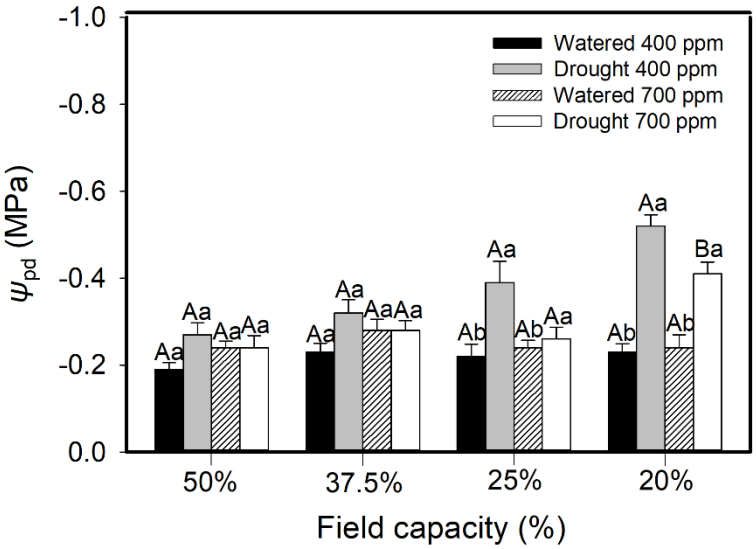


**Figure 1.** The effect of watering (well-watered or drought-stressed plants) and $CO_2$ supply (400 or 700 ppm) on the predawn leaf water potential ($\psi_{pd}$). For drought-stressed plants, measurements were made at 50, 37.5, 25 and 20% of field capacity. Different lowercase letters indicate differences between watering regimes within the same $CO_2$ supply; different capital letters indicate differences between $CO_2$ treatments within the same watering regime (*Student t*-test, α= 0.05; *n*= 6 ± SE).

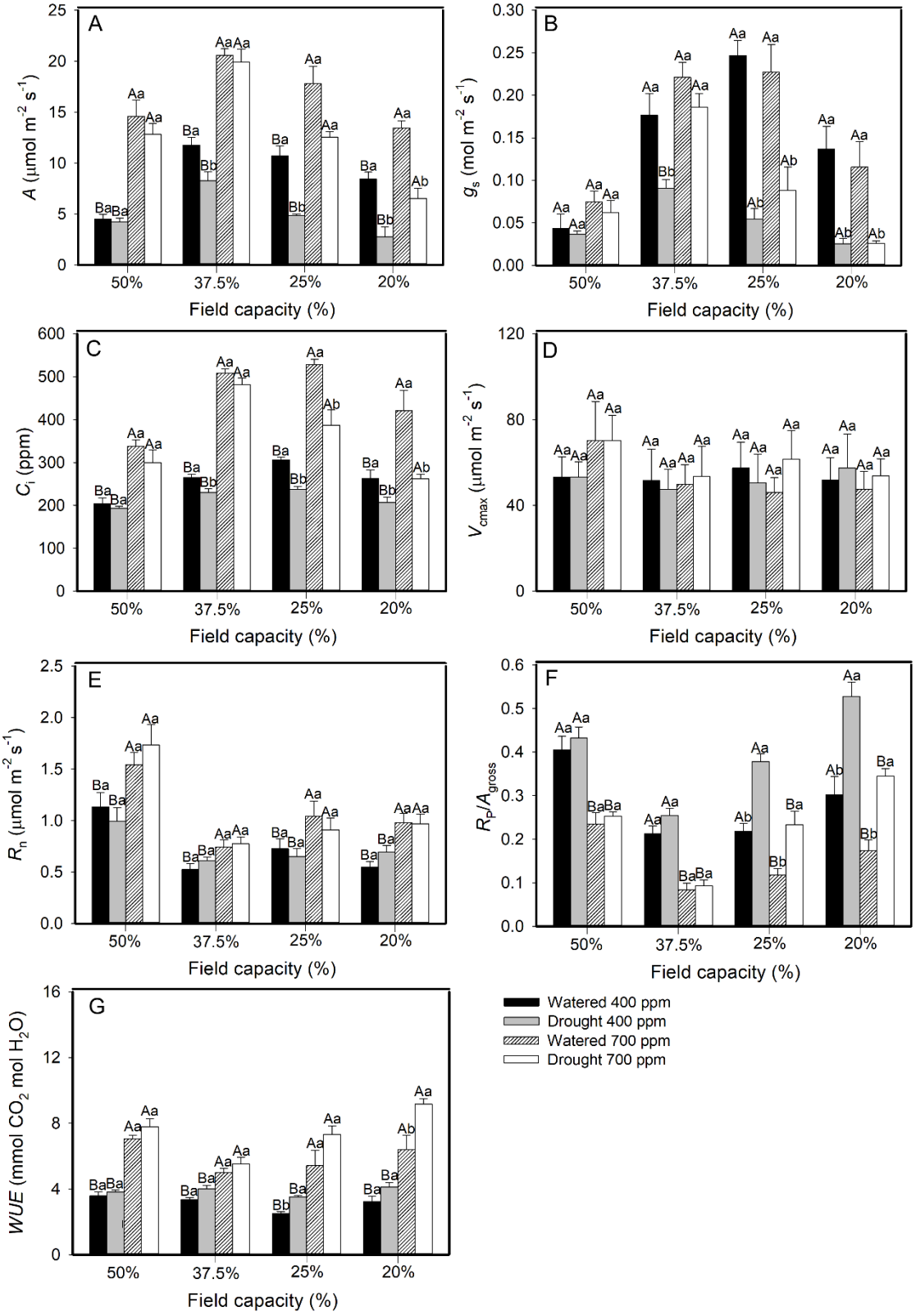


**Figure 2.** The effect of watering (well-watered or drought-stressed plants) and $CO_2$ supply (400 or 700 ppm) on the (A) net photosynthetic rate (*A*), (B) stomatal conductance ($g_s$), (C) internal $CO_2$ concentration ($C_i$), (D) single-point maximum apparent RuBisCO carboxylation capacity on a chloroplast $CO_2$ concentration basis

($V_{cmax}$), (E) nocturnal respiration ($R_n$), (F) photorespiration-to-gross photosynthetic rate ratio ($R_p/A_{gross}$), and water-use efficiency (WUE) (G). For drought-stressed plants, measurements were made at 50, 37.5, 25 and 20% of field capacity. Different lowercase letters indicate differences between watering regimes within a same $CO_2$ supply; different capital letters indicate differences between $CO_2$ treatments within a same watering regime (*Student t*-test, $\alpha = 0.05$; $n = 6 \pm$ SE).

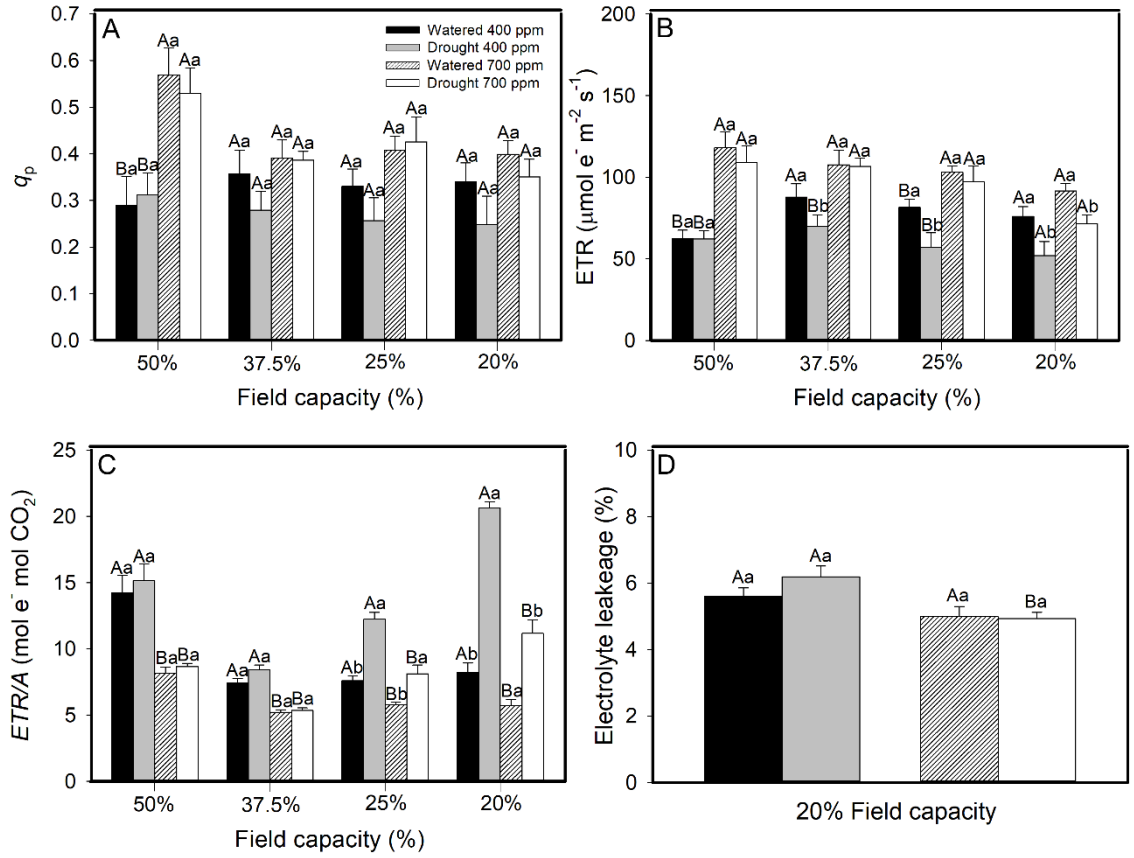


**Figure 3.** The effect of watering (well-watered or drought-stressed plants) and $CO_2$ supply (400 or 700 ppm) on the (A) photochemical quenching coefficient ($q_p$), (B) electron transport rate (ETR), (C) electron transport-to-net photosynthesis rate ratio (ETR*/A)* and (D) electrolyte leakage. For drought-stressed plants, measurements were made at 50, 37.5, 25 and 20% of field capacity (except electrolyte leakage). Different lowercase letters indicate differences between watering regimes within a same $CO_2$ supply; different capital letters indicate differences between $CO_2$ treatments within a same watering regime (*Student t*-test, α= 0.05; *n*= 6 ± SE).

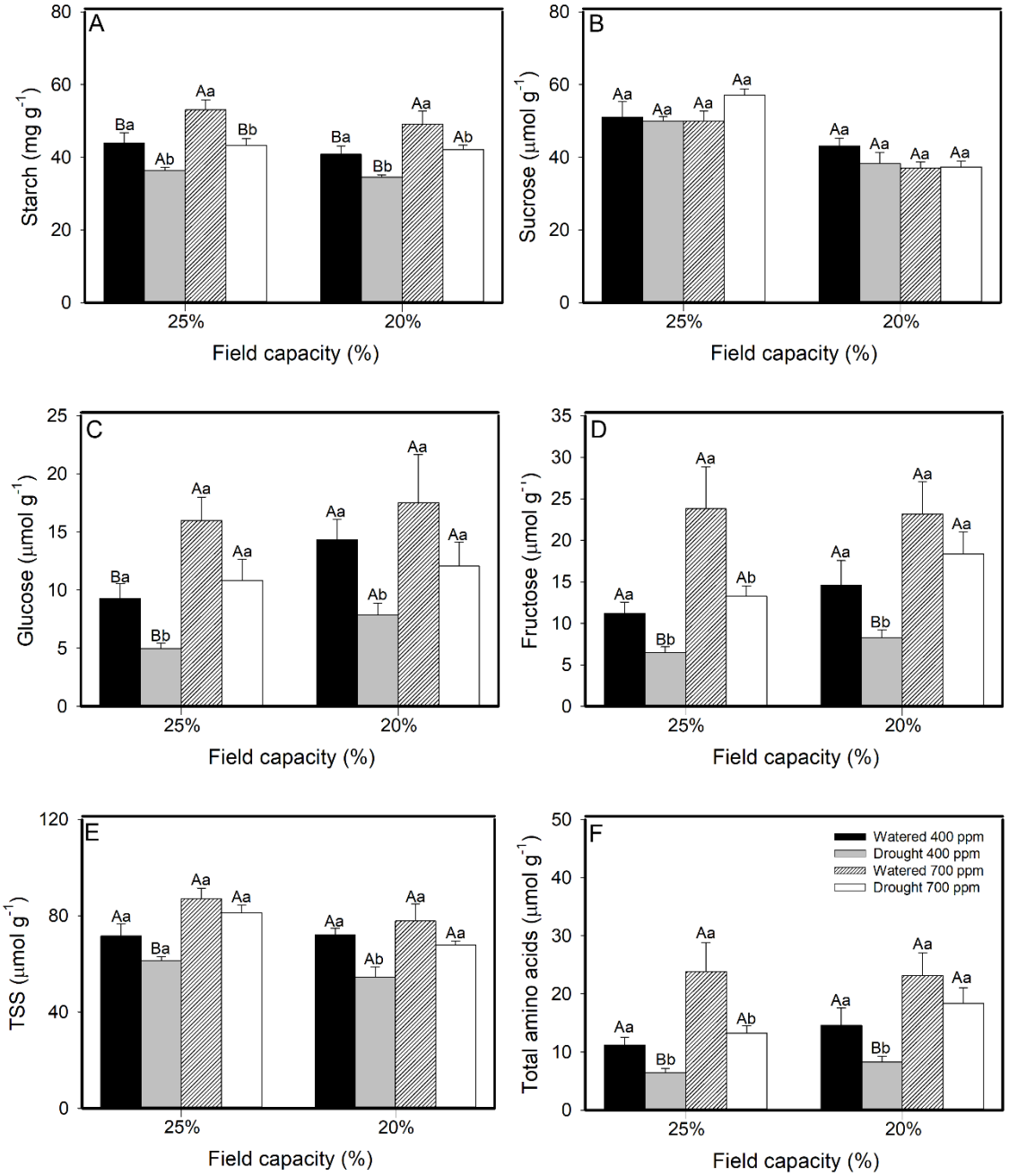


**Figure 4.** The effect of watering (well-watered or drought-stressed plants) and $CO_2$ supply (400 or 700 ppm) on the leaf contents (on a dry weight basis) of (A) starch, (B) sucrose, (C) glucose, (D) fructose, (E) total soluble sugar (TSS) and (F) total amino acids. For drought-stressed plants, measurements were made at 25 and 20% of field capacity. Different lowercase letters indicate differences between watering regimes within a same $CO_2$ supply; different capital letters indicate differences between $CO_2$ treatments within a same watering regime (*Student t*-test, $\alpha = 0.05$; $n = 6 \pm$ SE).

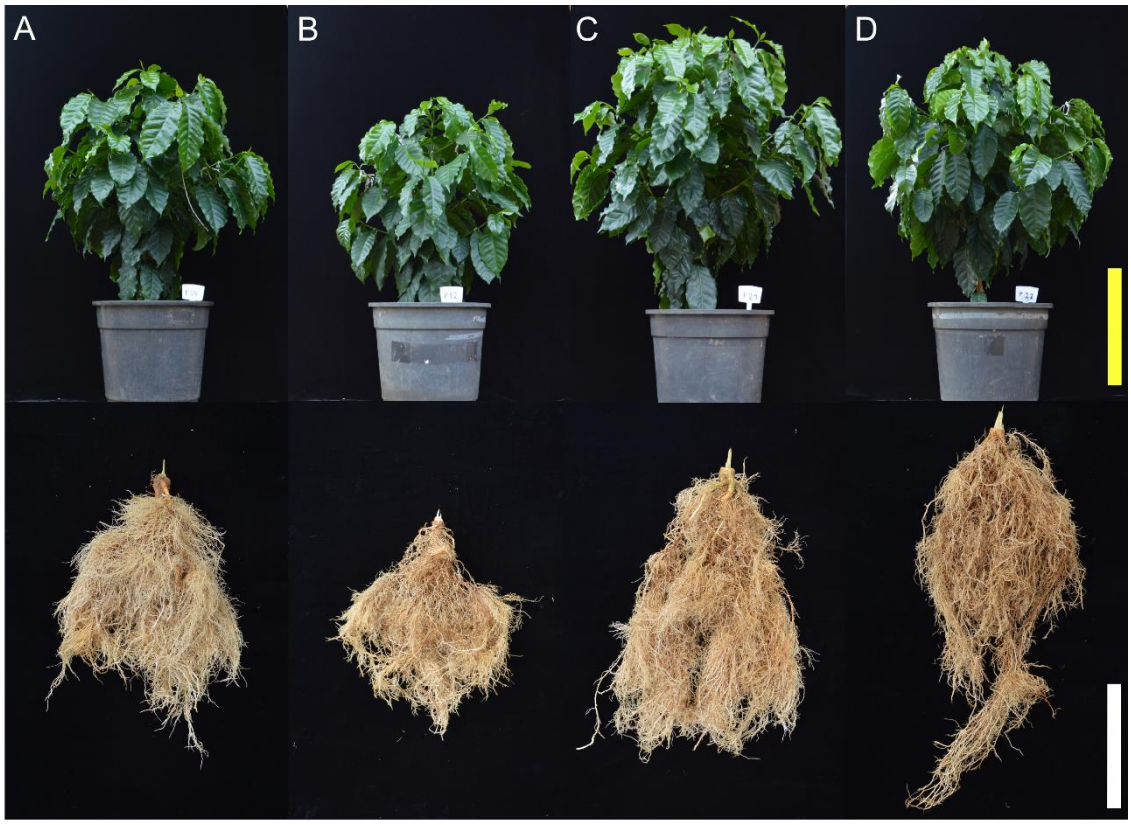


**Figure 5.** Phenotypic appearance of shoot and roots of coffee plants submitted to ambient [$CO_2$] (A, B, respectively, well-watered and drought-stressed plants) or enhanced [$CO_2$] (C, D, respectively well-watered and drought-stressed plants). Yellow (shoot) and white (root) scale bars represent respectively 30 and 20 cm.

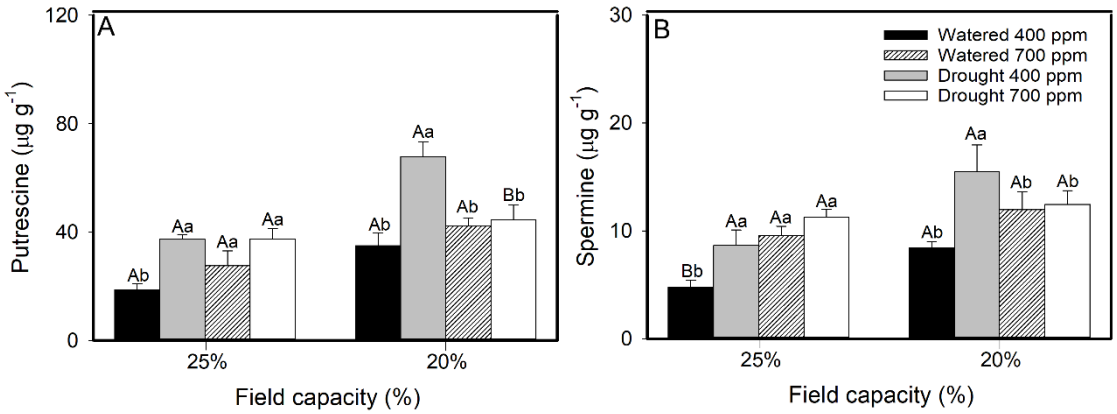


**Figure 6.** The effect of watering (well-watered or drought-stressed plants) and $CO_2$ supply (400 or 700 ppm) on the leaf contents (on a dry weight basis) of (A) putrescine and (B) spermine. For drought-stressed plants, measurements were made at 25 and 20% of field capacity. Different lowercase letters indicate differences between watering regimes within a same $CO_2$ supply; different capital letters indicate differences between $CO_2$ treatments within a same watering regime (*Student t*-test, $\alpha = 0.05$; $n = 6 \pm SE$).

# CHAPTER 3

## Vessel lumen fraction correlates with inter- and intraspecific variation in xylem vulnerability to embolism

**Abstract**

The resistance of xylem conduits to embolism correlates with plant tolerance to drought and can set the distributional limits of species across rainfall gradients. Despite the importance of embolism resistance in ecological and evolutionary adaptation to drought, we have very little understanding of the mechanisms driving differences in embolism resistance. Here, we investigated anatomical determinants of intrageneric variation in xylem embolism in species from the genera *Acer*, *Cinnamomum*, *Ilex*, *Quercus* and *Persea* that were native to environments differing in aridity. We further investigated inter-tree variation in stem and leaf embolism resistance of *Betula pubescens*, and if this potential variation is driven by light in *Phellodendron amurense* and *Ilex verticillata.* Vessel lumen fraction was the only anatomical trait measured that correlated with xylem embolism resistance across scales and species. Light was found to drive only minor differences in stem and not leaf embolism resistance. Our data suggest that conduits highly dispersed in a matrix of imperforate elements may be better protected against the spread of embolism than conduits that are packed in close proximity, which may contribute to our understanding of the mechanisms behind air-seeding.

Keywords: Embolism, xylem, drought, hydraulic segmentation, vessel.

## Introduction

During drought plants may die when the tension on the water column becomes so negative that air invades the xylem causing widespread embolism that permanently breaks the liquid connection between hydrated photosynthetic tissues and soil water (Sperry and Pockman, 1993; Brodribb and Cochard, 2009; Cochard and Delzon, 2013; Charrier *et al*., 2016; Lamarque *et al*., 2018). While there are a number of dynamic strategies plants employ to avoid reaching these lethal water potentials, like closing stomata to reduce water loss (Zhang *et al*., 2016a; Cardoso *et al*., 2018; Choat *et al*., 2018), plants that construct xylem that is able to resist embolism under more negative water potentials may ensure a prolonged survival during drought.

Many studies have presented correlations between the resistance of xylem conduits to embolism and plant tolerance to drought, and have found that embolism resistance can set the distributional limits of species across rainfall gradients (Blackman *et al*., 2009; Brodribb *et al*., 2010; Anderegg *et al*., 2012; Choat *et al*., 2012; Pittermann *et al*., 2012; Li *et al*., 2018). Despite the importance of embolism resistance in ecological and evolutionary adaptation to drought, as well as determining drought tolerance in plants, we have little understanding about the mechanisms driving differences in the vulnerability to embolism across species and within individuals. As homogeneous and heterogeneous nucleation of an air bubble in the xylem is physically unlikely in a reasonable time at water potential values between -1 and -10 MPa (Hölttä *et al*., 2002), air entry into a xylem conduit under negative tension likely occurs through pit membranes, with air having to traverse the porous medium of cellulose fibres to invade the neighbouring water-filled vessel (Sperry and Tyree, 1988; Kaack *et al*., 2019; Zhang *et al*., 2019). The physical and anatomical determinants of this process of air-seeding remain understudied and largely unknown (Jansen *et al*., 2018), thus studies have focused on gross anatomical traits of the xylem to provide potential explanations for differences in embolism resistance across species. To this end a number of traits have been associated with differences in $P_{50}$ (or the water potential at which 50% of the xylem is embolised) between species such as: cell wall thickness and vessel diameter ratio $(t/b)^2$ (Hacke *et al*., 2001; Blackman *et al*., 2010); vessel diameter (Scoffoni *et al*., 2016; Venturas *et al*., 2017); vessel length (Lens *et al*., 2011; Jacobsen *et al*., 2016); and pit membrane thickness (Choat *et al*., 2008; Brodersen *et al*., 2014; Li *et al*., 2016). Species that evolved in arid environments and present high resistance to embolism often have high values of $(t/b)^2$ and pit membrane thickness as

well as relatively narrow vessel diameter and short vessel lengths. The combination of these adaptive features has likely been selected for because they impair either the deformation of vessel conduits under negative tension, the initial seeding of embolism events, or the spread of air bubbles between conduits once an initial embolism has formed.

One of the best examples of the adaptive relevance of embolism resistance to plant survival in dry environments are provided by studies that examine variation in embolism resistance across genera with a wide distributional range. Larter *et al*. (2017) analysed the vulnerability to embolism in 23 species of *Callitris* from across the range of the genus. They found a large range of vulnerability in this clade with $P_{50}$ varying between -3.8 and -18.8 MPa. This extremely large difference in embolism resistance is believed to be ultimately driven by aridity gradients across the continent of Australia. Considerable variability has also been reported in *Quercus* by Skelton *et al*. (2018) with $P_{50}$ ranging from -2.72 to -6.27 MPa across species in this genus. This variation in *Quercus* was significantly correlated with the aridity of the native range of the species examined. Furthermore, across the genus *Acer* $P_{50}$ was found to be correlated with species habitat preferences (Lens *et al*., 2013; Schumann *et al*., 2019). *Acer campestre* a species which occurs commonly in more arid areas of Europe and Asia Minor, has a documented $P_{50}$ of -5.40, while the more mesic adapted species *A. pseudoplatanus* having a $P_{50}$ of -3.10. Schumann *et al*. (2019) analysed the xylem anatomy of these contrasting *Acer* species and found a close correlation between embolism resistance, wood density and pit membrane conductivity. These studies highlight the degree of intrageneric variation in embolism resistance that exists and for which we might use to better understand the anatomical determinants of embolism resistance.

While there is evidence from a number of intergeneric studies that embolism resistance varies across a genus in relation to the aridity of the native range of individual species, there is also evidence that this trait might also vary within a species. Cardoso *et al*. (2018) found that the vulnerability of xylem to embolism in sunflowers was highly responsive to environmental conditions, producing thicker cell walls under water-limited conditions translating into xylem conduits that were more resistant to embolism. A few studies have investigated whether intraspecific variation of $P_{50}$ occurs across the distributional range of a species (Wortemann *et al*., 2011a; David-schwartz *et al*., 2016; Hajek *et al*., 2016; Stojni *et al*., 2017; Lobo *et al*., 2018). Some have found

considerable intraspecific variation in $P_{50}$ (Wortemann *et al*., 2011b; David-schwartz *et al*., 2016; Stojni *et al*., 2017), while other studies have found low intraspecific variation (Hajek *et al*., 2016; Lobo *et al*., 2018).

Without an assessment of the variation in $P_{50}$ within an individual we do not know if intraspecific variation, if it exists, is determined by genetics or the environment. Considerable variation in $P_{50}$ between leaves of *Persea americana* has been associated with variation in drought-induced leaf death across a canopy (Cardoso *et al*., 2019). In terms of driving plasticity across a canopy, light availability comprises one of the greatest environmental factors to influence plant anatomy and thus physiological function. High light microenvironments within the canopy experience higher temperatures and higher vapor pressure deficits (VPD) in comparison to deep shade microenvironments (Bassow and Bazzaz, 1998; Rambo and North, 2008). Because of this, leaves and branches which expand or grow in full sun have higher transpiration rates and experience lower diurnal water potentials than their shaded counterparts (Cochard *et al*., 1999), resulting in extensive anatomical, morphological and consequently, physiological acclimation (Lemoine *et al*., 2002; Carins Murphy *et al*., 2012; Carins Murphy *et al*., 2016). High light acclimated leaves, generally, have reduced leaf area leading to considerable increases in vein density (Carins Murphy *et al*., 2016), increased lamina thickness (Oguchi *et al*., 2005), as well as modifications to xylem anatomy including increased vessel diameter (Cochard *et al*., 1999), pit membrane thickness (Plavcová *et al*., 2011) and possibly changes in vessel length. These morphological modifications have a major influence on the physiological capacity of leaves expanded under high light, with high light adapted leaves having higher leaf hydraulic conductivity, as well as higher rates of gas exchange compared to shade counterparts (Schultz and Matthews, 1993; Carins Murphy *et al*., 2017). There has been work suggesting that sun acclimated stems are more resistant to embolism than shade acclimated branches in angiosperms (Cochard *et al*., 1999; Lemoine *et al*., 2002; Barigah *et al*., 2006; Herbette *et al*., 2010). Exploring embolism resistance across sun and shade microenvironments within a canopy provides an opportunity to determine the drivers of potential intraspecific variation in embolism resistance.

Here we investigate the anatomical drivers behind acclimative and adaptive variation in embolism resistance in plants by examining embolism resistance and cellular anatomy across scales capturing both intrageneric and intraspecific variation in embolism resistance. We selected 11 species from five genera (*Acer*,

*Cinnamomum*, *Ilex*, *Quercus* and *Persea*) that evolved in contrasting environments varying in aridity to investigate the anatomical drivers underlying intrageneric variation in embolism resistance, namely vessel characteristics such as vessel diameter, $(t/b)^2$, and vessel lumen fraction. We further selected two temperate deciduous species, *Phellodendron amurense* and *Ilex verticillata,* in which to investigate anatomical and hydraulic adaptation to light intensity. With the inclusion of *Betula pubescens*, we further investigated the anatomical drivers of hydraulic segmentation between leaves and stems. We primarily used the optical method for detecting embolism in the xylem to construct vulnerability curves (Brodribb *et al*., 2016b). We conducted an experiment to test the validity of this non-hydraulic method by the simultaneous measurement of stem vulnerability curves in *Acer* with the Chinatron centrifuge (Wang *et al*., 2014).

**Material and methods**

*Plant material*

To assess intrageneric variation in embolism resistance and xylem anatomy we selected 11 species from *Acer*, *Cinnamomum*, *Ilex*, *Quercus* and *Persea* that evolved in contrasting environments (Supplementary Table S1). Plants of *A. pseudoplatanus* and *A. campestre* were grown outside in the Botanical Gardens of Ulm University, Ulm (Germany) (48° 25' N, 9° 57' E), *I. paraguariensis* in the glasshouses of the Botanical Gardens of Ulm University, *C. cassia*, *C. camphora*, *P. americana*, *P. indica*, *Q. falcata*, *Q. robur*, *Q. rubra* and some plants of *I. verticillata* (where indicated) were grown in the glasshouses of Purdue University, West Lafayette (Indiana, USA) (40° 25' N, 86° 54' W, elevation: 187 m). Experiments performed in West Lafayette and Ulm were conducted between August and early October 2018 and from June to July 2019, respectively.

To assess intraspecific variation in embolism resistance and xylem anatomy we used two temperate deciduous species, *Phellodendron amurense* Rupr. (Rutaceae) and *I. verticillata* that presented strongly decreased leaf area in high light environments; as well as the shade intolerant deciduous species *Betula pubescens* Ehrh. (Betulaceae), which did not grow any branches or leaves shaded in the canopy. Plants of *Ph. amurense* and *I. verticillata* were grown outside on the Purdue University campus, West Lafayette, Indiana (USA), while plants of *B. pubsecens* were grown outside in the Botanical Gardens of Ulm University, Ulm (Germany). Measurements on *Ph. amurense* and *I. verticillata,* were conducted in August 2018, a year that

experienced no drought with 437 mm of evenly distributed rainfall between May and August (the average annual rainfall for this time period is 424 mm), while measurements on *B. pubescens* were conducted in the late spring, May 2019. Light intensity in sun and shade microenvironments was measured using a light sensor *LI-COR* 6800 (model LI-6800, Li-COR Biosciences Inc., Lincoln, NE, USA). Light intensity in sun microenvironments within the canopy of *Ph. amurense* and *I. verticillata* was 1245 ± 50 μmol $m^{-2}$ $s^{-1}$ and 1152 ± 31 μmol $m^{-2}$ $s^{-1}$, respectively, while light intensity in shade microenvironment was 56 ±13 μmol $m^{-2}$ $s^{-1}$ and 45 ±19 μmol $m^{-2}$ $s^{-1}$, respectively. Stems and leaves grown in both light environments were sampled at the same canopy height to avoid possible variation caused by height induced reductions in intrinsic water potential.

*Vulnerability curves*

Vulnerability curves in stems were conducted using the optical vulnerability imaging method (Brodribb *et al*., 2016b) with stereo microscope (SZMT2, optika, Italy) and Raspberry Pi clamps (opensourceOV.org). Chinatron centrifuge vulnerability curves were also performed for 27 cm long stem segments of the two *Acer* species studied, since these species have relatively short vessels (Schumann *et al*., 2019). Two year old branches collected before dawn in July 2019, were used to construct centrifuge vulnerability curves. Samples were not flushed prior to assessing vulnerability, as flushing was not performed on paired branches for which the optical vulnerability method was used. A reference solution of 10 mM KCl was used.

For optical vulnerability curves, three to four stems of each species, were cut under water early in the morning (0.5 cm up to 2.5 meters long depending on the specie) and placed inside a closed bag containing moist paper towels for 1 hour to equilibrate water potential. A small, terminal stem of current year growth only, was selected for analysis between 0.35 to 2.2 m from the open cut to avoid open vessel artefacts. These had a diameter of 7-11 mm and were randomly selected, the bark was gently removed using a fingernail, with care taken to not touch the xylem. Immediately after bark removal, an adhesive gel (Tensive) was spread onto the exposed xylem and a coverslip placed over the gel. This region was enclosed in the imaging clamp or placed under a stereo microscope. Branches were allowed to dry under darkness while images were taken every 3 min and water potential assessed every 10 minutes using a PSY1 stem Psychrometer (ICT International, version 4.4). In *I. verticillata*,

water potential until leaf death was also concurrently measured in small branches bearing up to 5 leaves using a Scholander Pressure Chamber instrument, (PMS Instrument Company, Model 1505D).

Leaf vulnerability curves (for the intraspecific variation experiment) were performed using the same sampling approach used in stems. For each species, four leaves (still attached to individual branches in *I. verticillata*) or pinna (the dextral pinna immediately below the terminal pinna on the imparimonopinnate leaves of *Ph. amurense*, still attached to the rachis, which was attached to a branch), were scanned (Seiko Epson Corp., Model J371A) using transmitted light (LED lamps, Sungo lighting, model SI-003MFL-40) every 4 minutes. Leaves of *B. pubescens* were imaged using Raspberry Pi clamps. We refer to both leaves and pinna as leaves for simplicity. Initial water potentials for *Ph. amurense* were -1.24 MPa and -1.31 MPa for sun and shade stems, respectively, and for leaves was -1.37 MPa and -1.39 MPa. For *I. verticillata* initial water potential was -1.50 MPa and -0.9 MPa for sun and shade stems and for leaves was -0.46 MPa and -0.64 MPa, respectively. For *B. pubescens* initial leaf water potentials for leaves and stems was -1 MPa. Leaf vulnerability curves in *Ph. amurense* and *I. verticillata* were constructed from water potentials measured periodically in neighbouring leaves using the pressure chamber. Stem and leaf images were analysed in ImageJ (version 1.52h, NIH, USA) to quantify embolism accumulation through time and thus construct vulnerability curves as described by Brodribb *et al*. (2016b).

*Stem and Leaf Anatomy*

Stem xylem anatomy was observed in the segment that was imaged during optical vulnerability curves. For the centrifuge curves a sample was taken from the middle of the stem segment that was used to construct curves. Transverse sections of leaf midribs taken from the base of the lamina, (25 µm thick) were made using a freezing stage-microtome (Thermo scientific, model: HM 430) stained with aqueous 5% toluidine blue and mounted in phenol glycerine jelly. Leaf xylem vessels were identified by exposing the slides to UV light, as lignin in xylem cells auto-fluoresces under UV light. To determine vessel diameter, $(t/b)^2$ and the vessel lumen fraction in the xylem (VLF), images were taken with an Axiocam 506 color camera connected to a light microscope (Zeiss Axio Imager.A2 at 10x and 5x magnification and amplified by 1.6x magnification tube).

To determine $(t/b)^2$, the double wall thickness ($t$) and corresponding xylem lumen breadth ($b$) was determined in 75 vessels from leaves and 125 vessels from stems for each sample. Cell wall thickness was measured between two xylem vessels (avoiding cell wall corners) and the lumen diameter was calculated from vessel area. Assuming that vessel lumen in cross-section was an approximate circle diameter was estimated using equation 1, where $b$ is vessel lumen diameter and $A$ is the area of the vessel lumen.

$$b = 2\ x\ \sqrt{A/\pi}. \quad \text{(Eq. 1)}$$

VLF was determined by summing all $A$ values for each cross-section and expressing this area as a percentage of total xylem area using equation 2. For stems, the VLF values were based on wood tissue, while the VLF measurements of leaves were based on xylem of the vascular bundle. Despite major differences in mechanical properties and storage capacity between secondary xylem of the stem and xylem in vascular bundles, the water transport properties and in particular embolism resistance can directly be compared between tracheary elements in wood and vascular bundles.

$$VLF\ = \frac{\sum A}{Xylem\ area}\ x\ 100. \quad \text{(Eq. 2)}$$

To quantify vein density ($D_{vein}$), leaf tissue was placed in 10 % (m $v^{-1}$) NaOH in water for 3 h at 50 °C and then submerged in 20 % (v $v^{-1}$) NaOCl in water until completely transparent, washed twice in water for 20 minutes and stained with aqueous 5% toluidine blue (*Ph. amurense*) or aqueous safranin (*I. verticillata*). Images was placed at 5x magnification and amplified by 1.6x magnification tube using the above described microscope, $D_{\text{vein}}$ was determined as follows:

$$D_{\text{vein}}\ = \frac{Total\ length\ of\ veins\ (mm)}{Total\ area\ (mm^2)} \quad \text{(Eq. 3)}$$

*Physiological parameters*

Leaf gas exchange parameters [net photosynthetic rate ($A_N$) and stomatal conductance ($g_s$)] were measured using the *LI-COR* 6800. Measurements were carried out at the leaf level at an artificial photon irradiance of 1,000 and 100 µmol $m^{-2}$ $s^{-1}$ for sun and shade acclimated leaves respectively, and partial pressure of $CO_2$ of 40 Pa. Turgor lost point (TLP) and leaf capacitance at turgor lost point ($C_{leaf}$) were measured by pressure-volume curves following the methodology described in Tyree *et al*. (Tyree *et al*., 1972). Leaf hydraulic conductance ($K_{leaf}$) was calculated as described by Brodribb and Holbrook (2003).

## Results

*A large intrageneric variation in stem $P_{50}$*

We found a large variation in stem $P_{50}$ ranging from -2.07 up to -6.80 MPa across all species measured. Between species in the same genus we found significant differences in embolism resistance, with the exception of *Ilex* in which the Northern temperate deciduous species *Ilex vercitillata* and the Southern, subtropical evergreen species *I. paraguariensis* presented the same mean $P_{50}$ (-4.00 ± 0.42 MPa and -5.03 ± 0.89 MPa respectively) (Fig. 1*a*-*e*). *Persea americana*, native to subtropical rainforest was more vulnerable, with a mean stem $P_{50}$ of -2.30 ± 0.20 MPa, than the Macronesian native *P. indica*, with a mean stem $P_{50}$ of -4. 53 ± 0.47 MPa. *Cinnamomum cassia*, which is native to midly seasonal subtropical forest, had a mean stem $P_{50}$ of -3.08 ± -0.20 MPa, which was more vulnerable than the stems of *C. camphora*, native to very seasonal subtropical forests with a mean stem $P_{50}$ of -5.90 ± 0.35 MPa. Modest variation in mean stem $P_{50}$ was observed across *Quercus* species with *Q. falcata*, *Q. robur*, and *Q. rubra* having a mean stem $P_{50}$ of -3.53 ± 0.35 MPa, -4.00 ± 0.42 MPa and -5.03 ± 0.89 MPa, respectively. In *Acer* the optical method and the Chinatron centrifuge were used to construct vulnerability curves, these two methods resulted in identical embolism resistance curves in the stems of both species, with a mean $P_{50}$ of -2.87 ± 0.24 MPa and -5.2 ± 0.12 MPa respectively for *A. pseudoplatanus* and *A. campestre* (Figure 1*b*). Optical vulnerability curve montages of species demonstrating the embolised area are presented in Supplementary Figure S1 and S2.

Mean stem $P_{50}$ strongly correlated with VLF within each of the five genera examined, as well as across all samples pooled together ($r = 0.53$, $p$-value < 0.001) (Fig. 2*a*-*f*). Across all genera the higher the VLF, the more vulnerable the stem xylem was to embolism. Correlations within genera were generally very strong, with r values higher than 0.84 for four of the five genera. The weakest, yet still significant, correlation was observed across the three species from the ring-porous genus *Quercus* ($r = 0.53$, $p$-value < 0.001).

*Minor acclimation of $P_{50}$ to light in stems and leaves*

To test whether light intensity altered embolism resistance across the canopy, vulnerability curves were constructed within the canopy of two deciduous species. In *Phellodendron amurense* sun and shade acclimated stems had the same mean $P_{50}$, -4.6 ± 0.45 and -4.13 ± 0.46 MPa respectively ($P_{value} = 0.4734$) (Fig. 3*a*). Sun acclimated

stems of *Ilex verticillata* (-6.83 ± 0.31 MPa) were significantly ($P_{value}$ < 0.01) more resistant than shade-acclimated counterparts (-5.02 ± 0.24 MPa) (Fig. 3*b*). In stems acclimated to different light intensities in *I. verticillata* $P_{50}$ was significantly correlated with VLF, with less resistant stems having a higher VLF (Fig. 3*b*), in *Ph. amurense* there was no significant difference in VLF between sun and shade stems that had the same $P_{50}$ (Fig. 3).

No variation in $P_{50}$ between sun and shade acclimated leaves was observed in both *Ph. amurense* and *I. verticillata* (-2.67 ± 0.25 and -2.54 ± 0.28 MPa for *Ph. amurense* and -1.64 ± 0.13 and -1.63 ± 0.11 MPa for *I. verticillata*, sun and shade leaves respectively) (Fig. 3*a,c*). This lack of difference in embolism resistance between sun and shade acclimated leaves contrasted with the strong anatomical alterations triggered by light availability in *Ph. amurense* and *I. verticillata* that correlated with considerable variation in leaf physiology. Sun leaves had higher rates of gas exchange reflected in both higher $A_N$ and $g_s$ (70 and 80% for *Ph. amurense* and 79 and 42 % for *I. verticillata*, respectively) than shade acclimated leaves for both species (Table 1). Increased $D_{vein}$ (Table 1) in sun leaves corresponded with a higher $K_{leaf}$ (301% and 207%, for *Ph. amurense* and *I. vertcillata*, respectively) in comparison to their shade counterparts (Table 1).

The water potential at the onset embolism ($P_e$), did not vary in response to light condition in either stems or leaves in *Ph. amurense*, being -1.65 ± 0.06 and -2.13 ± 0.39 MPa, respectively; which was after the water potential at turgor loss point (TLP) (mean TLP = -1.20 ± 0.07 MPa) (Fig. 3*a*). However, in *I. verticillata,* $P_e$ for leaves (from both sun and shade) and shade acclimated stems occurred around TLP (-1.27 ± 0.09 MPa), while sun acclimated stems had a lower $P_e$ of -1.90 ± 0.18 MPa (Fig. 3*b*).

*Vessel lumen fraction explains hydraulic segmentation between stems and leaves*

Considerable segmentation in xylem embolism resistance was observed in both *Ph. amurense* and *I. verticillata*, while none was observed in the species *Betula pubescens* (Fig. 3*a-c*). *P. amurense* stems were 1.76 MPa more resistant to embolism than leaves, in terms of mean $P_{50}$ (Fig. 3*a*). *I. verticillata* sun acclimated stems were 5.19 MPa more resistant to embolism formation than sun acclimated leaves, while shade stems were 3.39 MPa more resistant than leaves in terms of mean $P_{50}$ (Fig. 3*b*). In all three species, embolism in leaves was first observed in the midrib followed by secondary and lastly minor veins. In *B. pubescens* which displayed no hydraulic segmentation between leaves and stems, no difference in VLF was observed between these tissues (Fig. 3*c*).

VLF was found to correlate with embolism resistance across leaf samples in all three species examined (Fig. S3). When data was pooled from all samples including stems and leaves, from the thirteen species examined across seven genera, a correlation was observed between VLF and $P_{50}$ ($r = 0.58$, $P<0.001$), with the most embolism resistant samples having the lowest VLF (Fig. 4). This correlation was observed despite considerable variation in the intercepts and slopes of regressions within individual genera or species. We also assessed whether embolism resistance correlated with $(t/b)^2$ and vessel diameter across scales. Neither of these traits were significantly correlated with $P_{50}$ between species, within genera or within a same individual (Fig S4 and S5). $(t/b)^2$ was extremely variable across samples (from 0.001 to 0.274) primarily because of large variability of diameter dimensions (7.5 to 53 µm in average), which did not correlate with embolism resistance.

**Discussion**

We found that vessel lumen area as a percentage of total xylem area (VLF) strongly correlated with $P_{50}$ across all scales. Across 13 species, as well as between leaves and stems, VLF correlates with both inter- and intraspecific variation observed in xylem vulnerability to embolism. In *B. pubescens* we did not find any hydraulic segmentation between leaves and stems, and concurrently we observed no difference in VLF between the xylem of stems and leaves. Our results suggest that VLF is not only selected for when species evolve into more arid or seasonal environments, but also varies across a canopy that develops under different environmental conditions such light levels, and may vary between and within organs. Consequently, VLF may be a driver of adaptation in embolism resistance across species, in response to changes in the environment and of hydraulic segmentation across the plant body.

Decreased VLF might offer protection against the spread of embolism between vessels when water potential declines. It could be suggested that the spreading of embolism by air-seeding through pit membranes is decreased by reducing the contact area between conduits. Bordered pits will only develop in a conduit wall that is connected to another vessel or a tracheid, while pits generally do not occur between a vessel and non-conductive imperforate tracheary elements (Sano *et al*., 2008; Sano *et al*., 2011). In this way, xylem tissue that does not embolises (Zhang *et al*., 2016b) and contributes very little to water transport, including fibres and parenchyma may impair the spread of bubbles through the xylem (Jacobsen *et al*., 2005). This avoidance of air-seeding by

the non-conduit xylem matrix may translate to changes in xylem vulnerability, with more negative water potentials required to trigger embolism formation in more protected vessels. In contrast, when vessels are packed into xylem in close proximity, with minimal non-vessel matrix, the chance of embolism spreading between vessels at negative water potentials increases, reducing the vulnerability of the xylem. Species with greater lignification, have more resistant xylem, this increased lignification and embolism resistance might be due to increased non-vessel lignification, such as increased fibres in the xylem matrix (Lens *et al*., 2016; Dória *et al*., 2018).

We found that vessel conduit dimensions did not correlate with xylem vulnerability. Although there have been many publications correlating cell wall thickness and vessel diameter ratio $(t/b)^2$ (Hacke *et al*., 2001; Blackman *et al*., 2010), the diameter of vessels (Scoffoni *et al*., 2016; Hacke *et al*., 2017) and vessel length (Lens *et al*., 2011; Jacobsen *et al*., 2016) to interspecific variation in xylem vulnerability, our results suggest that this might not be a rule to variations in $P_{50}$. Overall, although the exact mechanism remains unresolved, our results show that xylem vulnerability might be more a function of proximity of vessels in the xylem, possibly facilitating the spread of embolism between conduits. How alterations in VLF could interfere with vessel-to-vessel connectivity, vessel and imperforate tracheary connections and what the importance of these connections are for preventing embolism spread could be useful for a deeper understanding about the drivers of embolism resistance and should be a matter for future studies (Choat *et al*., 2005; Rockwell *et al*., 2014; Charrier *et al*., 2016; Choat *et al*., 2016; Hochberg *et al*., 2016; Hochberg *et al*., 2017). Despite variation in vessel diameter numerous studies, including here, have observed the midrib of leaves to be the first order of veins to embolise during dehydration [39,52,63]. It could be that the xylem of the midrib contains more highly vulnerable xylem elements, as has been proposed before [67], such as primary xylem has incompletely lignified secondary cell walls, or is more dispersed with intercellular air spaces [4].

Although the vulnerability segmentation hypothesis appears to not be a rule in all angiosperms species (Pivovaroff *et al*., 2014; Charrier *et al*., 2016; Johnson *et al*., 2016; Skelton *et al*., 2017; Klepsch *et al*., 2018; Skelton *et al*., 2018) as found here in *B. pubescens*, we found extreme segmentation in xylem resistance to embolism between stems and leaves in *Ph. amurense* and *I. verticillata*. In these three temperate deciduous species, we found that the presence and degree of hydraulic segmentation between leaves and stems was correlated with the VLF, with no segmentation

observed in *B. pubescens* in which no difference in VLF between stem and leaf xylem was found. The high degree of vulnerability segmentation in two of these species might be a strategy that evolved to allow leaves to operate as fuses, decreasing plant transpiration during mild drought thus protecting stems from further desiccation (Chen *et al*., 2009; Chen *et al*., 2010). However, it should be noted that the initial embolisms observed in stems of the two species with considerable hydraulic segmentation, which occurred over a substantial range in water potential, might have been caused by leaf death triggering these incipient embolism events. Perhaps strong segmentation in xylem resistance to embolism may have a cost for the plant, in that as leaves die, a small proportion of xylem in the stem is concurrently lost to embolism. However this will depend on whether there is a hydraulic connection of vessels through the abscission zone, or whether this connection is provided by tracheids (André *et al*., 1999).

Surprisingly, minor acclimation of xylem vulnerability to embolism in response to light availability was found in *Ph. amurense* and *I. verticillata* even though extensive anatomical and hydraulic acclimation in the xylem occurred. In contrast to our hypothesis, the vulnerability of leaves was not more plastic than stems. The only significant variation in $P_{50}$ between organs from different light environments in the canopy was found in *I. verticillata* stems, which presented the most tolerant xylem conduits in this study. We are tempted to hypothesize that species with more resistant xylem might present higher acclimation responses to environmental conditions. This might explain why there is higher variation in $P_{50}$ between similar organs in plants that have more resistant xylem (Lamarque *et al*., 2018; Rodriguez-Dominguez *et al*., 2018) compared to those that have less resistant xylem (Brodribb *et al*., 2016a; Cardoso *et al*., 2019). This concept might also explain why we did not see any acclimation at the leaf level, which has comparatively more vulnerable xylem. In contrast to our findings, Barigah *et al*. (Barigah *et al*., 2006), by generating vulnerability curves using air injection, found that sun acclimated stems from four species presented lower vulnerability than shade acclimated stems with $P_{50}$ ranging from 1.72 and 2.51 MPa in shade stems and from 2.05 to 2.72 MPa in sun stems. Cochard *et al*. (Cochard *et al*., 1999), Lemoine *et al*. (Lemoine *et al*., 2002) and Herbette *et al*. (Herbette *et al*., 2010) also found similar results by air injection or the cavitron respectively, measuring losses in hydraulic conductivity in 2-3 cm long stems in *Fagus sylvatica*, although vessel length was not determined. Further studies are required, using non-invasive methods

for assessing vulnerability to test acclimation responses to light availability in extremely tolerant species to better understand the capacity of xylem vulnerability to acclimate. Although anatomical changes in leaves correlated with leaf physiological parameters in both species, a lack of alteration in $P_{50}$ challenges the theory of a safety and efficiency trade-off in plant hydraulics (Wagner *et al*., 1998; Pratt *et al*., 2007; Gleason *et al*., 2016) operating within an individual. This theory states that plants with highly efficient xylem vessels are more vulnerable to the formation of embolism (Tyree *et al*., 1994). Sun leaves in *Ph. amurense* and *I. verticillata* did not present lower vulnerability to embolism even though they displayed higher hydraulic conductivity in comparison to shade leaves. Higher hydraulic conductivity is likely due to the decreased leaf area in sun leaves, which translates into an increased vein density (Carins Murphy *et al*., 2012; Carins Murphy *et al*., 2016). However, in sun leaf midribs there were fewer xylem vessels in comparison to shade leaves, suggesting that cell size and number may have changed as sun leaves developed. Sun microenvironments expose leaves to more negative water potentials because of higher evaporative demands in comparison to shade microenvironments, thus leaves in sun microenvironments require more efficient delivery of water for stomata to remain open. However, building more efficient yet more vulnerable leaves (as hypothesized by the trade-off theory) seems unlikely. We found that sun acclimated leaves have an increased efficiency to deliver water to stomata without being constructed in a way that compromises resistance to embolism formation.

In summary, we found that alterations in VLF correlate with differences in xylem resistance to embolism inter- and intra-specifically. It seems that vessels that are more dispersed in a matrix of tracheids, fibres and parenchyma may be more protected against the spread of embolism and thus more resistant to embolism formation. VLF was found to correlate with $P_{50}$ not just when xylem acclimates within a species to different environmental conditions, but also across clades of species adapted to different aridities. In this way, $P_{50}$ may be not just a function of how resistant an individual xylem vessel conduit is but also a function of how easily incipient embolism might spread through the xylem.

**References**

**Anderegg WRL, Berry JA, Smith DD, Sperry JS, Anderegg LDL** (2012) The roles of hydraulic and carbon stress in a widespread climate-induced forest die-off.

PNAS **109**: 233–237

**André JP, Catesson AM, Liberman M** (1999) Characters and origin of vessels with heterogenous structure in leaf and flower abscission zones. Can J Bot **77**: 253–261

**Barigah TS, Ibrahim T, Bogard A, Lagneau LA, Montpied P** (2006) Irradiance-induced plasticity in the hydraulic properties of saplings of different temperate broad-leaved forest tree species. Tree Physiol **26**: 1505–1516

**Bassow SL, Bazzaz FA** (1998) How enviromental conditions affect canopy leaf-level photosynthesis in four deciduous tree species. Ecology **79**: 2660–2675

**Blackman CJ, Brodribb TJ, Jordan GJ** (2010) Leaf hydraulic vulnerability is related to conduit dimensions and drought resistance across a diverse range of woody angiosperms. New Phytol **188**: 1113–1123

**Blackman CJ, Brodribb TJ, Jordan GJ** (2009) Leaf hydraulics and drought stress: response, recovery and survivorship in four woody temperate plant species. Plant Cell Environ **32**: 1584–1595

**Brodersen C, Jansen S, Choat B, Rico C, Pittermann J** (2014) Cavitation resistance in seedless vascular plants: the structure and function of interconduit pit membranes. Plant Physiol **165**: 895–904

**Brodribb TJ, Bienaimé D, Marmottant P** (2016a) Revealing catastrophic failure of leaf networks under stress. **113**: 4865–4869

**Brodribb TJ, Bowman DJMS, Nichols S, Delzon S, Burlett R** (2010) Xylem function and growth rate interact to determine recovery rates after exposure to extreme water deficit. New Phytol **188**: 533–542

**Brodribb TJ, Cochard H** (2009) Hydraulic failure defines the recovery and point of death in water-stressed conifers. Plant Physiol **149**: 575–584

**Brodribb TJ, Holbrook NM** (2003) Stomatal closure during leaf dehydration, correlation with other leaf physiological traits. Plant Physiol **132**: 2166–2173

**Brodribb TJ, Skelton RP, Mcadam SAM, Lucani CJ, Marmottant P** (2016b) Visual quantification of embolism reveals leaf vulnerability to hydraulic failure. New Phytol **209**: 1402–1409

**Cardoso AA, Batz TA, Mcadam SAM** (2019) Xylem embolism resistance determines leaf mortality during drought in Persea americana. Plant Physiol. doi: 10.1201/9781351072571

**Cardoso AA, Brodribb TJ, Lucani CJ, DaMatta FM, Mcadam SAM** (2018)

Coordinated plasticity maintains hydraulic safety in sunflower leaves. Plant Cell Environ **41**: 2567–2576

**Carins Murphy MR, Dow GJ, Jordan GJ, Brodribb TJ** (2017) Vein density is independent of epidermal cell size in Arabidopsis mutants. Funct Plant Biol **44**: 410

**Carins Murphy MR, Jordan GJ, Brodribb TJ** (2012) Differential leaf expansion can enable hydraulic acclimation to sun and shade. Plant, Cell Environ **35**: 1407–1418

**Carins Murphy MR, Jordan GJ, Brodribb TJ** (2016) Cell expansion not cell differentiation predominantly co-ordinates veins and stomata within and among herbs and woody angiosperms grown under sun and shade. Ann Bot **118**: 1127–1138

**Charrier G, Torres-ruiz JM, Badel E, Burlett R, Choat B, Cochard H, Delmas CEL, Domec J, Jansen S, King A, *et al*** (2016) Evidence for hydraulic vulnerability segmentation and lack of xylem refilling under tension. Plant Physiol **172**: 1657–1668

**Chen JW, Zhang Q, Li XS, Cao KF** (2009) Independence of stem and leaf hydraulic traits in six Euphorbiaceae tree species with contrasting leaf phenology. Planta **230**: 459–468

**Chen JW, Zhang Q, Li XS, Cao KF** (2010) Gas exchange and hydraulics in seedlings of *Hevea brasiliensis* during water stress and recovery. Tree Physiol **30**: 876–885

**Choat B, Badel E, Burlett R, Delzon S, Cochard H, Jansen S** (2016) Noninvasive measurement of vulnerability to drought-induced embolism by X-Ray microtomography. Plant Physiol **170**: 273–282

**Choat B, Brodribb TJ, Brodersen CR, Duursma RA, López R, Medlyn BE** (2018) Triggers of tree mortality under drought. Nature **558**: 531–539

**Choat B, Choat B, Cobb AR, Jansen S** (2008) Structure and function of bordered pit: new discoveries and impacts on whole-plant hydraulic function. New Phytol **177**: 608–626

**Choat B, Jansen S, Brodribb TJ, Cochard H, Delzon S, Bhaskar R, Bucci SJ, Feild TS, Gleason SM, Hacke UG, *et al*** (2012) Global convergence in the vulnerability of forests to drought. Nature **491**: 752–756

**Choat B, Lahr EC, Melcher PJ, Zwieniecki MA, Holbrook NM** (2005) The spatial pattern of air seeding thresholds in mature sugar maple trees. Plant, Cell Environ **28**: 1082–1089

**Cochard H, Delzon S** (2013) Hydraulic failure and repair are not routine in trees. Ann For Sci **70**: 659–661

**Cochard H, Lemoine D, Dreyer E** (1999) The effects of acclimation to sunlight on the xylem vulnerability to embolism in *Fagus sylvatica* L. Plant Cell Environ **22**: 101–108

**David-schwartz R, Paudel I, Mizrachi M, Delzon S, Werner C** (2016) Indirect evidence for genetic differentiation in vulnerability to embolism in *Pinus halepensis*. Front Plant Sci **7**: 1–13

**Dória LC, Podadera DS, del Arco M, Chauvin T, Smets E, Delzon S, Lens F** (2018) Insular woody daisies (*Argyranthemum, Asteraceae*) are more resistant to drought-induced hydraulic failure than their herbaceous relatives. Funct Ecol **32**: 1467–1478

**Gleason SM, Westoby M, Jansen S, Choat B, Hacke UG, Pratt RB, Bhaskar R, Brodribb TJ, Bucci SJ, Cao K, *et al*** (2016) Weak tradeoff between xylem safety and xylem-specific hydraulic efficiency across the world's woody plant species. New Phytol **209**: 123–136

**Hacke UG, Sperry JS, Pockman WT, Davis SD, Mcculloh KA** (2001) Trends in wood density and structure are linked to prevention of xylem implosion by negative pressure. Oecologia **126**: 457–461

**Hacke UG, Spicer R, Schreiber SG, Plavcová L** (2017) An ecophysiological and developmental perspective on variation in vessel diameter. Plant Cell Environ **40**: 831–845

**Hajek P, Kurjak D, Wühlisch G Von, Delzon S** (2016) Intraspecific variation in wood anatomical, hydraulic, and foliar traits in ten european beech provenances differing in growth yield. Front Plant Sci **7**: 1–14

**Herbette S, Wortemann R, Awad H, Huc R, Cochard H, Barigah TS** (2010) Insights into xylem vulnerability to cavitation in *Fagus sylvatica* L.: phenotypic and environmental sources of variability. Tree Physiol **30**: 1448–1455

**Hochberg U, Albuquerque C, Rachmilevitch S, Cochard H, David-Schwartz R, Brodersen CR, McElrone A, Windt CW** (2016) Grapevine petioles are more sensitive to drought induced embolism than stems: evidence from in vivo MRI and microcomputed tomography observations of hydraulic vulnerability segmentation. Plant Cell Environ **39**: 1886–1894

**Hochberg U, Windt CW, Ponomarenko A, Zhang YJ, Gersony J, Rockwell FE,**

**Holbrook NM** (2017) Stomatal closure, basal leaf embolism, and shedding protect the hydraulic integrity of grape stems. Plant Physiol **174**: 764–775

**Hölttä T, Vesala T, Perämäki M, Nikinmaa E** (2002) Relationships between embolism, stem water tension, and diameter changes. J Theor Biol **215**: 23–38

**Jacobsen AL, Ewers FW, Pratt RB, Ill WAP, Davis SD** (2005) Do xylem fibers affect vessel cavitation resistance? Plant Physiol **139**: 546–556

**Jacobsen AL, Tobin MF, Toschi HS, Percolla MI, Pratt RB** (2016) Structural determinants of increased susceptibility to dehydration-induced cavitation in post-fire resprouting chaparral shrubs. Plant Cell Environ **39**: 2473–2485

**Jansen S, Klepsch M, Li S, Kotowska MM, Schiele S, Zhang Y, Schenk HJ** (2018) Challenges in understanding air-seeding in angiosperm xylem. Acta Hortic **1222**: 13–20

**Johnson DM, Wortemann R, McCulloh KA, Jordan-Meille L, Ward E, Warren JM, Palmroth S, Domec JC** (2016) A test of the hydraulic vulnerability segmentation hypothesis in angiosperm and conifer tree species. Tree Physiol **36**: 983–993

**Kaack L, Altaner CM, Carmesin C, Diaz A, Holler M, Kranz C, Neusser G, Odstrcil M, Schenk H jochen, Schmidt V, *et al*** (2019) Function and three-dimensional structure of intervessel pit membranes in angiosperms: a review. IAWA J In Press

**Klepsch M, Zhang Y, Kotowska MM, Lamarque LJ, Nolf M, Schuldt B, Torres-Ruiz JM, Qin DW, Choat B, Delzon S, *et al*** (2018) Is xylem of angiosperm leaves less resistant to embolism than branches? Insights from microCT, hydraulics, and anatomy. J Exp Bot **69**: 5611–5623

**Lamarque LJ, Corso D, Torres-ruiz JM, Badel E, Brodribb TJ, Burlett R** (2018) An inconvenient truth about xylem resistance to embolism in the model species for refilling *Laurus nobilis* L. Ann For Sci **88**: 1–15

**Larter M, Pfautsch S, Domec JC, Trueba S, Nagalingum N, Delzon S** (2017) Aridity drove the evolution of extreme embolism resistance and the radiation of conifer genus *Callitris*. New Phytol **215**: 97–112

**Lemoine D, Jacquemin S, Granier A** (2002) Beech (*Fagus sylvatica* L.) branches show acclimation of xylem anatomy and hydraulic properties to increased light after thinning. Ann For Sci **59**: 761–766

**Lens F, Picon-Cochard C, Delmas CEL, Signarbieux C, Buttler A, Cochard H, Jansen S, Chauvin T, Doria LC, Del Arco M, *et al*** (2016) Herbaceous angiosperms are not more vulnerable to drought-induced embolism than

angiosperm trees. Plant Physiol **172**: 661–667

**Lens F, Sperry JS, Christman MA, Choat B, Rabaey D, Jansen S** (2011) Testing hypotheses that link wood anatomy to cavitation resistance and hydraulic conductivity in the genus *Acer*. New Phytol **709**: 709–723

**Lens F, Tixier A, Cochard H, Sperry JS, Jansen S, Herbette S** (2013) Embolism resistance as a key mechanism to understand adaptive plant strategies. Curr Opin Plant Biol **16**: 287–292

**Li S, Lens F, Karimi Z, Klepsch MM** (2016) Intervessel pit membrane thickness as a key determinant of embolism resistance in angiosperm xylem. IAWA J **37**: 152–171

**Li X, Blackman CJ, Choat B, Rymer PD, Medlyn BE, Tissue DT** (2018) Tree hydraulic traits are coordinated and strongly linked to climate-of-origin across a rainfall gradient. Plant Cell Physiol **41**: 646–660

**Lobo A, Torres-ruiz JM, Burlett R, Lemaire C, Parise C, Francioni C, Truffaut L, Tomásková I, Hansen JK, Kjaer ED, *et al*** (2018) Assessing inter- and intraespecific variability of xylem vulnerability to embolism in oaks. For Ecol Manage **424**: 53–61

**Oguchi R, Hikosaka K, Hirose T** (2005) Leaf anatomy as a constraint for photosynthetic acclimation: differential responses in leaf anatomy to increasing growth irradiance among three deciduous trees. Plant Cell Environ **28**: 916–927

**Pittermann J, Stuart SA, Dawson TE, Moreau A** (2012) Cenozoic climate change shaped the evolutionary ecophysiology of the Cupressaceae conifers. PNAS **109**: 9647–9652

**Pivovaroff AL, Sack L, Santiago LS** (2014) Coordination of stem and leaf hydraulic conductance in southern California shrubs: a test of the hydraulic segmentation hypothesis. New Phytol **203**: 842–850

**Plavcová L, Hacke UG, Sperry JS** (2011) Linking irradiance-induced changes in pit membrane ultrastructure with xylem vulnerability to cavitation. Plant, Cell Environ **34**: 501–513

**Pratt RB, Jacobsen AL, Ewers FW, Davis SD** (2007) Relationships among xylem transport, biomechanics and storage in stems and roots of nine Rhamnaceae species of the California chaparral. New Phytol **174**: 787–798

**Rambo ATR, North MP** (2008) Spatial and temporal variability of canopy microclimate in a sierra nevada riparian forest. Northwest Sci **82**: 259–268

**Rockwell FE, Wheeler JK, Holbrook NM** (2014) Cavitation and its discontents: opportunities for resolving current controversies. Plant Physiol **164**: 1649–1660

**Rodriguez-Dominguez CM, Carins Murphy MR, Lucani C, Brodribb TJ** (2018) Mapping xylem failure in disparate organs of whole plants reveals extreme resistance in olive roots. New Phytol **218**: 1025–1035

**Sano Y, Morris H, Shimada H, Ronse De Craene LP, Jansen S** (2011) Anatomical features associated with water transport in imperforate tracheary elements of vessel-bearing angiosperms. Ann Bot **107**: 953–964

**Sano Y, Ohta T, Jansen S** (2008) The distribution and structure of pits between vessels and imperforate tracheary elements in angiosperm woods. IAWA J **29**: 1–15

**Schultz HR, Matthews MA** (1993) Xylem development and hydraulic conductance in sun and shade shoots of grapevine (*Vitis vinifera* L.): evidence that low light uncouples water transport capacity from leaf area. Planta **190**: 393–406

**Schumann K, Leuschner C, Schuldt B** (2019) Xylem hydraulic safety and efficiency in relation to leaf and wood traits in three temperate *Acer* species differing in habitat preferences. Trees - Struct Funct **33**: 1475–1490

**Scoffoni C, Albuquerque C, Brodersen CR, Townes S V, John GP** (2016) Leaf vein xylem conduit diameter influences susceptibility to embolism and hydraulic decline. New Phytol **213**: 1076–1092

**Skelton RP, Brodribb TJ, Choat B** (2017) Casting light on xylem vulnerability in an herbaceous species reveals a lack of segmentation. 561–569

**Skelton RP, Dawson TE, Thompson SE, Shen Y, Weitz AP, Ackerly D** (2018) Low Vulnerability to Xylem Embolism in Leaves and Stems of North American Oaks. Plant Physiol **177**: 1066–1077

**Sperry JS, Pockman WT** (1993) Limitation of transpiration by hydraulic conductance and xyiem cavitation in *Betula occidentalis*. Plant Cell Environ **16**: 279–287

**Sperry JS, Tyree MT** (1988) Xylem embolism mechanism of water stress-induced. Plant Physiol **88**: 581–587

**Stojni S, Luis M De, Ræbild A, Tognetti R, Delzon S** (2017) Variation in xylem vulnerability to embolism in European beech from geographically marginal populations. Tree Physiol **38**: 173–185

**Tyree MT, Davis SD, Cochard H** (1994) Biophysical perspective of xylem evolution: is there a tradeoff of hydraulic efficiency for vulnerability to disfunction? IAWA J

**15**: 335–360

**Tyree MT, Hammel HT, Jolia L** (1972) The measurement of the turgor pressure and the water relations of plants by the pressure-bomb technique. J Exp Bot **23**: 267–282

**Venturas MD, Sperry JS, Hacke UG** (2017) Plant xylem hydraulics : What we understand , current research , and future challenges. **59**: 356–389

**Wagner KR, Ewers FW, Davis SD** (1998) Tradeoffs between hydraulic efficiency and mechanical strength in the stems of four co-occurring species of chaparral shrubs. Oecologia **117**: 53–62

**Wang Y, Burlett R, Feng F, Tyree MT** (2014) Improved precision of hydraulic conductance measurements using a Cochard rotor in two different centrifuges. J Plant Hydraul **1**: 007

**Wortemann R, Herbette S, Barigah TS, Fumanal B, Alia R, Ducousso A, Gomory D, Roeckel-drevet P, Cochard H** (2011a) Genotypic variability and phenotypic plasticity of cavitation resistance in *Fagus sylvatica* L. across Europe. Tree Physiol **31**: 1175–1182

**Wortemann R, Herbette S, Barigah TS, Fumanal B, Alia R, Ducousso A, Gomory D, Roeckel-Drevet P, Cochard H** (2011b) Genotypic variability and phenotypic plasticity of cavitation resistance in Fagus sylvatica L. across Europe. Tree Physiol **31**: 1175–1182

**Zhang J, Yu G, Wen W, Ma X, Xu B, Huang B** (2016a) Functional characterization and hormonal regulation of the PHEOPHYTINASE gene LpPPH controlling leaf senescence in perennial ryegrass. **67**: 935–945

**Zhang Y, Carmesin C, Kaack L, Klepsch MM, Kotowska M, Matei T, Schenk HJ, Weber M, Walther P, Schmidt V, *et al*** (2019) High porosity with tiny pore constrictions and unbending pathways characterise the 3D structure of intervessel pit membranes in angiosperm xylem. Plant Cell Environ 1–15

**Zhang Y, Rockwell FE, Graham AC, Alexander T, Holbrook NM** (2016b) Reversible leaf xylem collapse: a potential “circuit breaker” against cavitation. Plant Physiol **172**: 2261–2274

## Tables and figures

**Table 1.** Physiological parameters of sun and shade acclimated leaves of *Phellodendron amurense* and *Ilex verticillata*. Net photosynthetic rate ($A_N$), stomatal conductance ($g_s$), turgor lost point (TLP), and leaf hydraulic conductance ($K_{leaf}$) are presented as mean ($n$ =3 to 4, ± SE). Numbers followed by asterisks (*) are statistically significant (Student's $t$-test with 95% confidence interval).

| | *Phellodendron amurense* | | *Ilex verticillata* | |
|---|---|---|---|---|
| Traits | Sun | Shade | Sun | Shade |
| $A_N$ (μmol $m^{-2}$ $s^{-1}$) | 7.12* ± 0.70 | 4.18 ± 0.09 | 8.88* ± 0.81 | 4.97 ± 0.83 |
| $g_s$ (mol $m^{-2}$ $s^{-1}$) | 0.09* ± 0.01 | 0.05 ± 0.00 | 0.17* ± 0.02 | 0.12 ± 0.01 |
| TLP (MPa) | -1.30 ± 0.09 | -1.11 ± 0.04 | -1.46 ± 0.07 | -1.09 ± 0.11 |
| $K_{leaf}$ (mmol $m^{-2}$ $s^{-1}$ $MPa^{-1}$) | 6.30* ± 1.91 | 1.57 ± 0.39 | 23.4* ± 1.58 | 7.49 ± 0.70 |

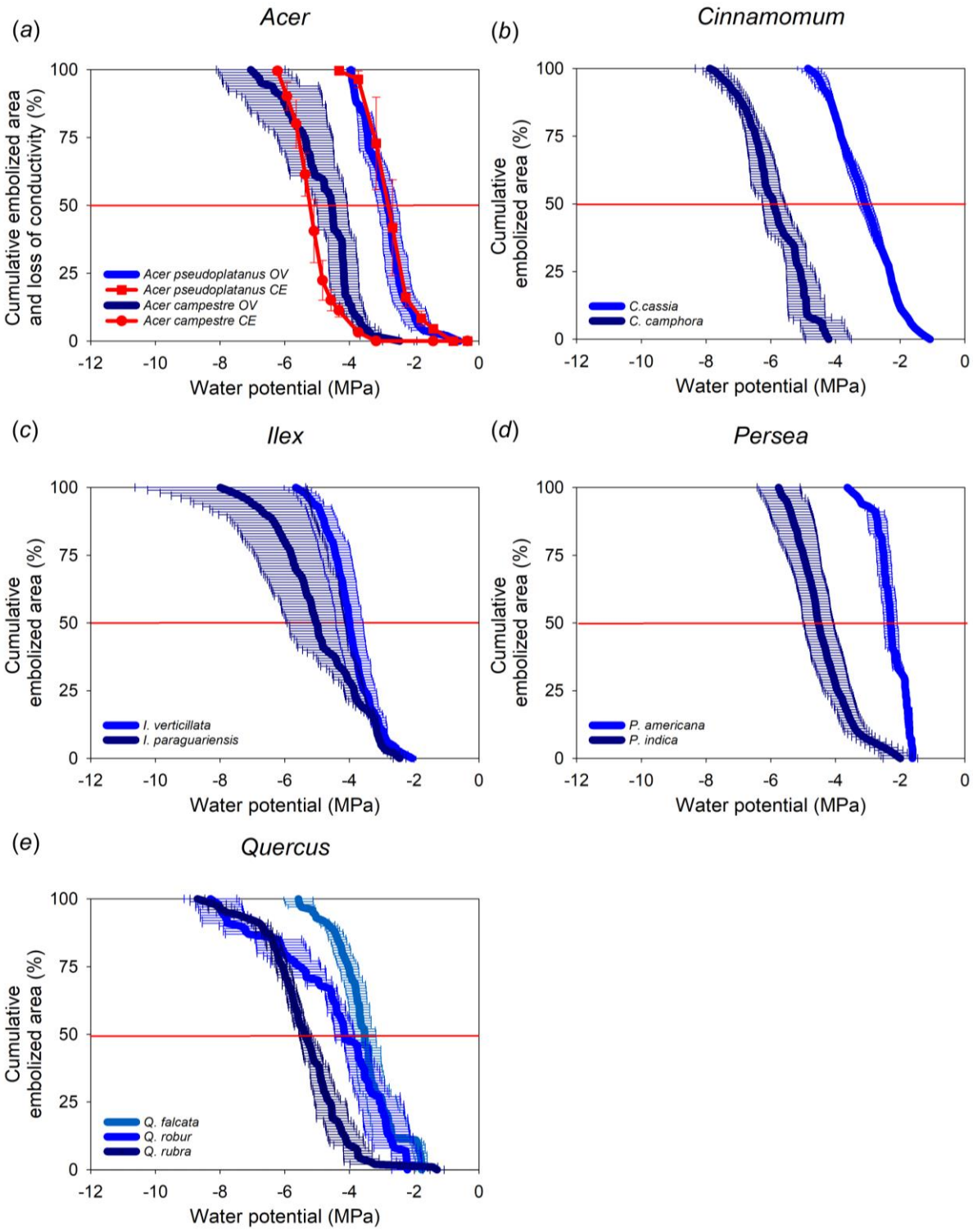


**Figure 1.** Optical (blue, OV), and centrifuge (red, CE), vulnerability curves of stems in species (each represented by curves of a different colour (OV), or symbol (CE)) of *Acer* (*a*), *Cinnamomum* (*b*), *Ilex* (*c*), *Persea* (*d*) and *Quercus* (*e*) (n=3, error bars represent ±SE). Montages constructed at the end of tissue dehydration once 100 % of xylem area was embolised are shown in Figure S1.

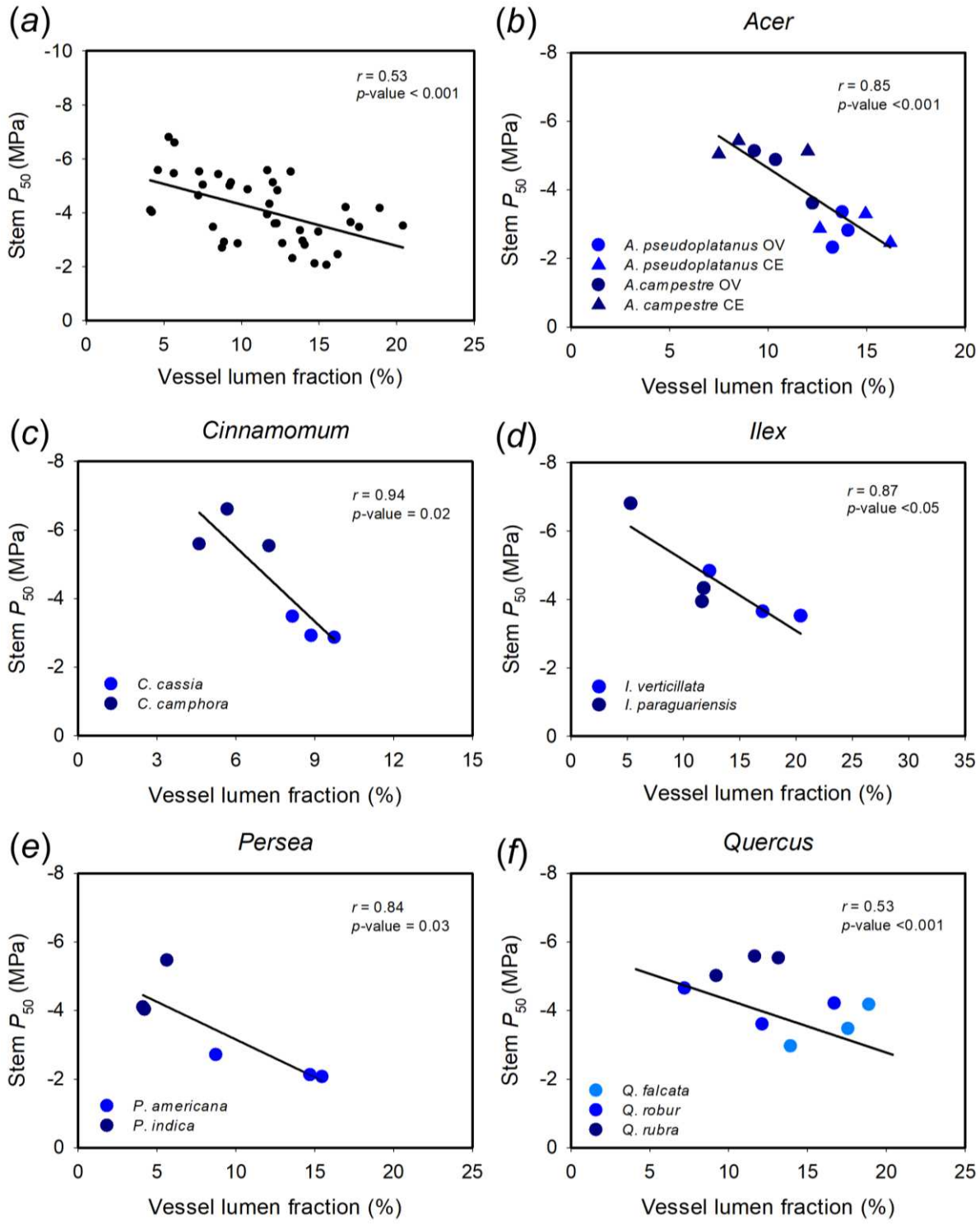


**Figure 2.** The relationship between vessel lumen fraction (VLF) and water potential at which 50% of xylem area was embolised or 50% of conductivity was lost ($P_{50}$) across all stems samples (*a*). $P_{50}$ was determined by the optical method (OV) in all species as well as by the centrifuge (CE) in *Acer* The relationships between VLF and $P_{50}$ within the genera *Acer* (including both the optical (circles) and centrifuge sampled stems

(triangles)) (*b*), *Cinnamomum* (*c*), *Ilex* (*d*), *Persea* (*e*) and *Quercus* (*f*). Species within each genera are represented by symbols of a different colour.

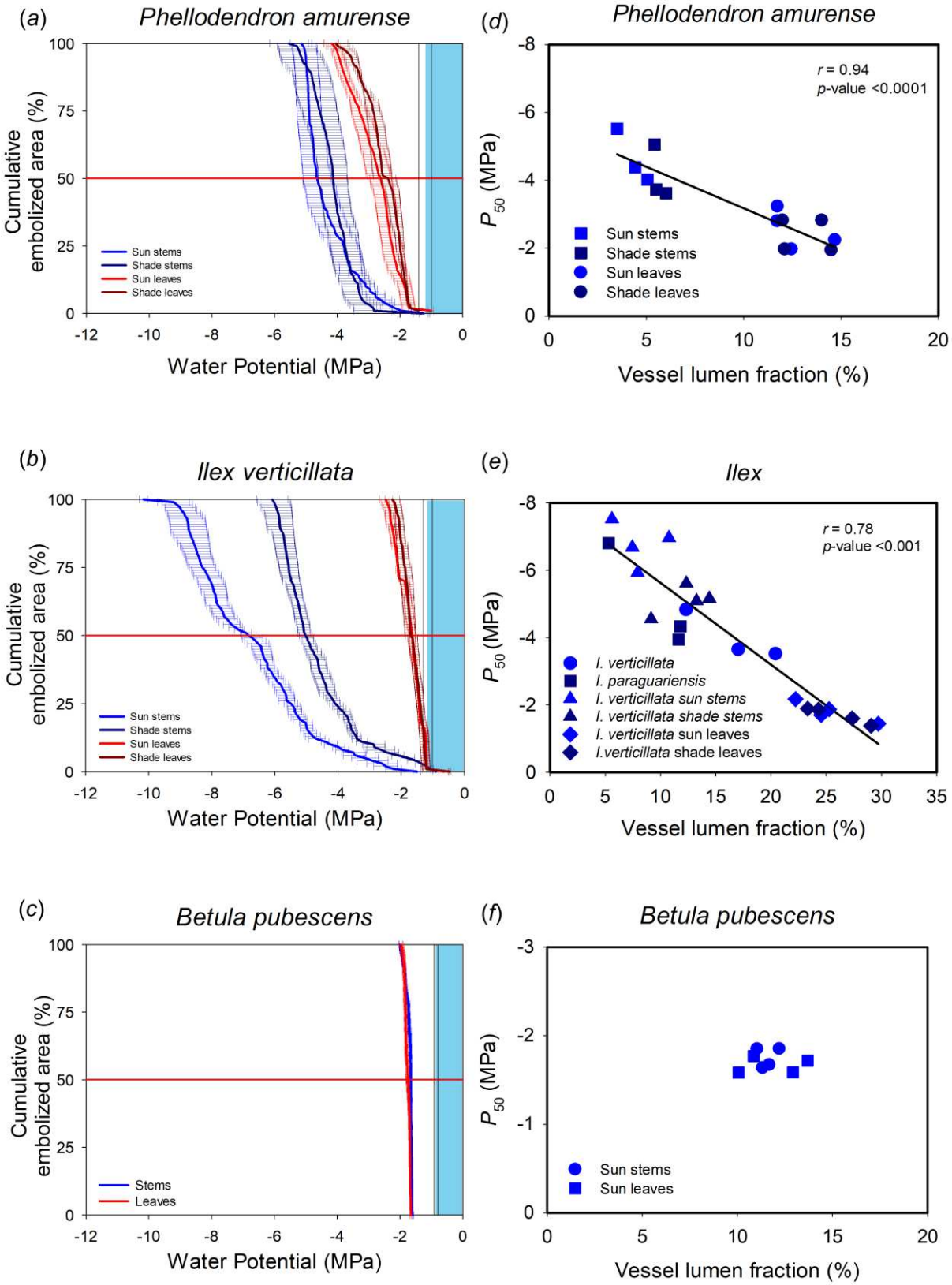


**Figure 3.** Optical vulnerability curves of stems (blue) and leaves (red) acclimated to sun (light) and shade (dark) microenviroments within an individual canopy of the two deciduous species *Phellodendron amurense* (*a*) and *Ilex verticillata* (*b*) and the leaves

and stems of the shade intolerant species *Betula pubescens* (*c*). Relationships between vessel lumen fraction and the water potential at which 50% of the xylem area was embolised for stems and leaves of *Ph. amurense* (*d*), all samples collected in this study from *Ilex* species, including stems and leaves from sun and shade microenvironments (*e*), and stems and leaves of *B. pubescens* (*f*). Red horizontal lines in the vulnerability curves indicate 50% cumulative embolised xylem area and vertical black lines indicate turgor lost point (±SE, $n$ = 3 to 4). The blue boxes represents the region of water potential prior to turgor lost point. Montages constructed at the end of tissue dehydration once 100 % of xylem area was embolised are shown on Figure S2.

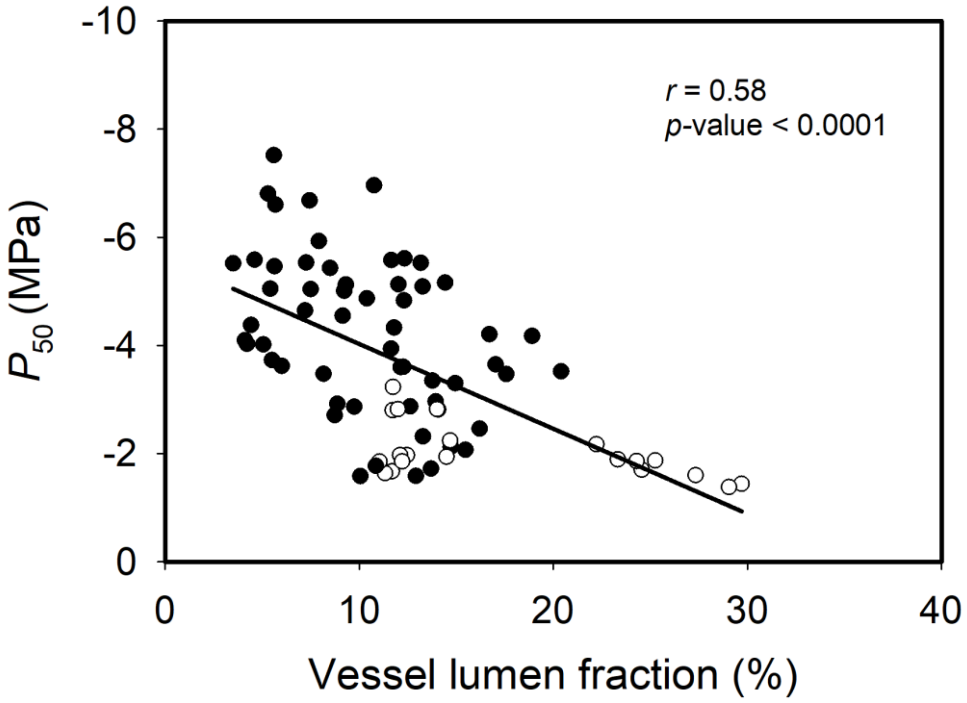


**Figure 4.** The relationship between the vessel lumen fraction and the water potential at which 50% of the xylem area was embolised in all samples analysed from thirteen species across seven genera, including data from stems (solid symbols) and leaves (open symbols), as well as tissue acclimated to different light environments.

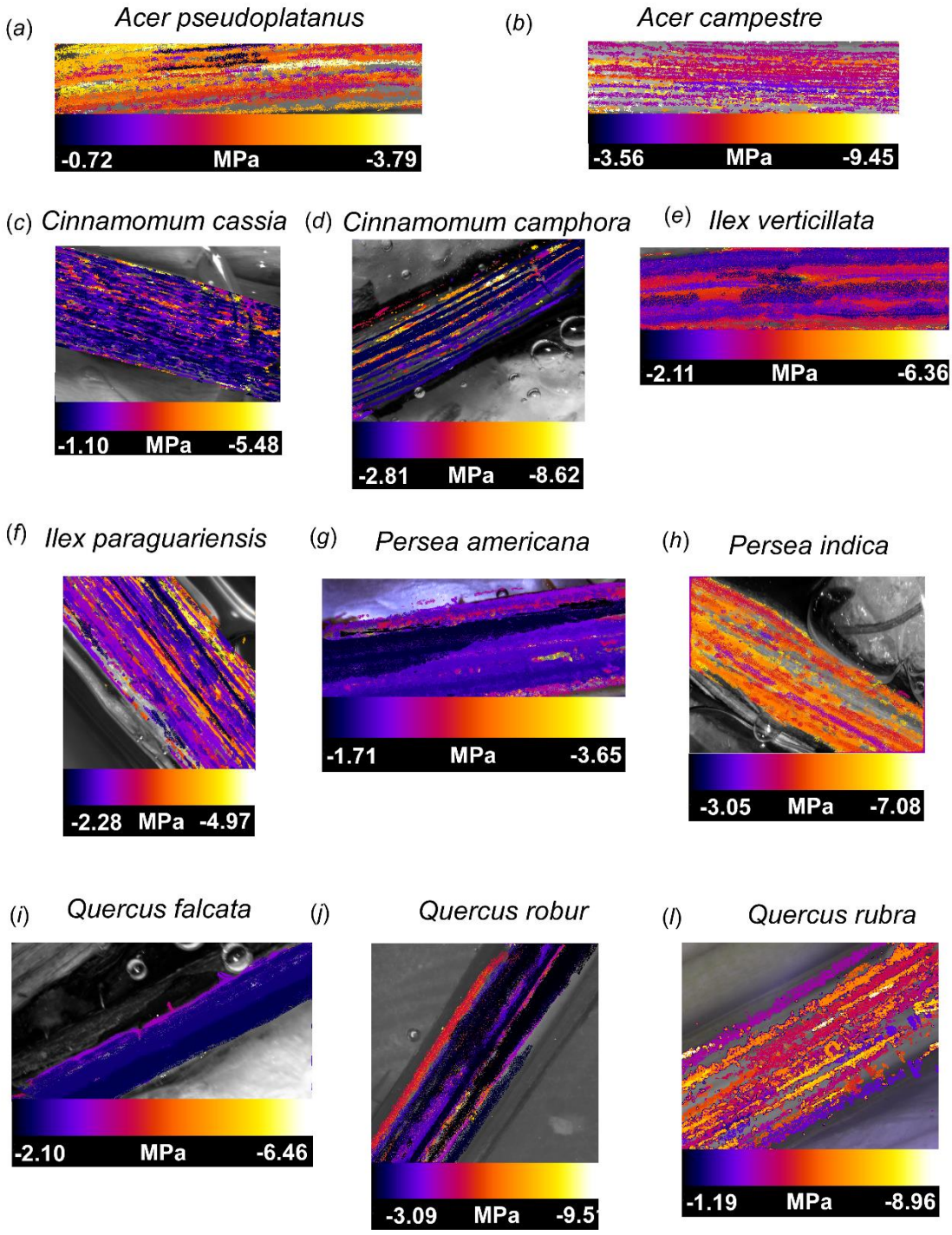


**Figure S1.** Representative montages used to construct optical vulnerability curves of stems of 11 species from 5 different genera showing the water potential based on the colour scale bar of each embolism event in *Acer pseudoplatanus* (a) and *Acer campestre* (b), *Cinnamomum cassia* (c) and *Cinnamomum camphora* (d), *Ilex verticillata* (e) and *Ilex paraguariensis* (f), *Persea americana* (g) and *Persea indica* (h) and *Quercus falcata* (i), *Quercus robur* (j) and *Quercus rubra* (l).

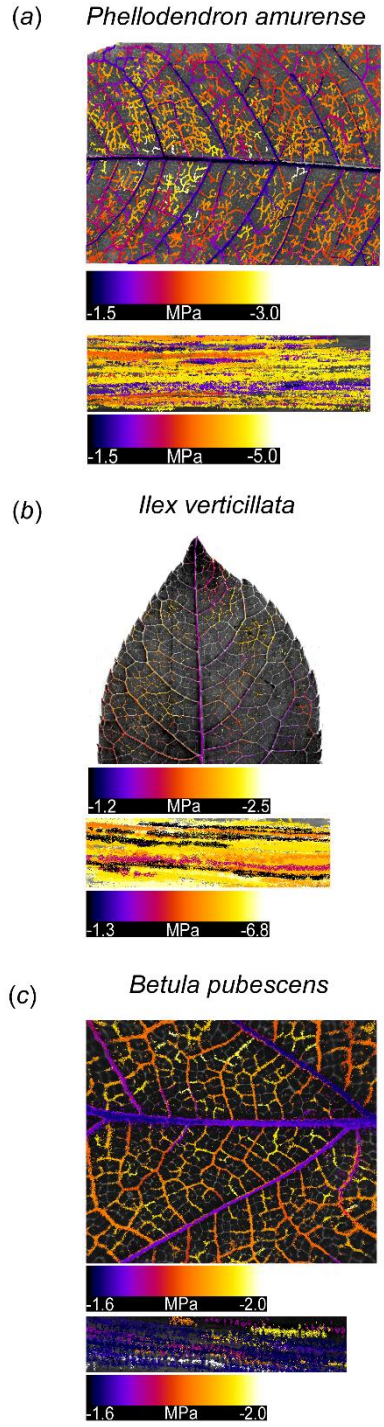


**Figure S2**. Representative montages of leaves and stems of *Phellodendron amurense* (a), *Ilex verticillata* (b) and *Betula pubescens* (c) used to construct optical vulnerability curves. The water potential, based on the colour scale bar, of each embolism event is indicated.

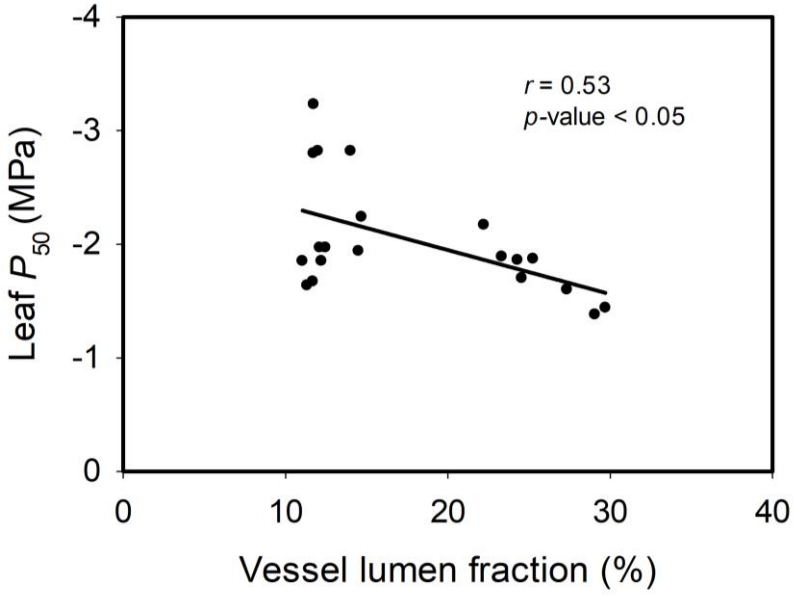


**Figure S3.** The relationship between vessel lumen fraction (VLF) and the water potential at which 50% of xylem area was embolised ($P_{50}$) of all leaf samples analyzed from *Phellodendron amurense*, *Ilex verticillata* and *Betula pubescens.*

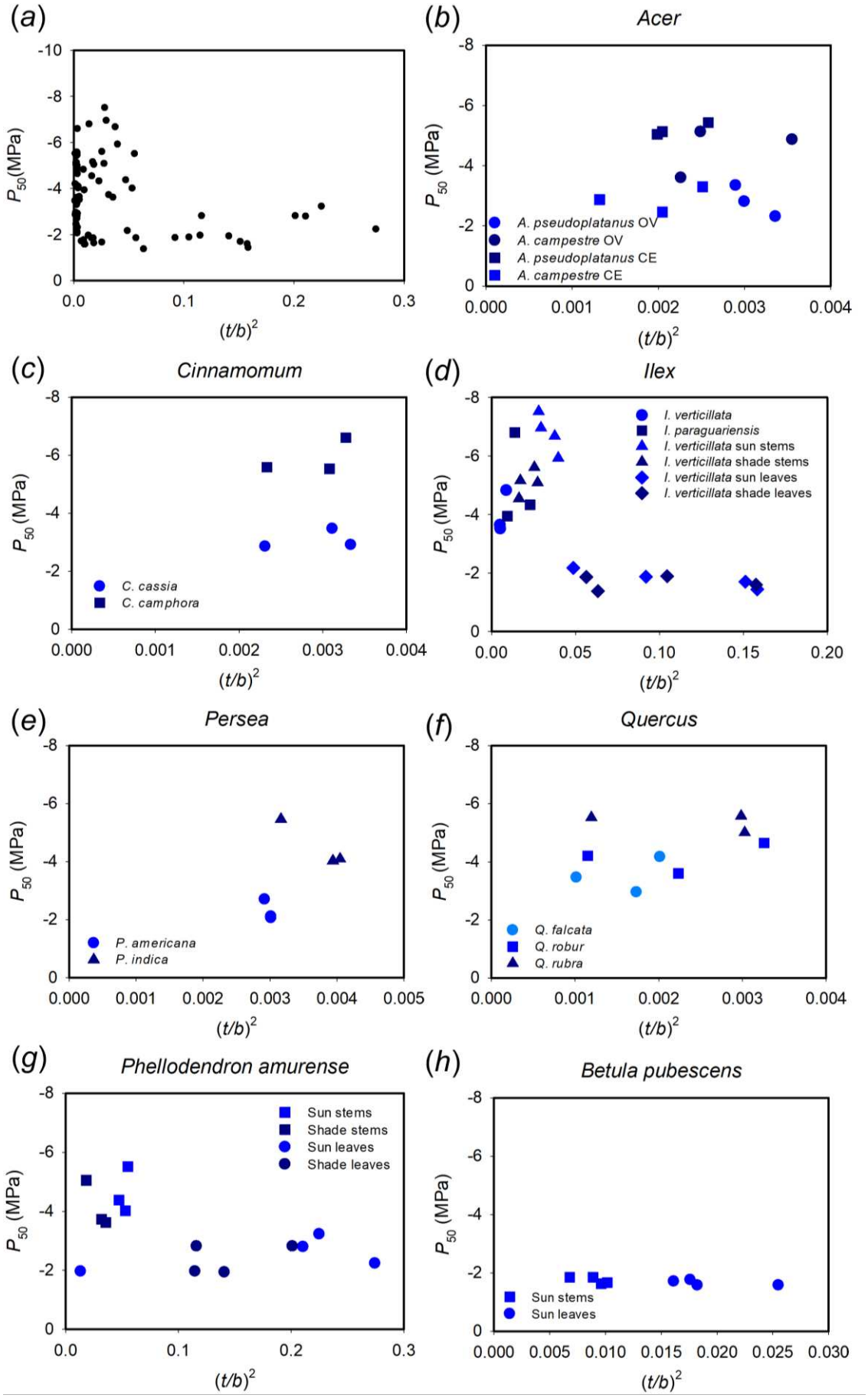
(a)
(b) Acer
(c) Cinnamomum
(d) Ilex
(e) Persea
(f) Quercus
(g) Phellodendron amurense
(h) Betula pubescens
P50 (MPa)
(t/b)2
A. pseudoplatanus OV
A. campestre OV
A. pseudoplatanus CE
A. campestre CE
C. cassia
C. camphora
I. verticillata
I. paraguariensis
I. verticillata sun stems
I. verticillata shade stems
I. verticillata sun leaves
I. verticillata shade leaves
P. americana
P. indica
Q. falcata
Q. robur
Q. rubra
Sun stems
Shade stems
Sun leaves
Shade leaves
Sun stems
Sun leaves

**Figure S4**. Relationships between the water potential at which 50% of xylem area was embolized ($P_{50}$) and $(t/b)^3$ in all samples (a), within the genera *Acer* (including optical and centrifuge data) (b), *Cinnamomum* (c), *Ilex* (including data from all samples including stems and leaves adaptated to different light environments) (d), *Persea* (e), *Quercus* (f) and intraspecific variation in *Phellodendron amurense* (g) and *Betula pubescens* (h).

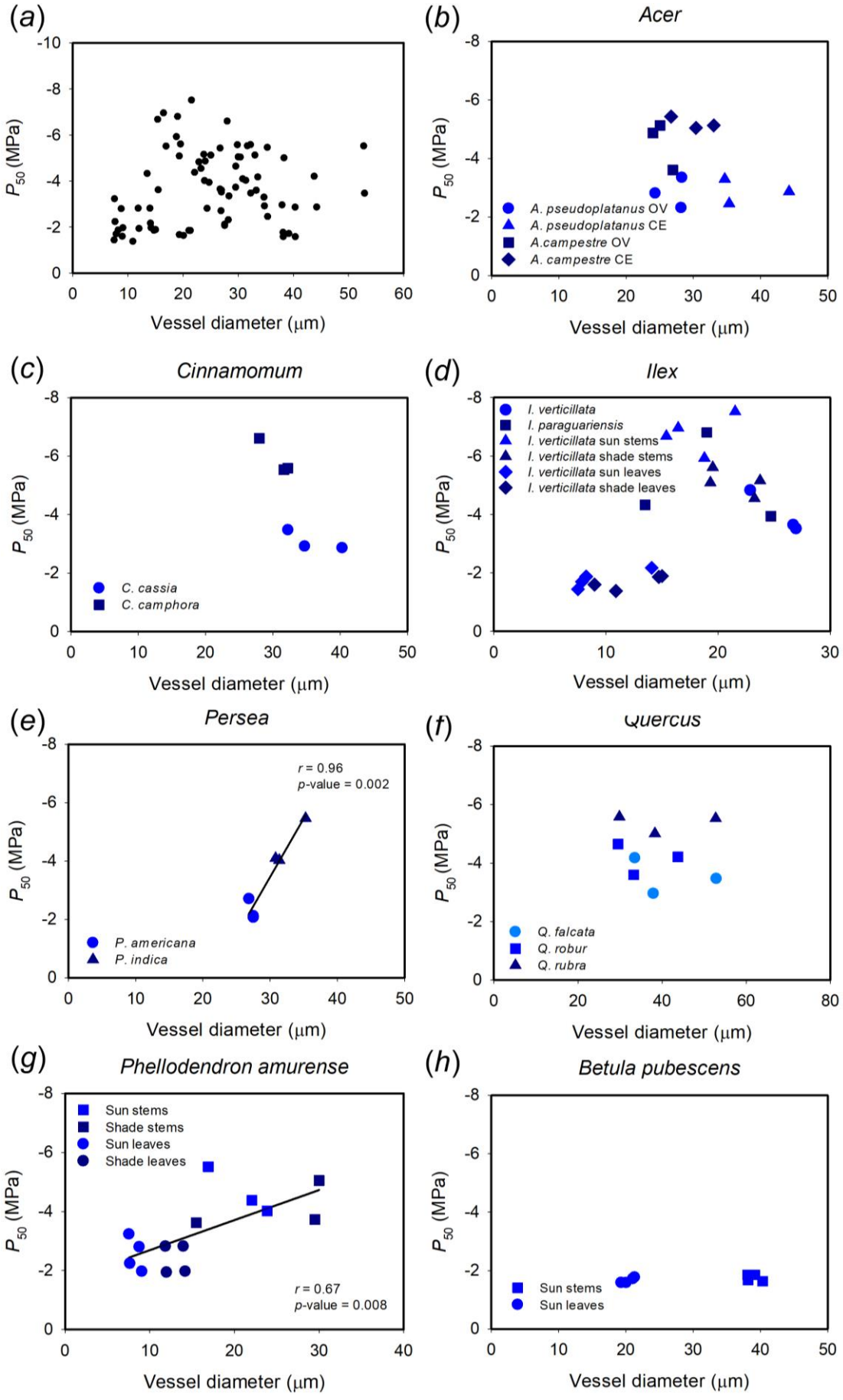
(a)
(b) Acer
(c) Cinnamomum
(d) Ilex
(e) Persea
(f) Quercus
(g) Phellodendron amurense
(h) Betula pubescens
P50 (MPa)
Vessel diameter (μm)
A. pseudoplatanus OV
A. pseudoplatanus CE
A.campestre OV
A. campestre CE
C. cassia
C. camphora
I. verticillata
I. paraguariensis
I. verticillata sun stems
I. verticillata shade stems
I. verticillata sun leaves
I. verticillata shade leaves
r = 0.96
p-value = 0.002
P. americana
P. indica
Q. falcata
Q. robur
Q. rubra
Sun stems
Shade stems
Sun leaves
Shade leaves
r = 0.67
p-value = 0.008

**Figure S5**. Relationships between the water potential at which 50% of xylem area was embolized ($P_{50}$) and vessel diameter in all samples (a), within the genera *Acer* (including optical and centrifuge data) (b), *Cinnamomum* (c), *Ilex* (including data from all samples including stems and leaves adapted to different light environments) (d), *Persea* (e), *Quercus* (f) and intraspecific variation in *Phellodendron amurense* (g) and *Betula pubescens* (h).

**Supplementary Table S1.** The native range, climate information and drought and freezing tolerance of the selected species.

| Species | Family | Native range | Dry season/frozen winter | Drought/freezing tolerance behavior | Reference |
|---|---|---|---|---|---|
| *Acer campestre* L. | Sapindaceae | Continental Europe, Britain, southwest Asia from Turkey to the Caucasus, and north Africa in the Atlas Mountains. | Native to regions with a dry and hot summer, including Spain and North Africa. | Drought tolerant. It prefers warmer climates but it can also be winter hardy. | (Caudullo *et al*., 2016; Schumann *et al*., 2019) |
| *Acer pseudoplatanus* L. | Sapindaceae | Mainly Central Europe and a small amount in Western Asia. | Native to mesic Central Europe. | Drought intolerant | (Lemoine *et al*., 2001; Pasta *et al*., 2016; Schumann *et al*., 2019) |
| *Cinnamomum camphora* (L.) J.Presl | Lauraceae | Warm temperate to subtropical areas of East Asia including China, Vietnam, Korea and Japan, specifically to the coastal areas from Cochin China (Vietnam) to the mouth of the Yang-tse-kiang River. | Native to regions with a prolonged dry season, rainfall of less than 40 mm in three months. Introduced to several arid areas including central of Australia West of United States, North Africa and Western Asia | Drought tolerant | Invasive species compendium (CABI) |
| *Cinnamomum cassia* (L.) J.Presl | Lauraceae | Southern China | Native to regions with only mild dry season and annual precipitation of 1200-2000 mm. | No information. | |
| *Ilex paraguariensis* A.St.-Hil. | Aquifoliaceae | Southern of South America, including Argentina; Bolivia, Plurinational States of; Brazil (Rio Grande do Sul, Santa Catarina); Colombia; Ecuador; Paraguay and Uruguay. | Native to Argentina and Paraguay, driest locations of annual rainfall no more than 500 mm per year and five month dry season with less than 40 mm per month.. | Drought tolerant | (Acevedo *et al*., 2019) |
| *Ilex verticillata* (L.) A.Gray | Aquifoliaceae | East North America in the United states and Southest Canada. | Temperature species can survive extremely temperatures below -40 °C. | Moderate drought tolerant. Resistant to extreme cold temperatures | (Gilman and Watson, 1993) |

| Species | Family | Native range | Dry season/frozen winter | Drought/freezing tolerance behavior | Reference |
|---|---|---|---|---|---|
| *Persea americana* Mill. | Lauraceae | South Central Mexico Guatemala, Costa Rica, Colombia, Ecuador and Peru. | Common in humid areas with rainfall ranging between 1000 up to 3000 mm per year. | Drought intolerant | (Barra *et al*., 2017) |
| *Persea indica* (L.) Spreng. | Lauraceae | Madeira and Canary islands. | Native to a Mediterranean semiarid climate. Rainfall of 250 mm per year | Drought tolerant | (González-Rodríguez *et al*., 2002; Sánchez-Díaz *et al*., 2007) |
| *Quercus falcata* Michx. | Fagaceae | Southern United States. | Annual rainfall of 1800 up to 2500 mm | Drought intolerant | (Pezeshki and Chambers, 1986) |
| *Quercus robur* L. | Fagaceae | Native to Europe West of the Caucasus. | Annual rainfall of 600 up to 1400 mm | Drought intolerant | (Tyree and Cochard, 1996; Nardini and Tyree, 1999) |
| *Quercus rubra* L. | Fagaceae | North America, in the eastern and central United States and southeast and south-central Canada. | Annual rainfall of 800 up to 1300 mm. Can survive extremely cold winter temperatures of below -40 °C. | Drought intolerant. Resistant to extreme cold temperatures. | (Tyree and Cochard, 1996) |
| *Phellodendron amurense* | Rutaceae | Eastern Asia: northern China, northeast China, Korea and Japan. | Mesic temperate native adapted to short warm and humid summers and cold and wet winters. | Drought tolerant. Resistant to cold temperatures. | (Wang *et al*., 2008) |
| *Betula pubescens* | Betulaceae | Northern Europe and Asia. | Native range rainfall ranging from 553 up to 1278 mm. Well adapted to extremely cold winters. | Drought tolerant. Resistant to extreme cold temperatures. | (Rinne *et al*., 1998; Welling *et al*., 2004; Aspelmeier and Leuschner, 2006) |

## References

**Acevedo RM, Avico EH, González S, Salvador AR, Rivarola M, Paniego N, Nunes-Nesi A, Ruiz OA, Sansberro PA** (2019) Transcript and metabolic adjustments triggered by drought in *Ilex paraguariensis* leaves. Planta **250**: 445–462

**Aspelmeier S, Leuschner C** (2006) Genotypic variation in drought response of silver birch (*Betula pendula* Roth): leaf and root morphology and carbon partitioning. Trees - Struct Funct **20**: 42–52

**Barra PJ, Inostroza NG, Mora ML, Crowley DE, Jorquera MA** (2017) Bacterial consortia inoculation mitigates the water shortage and salt stress in an avocado (*Persea americana* Mill.) nursery. Appl Soil Ecol **111**: 39–47

**Caudullo G, Commission E, Rigo D De** (2016) *Acer campestre* in Europe: distribution, habitat, usage and threats. Eur Atlas For Tree Species 52–53

**Gilman EF, Watson DG** (1993) Ilex verticillata. Fact sheet ST-309 1–3

**González-Rodríguez ÁM, Bertamini M, Nedunchezhian N** (2002) Leaf gas exchange characteristics of a Canarian laurel forest tree species [*Persea indica* (L.) K. Spreng.] under natural conditions. J Plant Physiol **159**: 695–704

**Lemoine D, Peltier JP, Marigo G** (2001) Comparative studies of the water relations and the hydraulic characteristics in *Fraxinus excelsior, Acer pseudoplatanus* and *A. opalus* trees under soil water contrasted conditions. Ann For Sci **58**: 723–731

**Nardini A, Tyree MT** (1999) Root and shoot hydraulic conductance of seven *Quercus* species. Ann For Sci **56**: 371–377

**Pasta S, Rigo D De, Caudullo G, Houston Durrant T, Mauri A** (2016) *Acer pseudoplatanus* in Europe: distribution, habitat, usage and threats. Eur Atlas For Tree Species 56–58

**Pezeshki SR, Chambers JL** (1986) Stomatal and photosynthetic response of drough-stressed cherrybark oak (*Quercus falcata* var. *pagodaefolia*) and sweet gum (*Liquidambar styraciflua*). Can J For Res **16**: 841–845

**Rinne P, Welling A, Kaikuranta P** (1998) Onset of freezing tolerance in birch (*Betula pubescens* Ehrh.) involves LEA proteins and osmoregulation and is impaired in an ABA-deficient genotype. Plant, Cell Environ **21**: 601–611

**Sánchez-Díaz M, Tapia C, Antolín MC** (2007) Drought-induced oxidative stress in Canarian laurel forest tree species growing under controlled conditions. Tree Physiol **27**: 1415–1422

**Schumann K, Leuschner C, Schuldt B** (2019) Xylem hydraulic safety and efficiency in relation to leaf and wood traits in three temperate *Acer* species differing in habitat preferences. Trees - Struct Funct **33**: 1475–1490

**Tyree M, Cochard H** (1996) Summer and winter embolism in oak: impact on water relations. Ann des Sci For **53**: 173–180

**Wang H, Wang Y, Zu Y, Sun L** (2008) Construction and analysis of subtractive cDNA library of *Phellodendron amurense* under drought stress. Shengwu Gongcheng Xuebao/Chinese J Biotechnol **24**: 198–202

**Welling A, Rinne P, Viherä-Aarnio A, Kontunen-Soppela S, Heino P, Palva ET** (2004) Photoperiod and temperature differentially regulate the expression of two dehydrin genes during overwintering of birch (*Betula pubescens* Ehrh.). J Exp Bot **55**: 507–516

# CHAPTER 4

## The presence of embolism influences embolism resistance differentially in tracheid- and vessel-based xylem

**Abstract**

When assessing embolism resistance by hydraulic methods, the gradual decline in hydraulic conductance as leaf water potential declines suggests that there can be a wide range of water potentials at which embolism forms in each conduit. In the past decade, with the advent of methods capable of visualizing embolism in xylem conduits, there is now confirmatory evidence that embolism does indeed form in particular xylem elements across a range of water potentials. It is believed that the threshold for embolism resistance, in individual conduits, it is determined by macro-anatomy traits as conduit dimension, pit membrane structure in angiosperms and the relation between the size of torus and the pit chamber in conifers and cell-wall thickness. Herein, we designed an experiment using a cycle of dehydration, rehydration and subsequent dehydration to death to test (*i*) whether there is a specific water potential at which individual conduits will embolise and (*ii*) how the degree of pre-existing embolism in the xylem can influence the resistance to embolism in remaining water-filled conduits. We found that, in vessel-based xylem species, individual xylem conduits had a more well-defined water potential at which embolism occur, with considerable pre-existing embolism being able to influence the vulnerability of the xylem. In contrast, conduits in tracheid-based xylem did not display a well-defined individual water potential threshold at which embolism occurs and thus pre-existing embolism did not alter the vulnerability of xylem.

**Keywords:** rehydration, individual conduits, pre-existing embolism; $P_{50}$

## Introduction

Plants transport water under negative tension from the roots to the stomata through xylem. During drought the water column experiences increasing tension which ultimately leads to the invasion of the conduits by air, causing an embolism which irreversibly disrupts the water column (Sperry & Pockman, 1993; Brodribb & Cochard, 2009; Cochard & Delzon, 2013; Charrier *et al.*, 2016; Lamarque *et al.*, 2018). The continual formation of embolism under negative tension ultimately lead to complete hydraulic failure (Brodribb & Cochard, 2009).

Plants have evolved a number of strategies to prevent the formation of embolism at increasingly negative tensions on the water column and thus surviving without embolism in dry environments. Many of these adaptations are believed to be associated with the macro-anatomy of the xylem conduits, including conduit dimensions (Hacke *et al.*, 2009; Blackman *et al.*, 2010), pit membrane structure in angiosperms (Choat *et al.*, 2008; Brodersen *et al.*, 2014; Li *et al.*, 2016), the relation between the size of torus and the pit chamber in conifers (Choat & Pittermann, 2009; Hacke & Jansen, 2009) and cell-wall thickness (Hacke *et al.*, 2001; Blackman *et al.*, 2010). Each of these traits has been linked to xylem embolism resistance, correlating with $P_{50}$, or the water potential at which 50% of the conduits are embolised. When assessing embolism resistance by hydraulic methods, the gradual decline in hydraulic conductance as leaf water potential declines suggests that there can be a wide range of water potentials at which embolism forms in each conduit (Sperry & Tyree, 1988; Pockman *et al.*, 1995; Cochard *et al.*, 2013; Brodribb *et al.*, 2016). In the past decade, with the advent of methods capable of visualizing embolism in xylem conduits there is now confirmatory evidence that embolism does indeed form in particular xylem elements across a range of water potentials (Cochard *et al.*, 2015; Brodribb *et al.*, 2016).

If each xylem conduit has an anatomically determined threshold for embolism resistance, then early during a drought event the first embolism events would be expected to occur in the most vulnerable conduits. As drought progresses conduits will embolise gradually such that by $P_{50}$ only the most embolism resistant conduits will remain water filled. If the drought ceases before hydraulic conductivity is completely lost, we would expect embolism events to cease, and water filled conduits resuming the transport of water, albeit in close proximity to air filled conduits thereby reducing

maximum hydraulic conductance (Blackman *et al.*, 2009; Brodribb & Cochard, 2009; Choat *et al.*, 2015). These embolised, or air filled, conduits can potentially act as sources of air for future embolism events should the plant experience another drought event. The air in embolised conduits has the potential to traverse pit membranes, embolising adjacent xylem (Zimmermann, 1983). In angiosperms, surfactants coating the cellulose of the pit membranes is believed to mitigate this air seeding (Jansen & Schenk, 2015; Schenk *et al.*, 2015, 2017). In conifers, with torus and margo pit membranes the aspiration of the pits is believed to prevent the spread of air between embolised conduits into neighbouring water filled tracheids (Walter & Bauch, 1967; Petty & B, 1972; Sperry, J. & Tyree, 1990). If an air-filled conduit neighbours water filled conduits there is the potential that the presence of this pre-exisiting embolism will make neighbouring conduits more vulnerable and thus alter the vulnerability of the shoot. Plants in nature can experience several cycles of dehydration sufficient to cause embolism during a season.

In this study we designed an experiment using a cycle of dehydration, rehydration and subsequent dehydration to death to test (i) whether there is a specific water potential at which individual conduits will embolise and (ii) how the degree of pre-existing embolism in the xylem can influence the resistance to embolism in remaining water-filled conduits. We selected 5 angiosperm species with xylem consisting of vessels and 1 vessel-less angiosperm and 3 conifers all with tracheid-based xylem. Embolism was observed using the optical method, which is nondestructive, and permits a clear visualization of embolism events in the stem. In vessel-based xylem species, we found that individual xylem conduits had a more well-defined water potential at which embolism occur, with considerable pre-existing embolism able to influence the vulnerability of the xylem. In contrast, conduits in tracheid-based xylem did not display a well-defined individual water potential threshold at which embolism occurs and thus pre-existing embolism did not alter the vulnerability of xylem.

**Material and methods**

We selected five vessel-bearing angiosperms (*Ilex verticillata* (L.) A. Gray [Aquifoliaceae]*, Rhododendron hirsutum* L. [Ericaceae]*, Ficus religiosa* L. [Moraceae], *Tilia cordata* Mill. [Malvaceae] and *Lindera benzoin* L. [Lauraceae]) and one vessel-less angiosperm (*Drimys winteri* J.R. Forst & G. Forst. [Winteraceae]), as well as three

conifers (*Agathis robusta* (C.Moore ex. F.Muell) Bailey [Araucariaceae], *Tsuga canadenses* (L.) Carrière [Pinaceae] and *Torreya californica* Torr. [Taxaceae]). Plants of *T. cordata*, *A. robusta* and *T. canadenses* were grown outside in the Botanical Gardens of Ulm University, Ulm (Germany) (48° 25' N, 9° 57' E), *F. religiosa*, *D. winteri* in the glasshouses of the Botanical Gardens of Ulm University, *I. verticillata*, *L. benzoin* and *T. californica* were grown in the glasshouses of Purdue University, West Lafayette (Indiana, USA) (40° 25' N, 86° 54' W, elevation: 187 m). *R. hirsutum* was collected in the Allgäu Alps near Oberstdorf (Germany) (47° 25' N, 10° 17' E, elevation: 2600 m).
Branches ranging from 30 cm to 2 m long (all exceeding the length of the longest vessel as determined by air injection) were collected early in the morning, cut under water and bagged for approximately 1 hour so that all experiments started with a stem water potential of at least -0.54 MPa. Branches, or leaves in *L. benzoin*, were fixed to a stereo microscope (SZMT2, optika, Italy) or Raspberry Pi clamps (opensourceOV.org), and a 2-cm-segment of bark was gently removed using a fingernail without touching the xylem and immediately an adhesive gel (Tensive) immediately applied to the surface of the xylem to avoid dehydration. A glass cover slide was placed on top of the adhesive gel to air imaging. Images were collected every 3 minutes, a psychrometer (ICT International, version 4.4) was then attached as close as possible to the segment in which the bark was removed. Branches were allowed to bench dry while embolism images were captured. Rehydrations were performed across a range of water potentials for each species to build a data set spanning a range of variation in the percentage of embolism. The end of the branch was excised under water (removing only 1 cm from the cut end) until water potential ranging from 0 MPa to -1.07 MPa, depending on the resistance of the specie against embolism (rehydrations took no more than 306 mins). The cut end of the stem was removed from water and the branch was allowed to bench dry again this time until all conduits had visibly embolised. Stem and leaf images were analyzed in ImageJ (version 1.52h, NIH, USA) to quantify embolism accumulation through time and thus construct vulnerability curves as described by (Brodribb *et al.*, 2016).
The percentage of embolised area that occurred prior to the water potential of rehydration ($E_{pr}$) in the second round of dehydrations was determined as follows:

$$E_{pr} = \left(\frac{E_{r2} - E_{r1}}{E_{100} - E_{r1}}\right) X\ 100$$

Where $E_{r1}$ is the percentage of embolised xylem area at the moment of rehydration and $E_{r2}$ is the percentage of embolised xylem area accumulated in the sample when it reached the same water potential at which rehydration occurred during the second period of bench dehydration.

Furthermore, the samples rehydrated around or less than 80% of $E_{r1}$ were used to determined two values of $P_{50}$ (or the water potential at which 50% of the xylem area was embolised). The first one was similar to a traditional $P_{50}$ considering all events of embolism since the first round of dehydration until the death of the sample. The second one, disregarding the embolism events that happened prior to the first round of dehydration, and considering the second dehydration as starting with no embolism ($P_{50r}$) (Figure 1) (for complete details see supplementary information S2). The percentage of alteration on $P_{50}$ was then calculated using the follow equation:

$$Decrease\ in\ apparent\ P_{50} = \left(\frac{P_{50} - P_{50r}}{P_{50}}\right) X\ 100$$

For *I. verticillata* and *R. hirsutum* the experiment was performed three times while two rehydration curves were done for *L benzoin* and *F. religiosa,* for all these species the curves were executed in different quantities of $E_{r1}$, thus not configuring repetitions. However, for *T. californica*, the three rehydration were performed at the same $E_{r1}$ and the results presented as the average of these three events (further details with all the calculations are presented in both Figure S1, and Supplementary information S2).

**Results**

In a representative trace from a branch of the angiosperm *R. hirsutum* with vessel-based xylem, embolism first started to accumulate in the xylem once the stem reached -1 MPa and continued until -3 MPa when approximately 50% of the xylem area was embolised and the branch was rehydrated. Upon rehydration there was a cessation of embolism accumulation for approximately 600 minutes during which time the xylem water potential returned to near 0 MPa and on bench dehydration began to decline again (Fig. 2A). Only once water potential again declined to -3 MPa after rehydration was embolism observed to form in the xylem (Fig. 2B). In the conifer *T. canadensis* with tracheid-based xylem the first embolism in the stem was also observed at approximately -1 MPa and approximately 50% of the xylem area was embolized at -3 MPa (Fig. 2B). In *T. canadensis* rehydration caused water potential to

return to near 0 MPa after which bench dehydration caused it to decline again (Fig. 2B). Unlike *R. hirsutum* embolism began to accumulate as soon as water potential had declined to -1 MPa on the second dehydration and approximately 50% of the remaining xylem are was embolised by -3 MPa on the second rehydration. When branches in angiosperm species with vessel-based xylem were rehydrated when less than 50% of the xylem area had embolized there was very limited embolism that occurred when water potentials were higher than the water potential at which rehydration occurred (Fig. 2C). In these plants however once 50% of the xylem area had embolised, an increasing percentage of the remaining xylem embolised at water potentials higher than when the stem was rehydrated on the first dehydration cycle (Fig. 2C). In contrast to plants with vessel-based xylem, in plants with tracheid-based xylem there was a linear relationship between the percentage of pre-exisiting embolism and the area of embolism that occurred in xylem at water potentials greater than the water potential at which rehydration occurred (Figure 2C). Overall, all samples presented ate least some events of embolism before the water potential of rehydration in the second round of dehydration (Fig. S1) with the exception of the curve of *R. hirsutum* presented in Fig. 2A.

In angiosperm species with vessel-based xylem there was a positive linear relationship between the area of pre-existing embolism in the xylem and apparent embolism resistance (as determined by apparent changes in $P_{50}$) (Fig. 3A). The more pre-existing embolism in the xylem correlated with an increase in apparent xylem embolism resistance (Fig. 3A). This shift in apparent xylem embolism resistance was most pronounced in vessel-bearing angiosperm species in which more than 25% of the xylem area was already embolised (Fig. 3A). In the most extreme case, in which 48% of xylem area was embolised, apparent $P_{50}$ was 24% more negative than when there was no pre-existing embolism in the xylem (Fig. 3A). In species with tracheid-based xylem, there was no consistent effect of the degree of pre-existing embolism on apparent xylem embolism resistance (Fig. 3B). In some tracheid-based xylem stems, with pre-existing embolism, apparent $P_{50}$ was lightly more negative, while in others apparent $P_{50}$ was less negative or even irresponsive to pre-existing embolism (Fig. S1).

## Discussion

Here, we conducted a simple rehydration experiment during a progressive branch dehydration and observed embolism events in the xylem across a diversity of species. Our experiment revealed insight into whether xylem conduits had individual thresholds of embolism resistance as well as the effect of pre-existing embolism on the apparent embolism resistance of xylem. We found that individual xylem elements in plants with vessel-based xylem had a more well-defined individual conduit threshold embolism resistance, while tracheids had a poorly-defined individual conduit embolism resistance. The consequence of this observation of each individual conduit in vessel-based xylem having a particularly individual conduit threshold of embolism resistance is that the degree of pre-existing embolism in xylem appears to linearly influence apparent xylem embolism resistance.

It is clear and well documented that traits like $(t/b)^2$ (Hacke *et al.*, 2001; Blackman *et al.*, 2010), diameter and length of conduits (Hacke *et al.*, 2009; Blackman *et al.*, 2010), pit membrane structure (Choat *et al.*, 2008; Brodersen *et al.*, 2014; Li *et al.*, 2016) and sealing determine how easily a conduit will embolise.. Considering an individual plant, we can obviously find a range of diameters and lengths and cell wall thickness anatomically determining the susceptibility to embolism in an individual scale. Because of this diversity, vulnerability curves have an *S*-type shape with a sigmoidal behavior following a normal distribution of susceptibility against embolism. Thus, those traits are believed to determine, by themselves, the water potential at witch individual conduits would embolize, however, our data suggests that this is also dependent to how much gas-filled conduits are adjacent to this water-filled conduit. In other words, how many sites of nucleation a particular conduit has around it. Since the water inside conduits it is in a metaphasic state, the occurrence of leaking through less well sealed pit membranes could trigger embolism. Both vessels and tracheid are influenced by the amount of the pre-existing embolism. However, tracheids are much more prompt to embolise than vessel at the same level of pre-existing embolism. This implicates that when vessel-based xylem plants have a certain amount of pre-existing embolism, the remained water-filled vessels are more resistant them the previous embolized. Thus shifting the $P_{50}$ towards a water potential more negative and increasing the apparent resistance of the xylem which does not occur in tracheid-based xylem plants. Ultimately, our results also demonstrate that vulnerability curves performed in vessel-based xylem samples with pre-existing embolism could lead to overestimation of $P_{50}$. Although, the mechanistic behind this behavior is still obscure,

we can infer that the different distribution between tracheids and vessels and the sealing of torus margo are, probably, major triggers for this phenomenon.

Taken together, our results highlight how embolism events are also a function of probability of nucleation events in water-filled conduits and not just limited to a threshold water potential determined by anatomical structure of conduits. This in consonance to recent finds relating decreased vessel connectivity, and vessel lumen fraction in xylem to higher embolism resistance (Zhao *et al.*, 2019). Both of these traits are likely to interfere in xylem resistance by the same mechanism as pre-existing embolism does, which it is ultimately increasing the probability for air-seeding. Following this line, it is not a surprise that tracheid is more influenced by the amount of preexisting embolism since they are packed extremely close one to another being dimensionally connected to several of them, on the other hand in the case of vessels, it is not rare in a transverse section to find them without no linkage to others.

**References**

**Blackman CJ, Brodribb TJ, Jordan GJ**. **2009**. Leaf hydraulics and drought stress: response, recovery and survivorship in four woody temperate plant species. *Plant Cell and Environment* **32**: 1584–1595.

**Blackman CJ, Brodribb TJ, Jordan GJ**. **2010**. Leaf hydraulic vulnerability is related to conduit dimensions and drought resistance across a diverse range of woody angiosperms. *New Phytologist* **188**: 1113–1123.

**Brodersen C, Jansen S, Choat B, Rico C, Pittermann J**. **2014**. Cavitation resistance in seedless vascular plants: the structure and function of interconduit pit membranes. *Plant Physiology* **165**: 895–904.

**Brodribb TJ, Cochard H**. **2009**. Hydraulic failure defines the recovery and point of death in water-stressed conifers. *Plant Physiology* **149**: 575–584.

**Brodribb TJ, Skelton RP, Mcadam SAM, Lucani CJ, Marmottant P**. **2016**. Visual quantification of embolism reveals leaf vulnerability to hydraulic failure. *New Phytologist* **209**: 1402–1409.

**Charrier G, Torres-ruiz JM, Badel E, Burlett R, Choat B, Cochard H, Delmas CEL, Domec J, Jansen S, King A, *et al.* 2016**. Evidence for hydraulic vulnerability segmentation and lack of xylem refilling under tension. *Plant Physiology* **172**: 1657–1668.

**Choat B, Brodersen CR, Mcelrone AJ**. **2015**. Synchrotron X-ray microtomography of

xylem embolism in Sequoia sempervirens saplings during cycles of drought and recovery. *New Phytologist* **205**: 1095–1105.

**Choat B, Brodribb TJ, Brodersen CR, Duursma RA, López R, Medlyn BE**. **2018**. Triggers of tree mortality under drought. *Nature* **558**: 531–539.

**Choat B, Choat B, Cobb AR, Jansen S**. **2008**. Structure and function of bordered pit: new discoveries and impacts on whole-plant hydraulic function. *New Phytologist* **177**: 608–626.

**Choat B, Pittermann J**. **2009**. New insights into bordered pit structure and cavitation resistance in angiosperms and conifers. *New Phytologist* **182**: 557–560.

**Cochard H, Badel E, Herbette S, Delzon S, Choat B, Jansen S**. **2013**. Methods for measuring plant vulnerability to cavitation: a critical review. *Journal of Experimental Botany* **64**: 4779–4791.

**Cochard H, Delzon S**. **2013**. Hydraulic failure and repair are not routine in trees. *Annals of Forest Science* **70**: 659–661.

**Cochard H, Delzon S, Badel E**. **2015**. X-ray microtomography (micro-CT): A reference technology for high-resolution quantification of xylem embolism in trees. *Plant, Cell and Environment* **38**: 201–206.

**Hacke UG, Jacobsen AL, Pratt RB**. **2009**. Xylem function of arid-land shrubs from California, USA: An ecological and evolutionary analysis. *Plant, Cell and Environment* **32**: 1324–1333.

**Hacke UG, Jansen S**. **2009**. Embolism resistance of three boreal conifer species varies with pit structure. *New Phytologist* **182**: 675–686.

**Hacke UG, Sperry JS, Pockman WT, Davis SD, Mcculloh KA**. **2001**. Trends in wood density and structure are linked to prevention of xylem implosion by negative pressure. *Oecologia* **126**: 457–461.

**Jansen S, Schenk HJ**. **2015**. On the ascent of sap in the presence of bubbles. *American Journal of Botany* **102**: 1561–1563.

**Lamarque LJ, Corso D, Torres-ruiz JM, Badel E, Brodribb TJ, Burlett R**. **2018**. An inconvenient truth about xylem resistance to embolism in the model species for refilling *Laurus nobilis* L. *Annals of Forest Science* **88**: 1–15.

**Li S, Lens F, Karimi Z, Klepsch MM**. **2016**. Intervessel pit membrane thickness as a key determinant of embolism resistance in angiosperm xylem. *IAWA jornal* **37**: 152–171.

**Petty JA, B PRSL**. **1972**. The aspiration of bordered pits in conifer wood. *Proceedings*

*of the Royal Society of London. Series B. Biological Sciences* **181**: 395–406.

**Pockman WT, Sperry JS, O'leary JW**. **1995**. Sustained and significant negative water pressure in xylem. *Nature* **378**: 715–716.

**Schenk H j., Espino S, Romo DM, Nima N, Do AYT, Michaud JM, Papahadjopoulos-Sternberg B, Yang J, Zuo YY, Steppe K, *et al.* 2017**. Xylem surfactants introduce a new element to the cohesion-tension theory. *Plant Physiology* **173**: 1177–1196.

**Schenk HJ, Steppe K, Jansen S**. **2015**. Nanobubbles: A new paradigm for air-seeding in xylem. *Trends in Plant Science* **20**: 199–205.

**Sperry, J. S, Tyree MT**. **1990**. Water-stress-induced xylem embolism in three species of conifers. *Plant, cell & environment* **13**: 427–436.

**Sperry JS, Pockman WT**. **1993**. Limitation of transpiration by hydraulic conductance and xyiem cavitation in *Betula occidentalis*. *Plant Cell and Environment* **16**: 279–287.

**Sperry JS, Tyree MT**. **1988**. Xylem embolism mechanism of water stress-induced. *Plant Physiology* **88**: 581–587.

**Walter L, Bauch J**. **1967**. On the closure of bordered pits in conifers. *Wood Science and Technology* **1**: 1–13.

**Zhao H, Jiang Z, Ma J, Cai J**. **2019**. What causes the differences in cavitation resistance of two shrubs? Wood anatomical explanations and reliability testing of vulnerability curves. *Physiologia Plantarum*.

**Zimmermann MH**. **1983**. Xylem structure and the ascent of sap. *Springer-Verlag*.

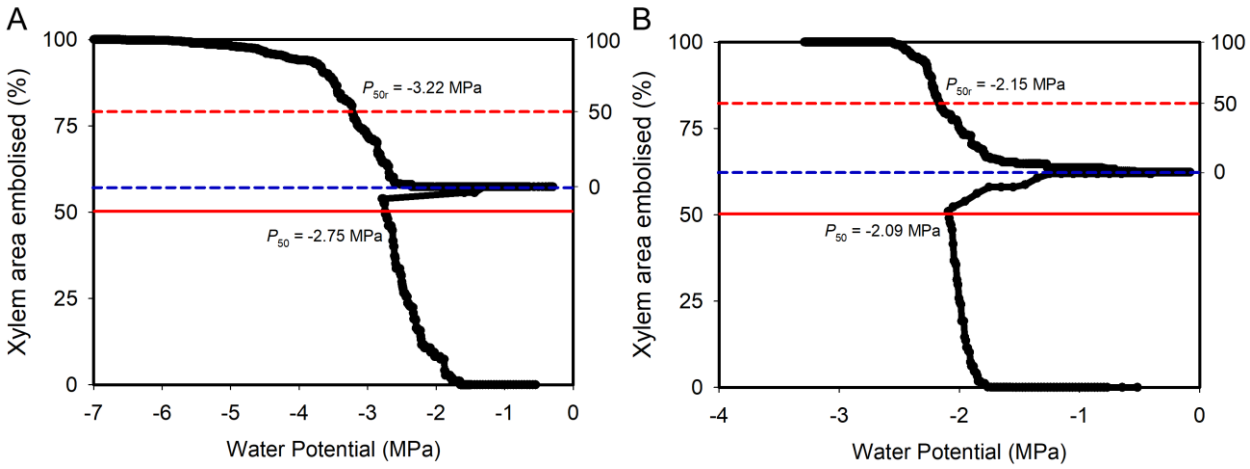


**Figure 1.** Rehydration curves performed in *Ilex verticillata* (A) and *Agathis robusta* (B) which are vessel and tracheid-based xylem respectively. Red line highlights the water potential at which 50% of all xylem conduits of the sample were embolised ($P_{50}$). Dashed red line highlights the water potential at which 50% of the remaining water-filled conduits were embolised ($P_{50r}$) at the second round of dehydration. Dashed blue line represents the end of the rehydration and consequently beginning of dehydration; preexisting. Complete data are presented in supplementary information S2)

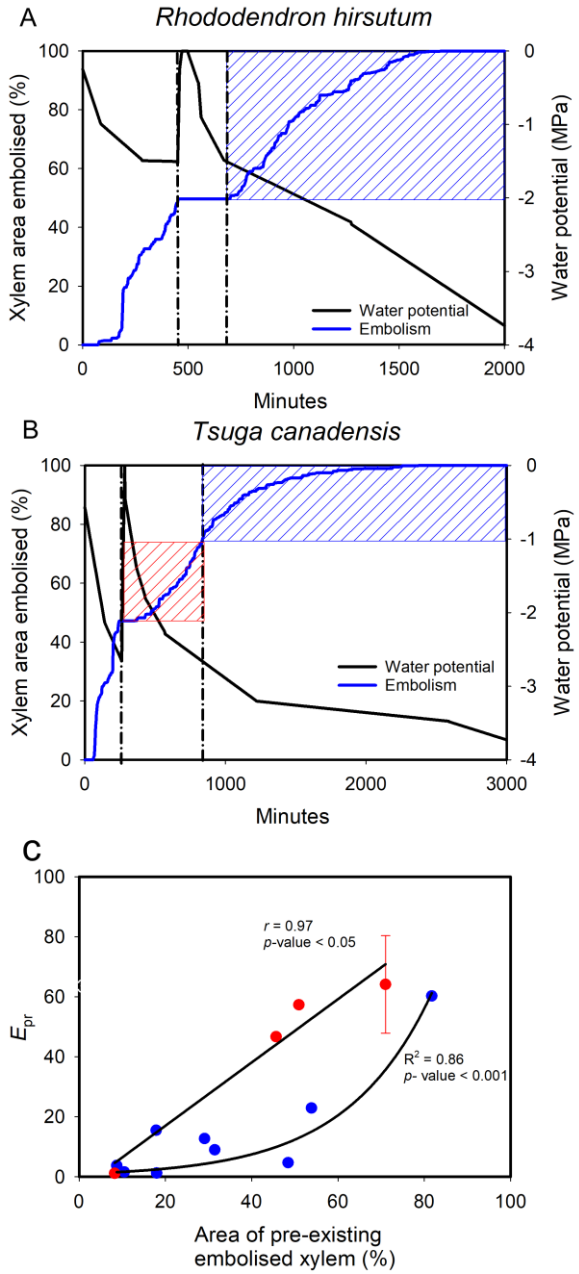


**Figure 2.** Examples of traces of the percentage of embolized xylem area (blue) and water potential (black) plotted against time in a branch of the vessel-bearing angiosperm *Rhododendron hirsutum* (A) and the conifer *Tsuga canadensis* (B). The verticals dashed lines mark the period of time between the rehydration and the and the point in which the water potential on the second dehydration had declined to the water potential when the branch was first rehydrated. The red box surrounds the percentage of embolized xylem area which occurred prior to the water potential when the branch was first rehydrated. The blue box represents the amount of embolism on the second dehydration that occurred after the water potential of the branch had declined to the water potential when the branch was rehydrated. The effect of the area of pre-existing

embolised xylem on the percentage of xylem area in which embolism occurred prior to the water potential of the branch declining to the water potential reached when it was rehydrated on the first period of dehydration, in plants with vessel-bearing xylem (blue) and tracheid-based xylem (red) (C). Linear (in data from tracheid-based xylem) and exponential (in data from vessel-bearing xylem) regression are plotted for each dataset. The tracheid-based xylem dataset includes a mean (n =3, ±SE) datum from *Torreya californica*. All traces used to assemble this dataset are included in Figure S1 and supplementary information S2.

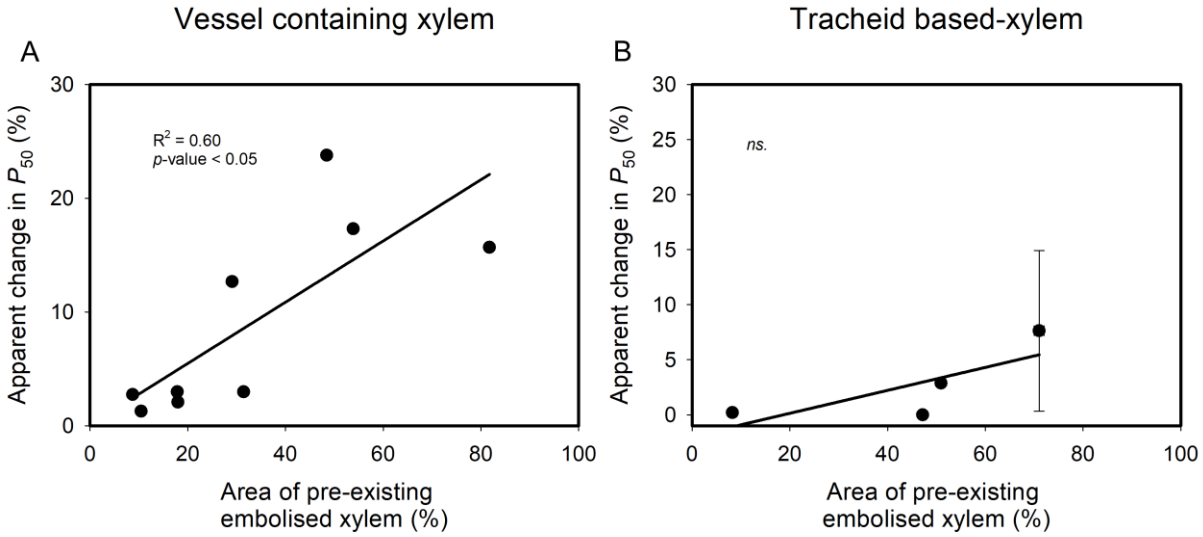


**Figure 3.** The effect of pre-existing embolised xylem area on apparent change in $P_{50}$ of plants with vessel-containing xylem (A) and tracheid-based xylem (B).

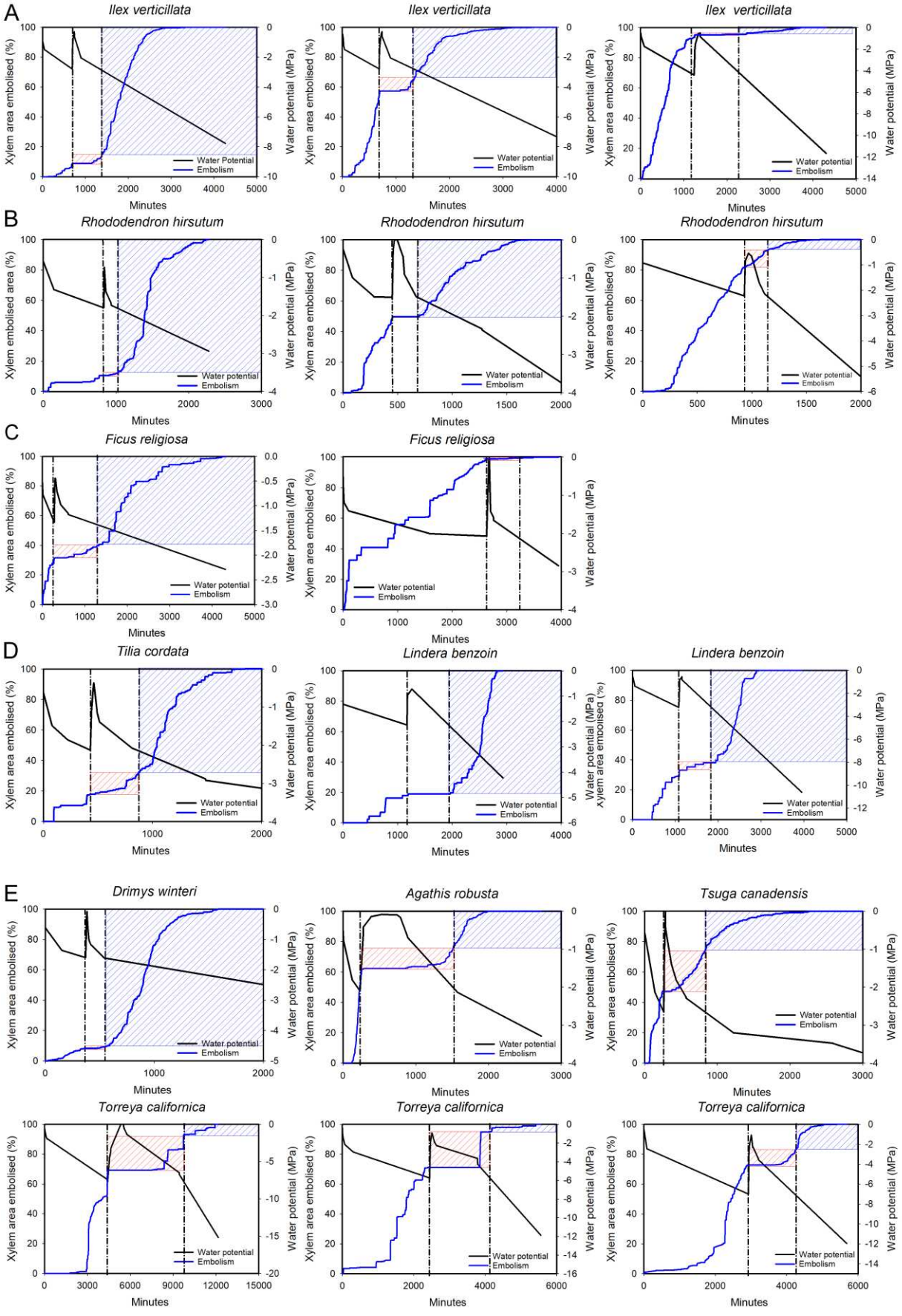
A
Ilex verticillata
Ilex verticillata
Ilex verticillata
B
Rhododendron hirsutum
Rhododendron hirsutum
Rhododendron hirsutum
C
Ficus religiosa
Ficus religiosa
D
Tilia cordata
Lindera benzoin
Lindera benzoin
E
Drimys winteri
Agathis robusta
Tsuga canadensis
Torreya californica
Torreya californica
Torreya californica
Xylem area embolised (%)
Xylem embolised area (%)
Water potential (MPa)
Minutes
Water Potential
Water potential
Embolism

**Figure S1.** Rehydration curve on stems of the angiosperms *Ilex verticillata* (A), *Rhododendron hirsutum* (B), *Ficus religiosa* (C), *Tilia cordata* and on leaves of *Lindera benzoin* (D); on tracheid angiosperm *Drymis winteri* and the conifers *Tsuga canadensis, Agathis robusta* and *Torreya californica* (E). Blue line and black lines represent respectively the accumulative curve of embolism and the behavior of water potential (WP) during the experiment. Dashed lines represent the WP of rehydration. The red box represents the amount of embolism which occurred previous to the WP of rehydration in the second round of dehydration. The blue box represents the amount of embolism that occurred after the WP of rehydration in the second round of dehydration.

## General conclusions

At the present work, we have revisited well known strategies plants employ against drought. As a result, we found interesting interactions between drought responses and other environmental factors as $CO_2$ concentration ($[CO_2]$) and light. In the first chapter, drought-stressed coffee plants acclimated to elevated $[CO_2]$ displayed a higher hydraulic conductance which might have been related to an overall increase in the expression of aquaporin genes when compared to their counterparts acclimated to ambient $[CO_2]$. We also found that well-watered coffee plants acclimated to elevated $[CO_2]$ had a faster stomatal response to vapor pressure deficit when compared to coffee plants acclimated to ambient $[CO_2]$ ultimately having a decreased transpiration at whole plant scale. This was associated with an upregulation of CaPiP2;1, an aquaporin believed to be essential for the well-described $CO_2$-dependent decrease of stomatal conductance. Further at the second chapter, elevated $[CO_2]$ improved carbon assimilation, water use-efficiency and biomass accumulation regardless watering, in addition to decreasing the oxidative pressure under drought conditions. Elevated $[CO_2]$ also promoted key allometric adjustments linked to drought tolerance, *e.g.* more biomass partitioning towards roots with a deeper root system. Improved growth under enhanced air $[CO_2]$ was unlikely to have been associated with global changes on hormonal pools but rather with shifts on carbon fluxeswe found that an increased These results demonstrate how $[CO_2]$ it is sensed as an important environmental factor being able to transcriptionally reprogram plants changing the way they sense and respond to drought events, which can help to keep the sustainability of the coffee-chain-of-value on a climate changing scenario. On the third chapter, in our search for anatomical drivers for plant resistance against embolism, we found that the vessel lumen fraction seems to be a major determinant not just for inter but also intraspecific variation of embolism resistance. In this way we found that plants evolved in environments with water scarcity or freezing events presented more negative values of $P_{50}$ (water potential at which 50% of xylem vessel are embolized) and decreased values of vessel lumen fraction. Also, irradiance have minor changes in embolism resistance on stems. Stems acclimated at high irradiance presented a more negative values of $P_{50}$, also associated with decreased values of vessel lumen fraction. Although we do not present a mechanistic explanation for these observations, we believed that a higher vessel lumen fraction would confine xylem vessels closer to one another and

permit an easier spread of embolism contributing to decrease the resistance against embolism. Finally, in our fourth chapter, we demonstrated that vessels have a more well-defined water potential threshold beyond which they will embolize which does not happen with tracheids. This feature implicates that measurement of $P_{50}$ of plants vessel-based xylem plants presenting pre-existing embolism might lead to overestimations of resistance against embolism.